



**DESIGN TOOLS FOR SOLID-FUELED RAMJET MISSILE
PRELIMINARY DEVELOPMENT**

ROGÉRIO LUIZ VERISSIMO CRUZ

**DISSERTAÇÃO DE MESTRADO EM CIÊNCIAS MECÂNICAS
DEPARTAMENTO DE CIÊNCIAS MECÂNICAS**

FACULDADE DE TECNOLOGIA

UNIVERSIDADE DE BRASÍLIA

**UNIVERSIDADE DE BRASÍLIA
FACULDADE DE TECNOLOGIA
DEPARTAMENTO DE CIÊNCIAS MECÂNICAS**

**DESIGN TOOLS FOR SOLID-FUELED RAMJET MISSILE
PRELIMINARY DEVELOPMENT**

ROGÉRIO LUIZ VERISSIMO CRUZ

Orientador: PROF. DR. CARLOS ALBERTO GURGEL VERAS, ENM/UNB

Co-Orientador: PROF. DR. OLEXIY SHYNKARENKO, ENM/UNB

DISSERTAÇÃO DE MESTRADO EM CIÊNCIAS MECÂNICAS

**PUBLICAÇÃO PPGENM.DM - XXX/AAAA
BRASÍLIA-DF, 18 DE DEZEMBRO DE 2023.**

**UNIVERSIDADE DE BRASÍLIA
FACULDADE DE TECNOLOGIA
DEPARTAMENTO DE CIÊNCIAS MECÂNICAS**

**DESIGN TOOLS FOR SOLID-FUELED RAMJET MISSILE
PRELIMINARY DEVELOPMENT**

ROGÉRIO LUIZ VERISSIMO CRUZ

DISSERTAÇÃO DE MESTRADO ACADÊMICO SUBMETIDA AO DEPARTAMENTO DE CIÊNCIAS MECÂNICAS DA FACULDADE DE TECNOLOGIA DA UNIVERSIDADE DE BRASÍLIA, COMO PARTE DOS REQUISITOS NECESSÁRIOS PARA A OBTENÇÃO DO GRAU DE MESTRE EM CIÊNCIAS MECÂNICAS.

APROVADA POR:

Prof. Dr. CARLOS ALBERTO GURGEL VERAS, ENM/UnB
Orientador

Prof. Dr. Olexiy Shynkarenko, ENM/UnB
Co-orientador

Prof. Dr. Armando de Azevedo Caldeira Pires & Prof. Dr. Paolo Gessini, ENM/UnB
Examinadores internos

Prof. Dr. Pedro Teixeira Lacava, ITA
Examinador externo

BRASÍLIA, 18 DE DEZEMBRO DE 2023.

FICHA CATALOGRÁFICA

ROGÉRIO LUIZ VERISSIMO CRUZ

Design Tools for Solid-Fueled Ramjet Missile Preliminary Development

2023xv, 121p., 201x297 mm

(ENM/FT/UnB, Mestre, Ciências Mecânicas, 2023)

Dissertação de Mestrado - Universidade de Brasília

Faculdade de Tecnologia - Departamento de Ciências Mecânicas

REFERÊNCIA BIBLIOGRÁFICA

ROGÉRIO LUIZ VERISSIMO CRUZ (2023) Design Tools for Solid-Fueled Ramjet Missile Preliminary Development. Dissertação de Mestrado em Ciências Mecânicas, Publicação xxx/AAAA, Departamento de Ciências Mecânicas, Universidade de Brasília, Brasília, DF, 121p.

CESSÃO DE DIREITOS

AUTOR: ROGÉRIO LUIZ VERISSIMO CRUZ

TÍTULO: Design Tools for Solid-Fueled Ramjet Missile Preliminary Development.

GRAU: Mestre ANO: 2023

É concedida à Universidade de Brasília permissão para reproduzir cópias desta dissertação de Mestrado e para emprestar ou vender tais cópias somente para propósitos acadêmicos e científicos. O autor se reserva a outros direitos de publicação e nenhuma parte desta dissertação de Mestrado pode ser reproduzida sem a autorização por escrito do autor.

ROGÉRIO LUIZ VERISSIMO CRUZ

Faculdade de Tecnologia da Universidade de Brasília - FT/UnB - Campus Darcy Ribeiro

Acknowledgments

First, I thank God for granting me physical and mental health to overcome every challenge throughout the various stages of the master's degree process. I would like to express my gratitude to my wife, Eliete, and my children, Breno and Sara, for their unwavering encouragement and support in accomplishing this significant milestone. Furthermore, I would like to extend a special thank you to my advisor, Carlos Alberto Gurgel Veras. Professor Gurgel is a highly competent professional with exceptional reasoning skills and an admirable level of dynamism. It has been a privilege to receive Professor Gurgel's meticulous, patient, and motivating guidance.

Resumo

Ferramentas de Projeto para Desenvolvimento Preliminar de Míssil com Estatorreator a Propelente Sólido - Esta pesquisa apresenta uma metodologia para o desenvolvimento conceitual da primeira versão naval brasileira de um míssil antinavio supersônico, superfície-superfície, empregando estatorreator a propelente sólido. Este sistema tático será capaz de desempenhar um papel crucial na proteção de instalações sensíveis e linhas de comunicação marítima na zona econômica exclusiva. O projeto conceitual do míssil proposto segue, como referência, as práticas de padronização da Cooperação Europeia para a Padronização Espacial, comumente empregadas em atividades espaciais. Para alcançar os objetivos do estudo, ferramentas numéricas são introduzidas para avaliar o desempenho balístico externo e interno, permitindo análise e otimização abrangentes do sistema. Esses programas computacionais utilizam equações de movimento e cálculos de balística interna para estimar várias etapas da trajetória do míssil, incluindo ascensão, cruzeiro e descida para o alvo. Eles também facilitam o projeto de um motor ramjet de combustível sólido. Posteriormente, a metodologia proposta é implementada para desenvolver duas versões conceituais de míssil supersônico. A primeira versão incorpora como primeiro estágio um propulsor que foi testado no Brasil, seguido por um motor ramjet como segundo estágio. Esse míssil possui diâmetro de 300 mm, atinge Mach 2.9 em voo de cruzeiro e é capaz transportar uma carga útil de 100 kg a 166 km de distância do local de lançamento. O segundo míssil conceitual é totalmente definido por uma metodologia específica, apresentando um diâmetro de 600 mm e um comprimento de 8.300 mm. Esse míssil é projetado para voar a Mach 3, a uma altitude de 14.000 m, e é capaz de transportar uma ogiva com peso de 200 kg, com um alcance superior a 300 km.

Keywords: ECSS, Propulsão ramjet, projeto preliminar de mísseis, mísseis táticos.

Abstract

This study presents a methodology for the conceptual development of the first Brazilian naval version of a surface-to-surface supersonic solid-fuel-based ramjet anti-ship missile. This tactical weapon plays a crucial role in safeguarding sensitive installations and maritime communication lines within the exclusive economic zone. The research draws upon the European Cooperation for Space Standardization practices, commonly employed in space activities, as a reference for the conceptual design of the missile. To achieve the study's objectives, numerical tools for assessing external and internal ballistics performance are introduced, enabling comprehensive system analysis and optimization. These computational programs utilize motion equations and internal ballistics calculations to estimate various stages of the missile's trajectory, including ascent, cruise, and coasting. They also facilitate the design of a solid-fueled ramjet engine. Subsequently, the proposed methodology is implemented to develop two baseline conceptual versions of the supersonic missile. The first version incorporates a booster that has been tested in Brazil as its first stage, followed by a ramjet engine as the second stage. This missile has a diameter of 300 mm, reaches Mach 2.9 in cruise flight, and is capable of carrying a payload of 100 kg up to 166 km from the launch site. The second conceptual missile is entirely defined by a specific methodology, featuring a diameter of 600 mm and a length of 8,300 mm. This missile is designed to fly at Mach 3, at an altitude of 14,000 m, and can carry a warhead weighing 200 kg, with a range exceeding 300 km.

Keywords: ECSS, Missile preliminary design, Ramjet propulsion, Tactical missiles.

CONTENTS

ACKNOWLEDGMENTS	I
RESUMO	II
ABSTRACT	III
1 INTRODUCTION	1
1.1 GENERAL OBJECTIVE	2
1.2 SPECIFIC OBJECTIVES	2
2 LITERATURE REVIEW	3
2.1 SOLID FUEL RAMJET MAIN CHARACTERISTICS	3
2.2 SOLID FUEL RAMJETS STUDIES OVERVIEW.....	4
2.3 TRAJECTOGRAPHY	8
3 PRELIMINARY DESIGN	10
3.1 PROJECT DESIGN REFERENCE	11
3.1.1 PHASE 0.....	13
3.1.2 PHASE A	22
4 PHYSICAL AND COMPUTATIONAL MODELS	26
4.1 PHYSICAL MODEL	26
4.1.1 FLIGHT DYNAMIC	26
4.1.2 EXTERNAL BALISTICS.....	26
4.1.3 GRAVITY AND AERODYNAMIC MODEL.....	29
4.1.4 ATMOSPHERE MODEL	34
4.1.5 MISSILE GEOMETRY.....	35
4.2 INTERNAL BALLISTIC	36
4.2.1 DIFFUSER	37
4.2.2 BURNER.....	39
4.2.3 LAVAL NOZZLE	41
4.2.4 THRUST	43
4.2.5 SPECIFIC IMPULSE	43
4.3 POWER AND EFFICIENCY	44

4.4	MISCELLANEOUS EQUATIONS.....	45
4.5	ALGORITHM	46
4.6	COST ASSESSMENT	46
4.7	NUMERICAL SOLUTION AND CODE VALIDATION	48
5	RESULTS AND DISCUSSION	53
5.1	BASELINE MISSILE DEVELOPMENT.....	53
5.2	MISSILE 1 DEVELOPMENT.....	56
5.3	MISSILE 2 DEVELOPMENT.....	61
	CONCLUSION.....	69
	BIBLIOGRAPHY.....	71
	APPENDIX A: BIBLIOMETRIC NETWORKS.....	78
	APPENDIX B: TECHNICAL REQUIREMENTS.....	80
	APPENDIX C: RISK MANAGEMENT	95
	APPENDIX D: EES CODE FOR MISSILE PROFILE DESIGN.....	103
	APPENDIX G: ACCEPTED PUBLICATION	104

LIST OF FIGURES

2.1	Solid-fuel ramjet missile.....	3
3.1	Conceptual missile design.....	10
3.2	The steps and cycles in the risk management process	20
3.3	Risk magnitude designations and proposed actions.....	21
4.1	Forces acting on flight.....	27
4.2	Control volume	36
4.3	Code validation	52
5.1	Successive process for preliminary missile design.....	55
5.2	FTI training rocket solid motor.....	56
5.3	subsystems volume arrangement without the booster.....	59
5.4	Missile 1 flight altitude and velocity profile.....	60
5.5	Missile 1 lift force and angle of attack during the flight.....	60
5.6	Missile 1 drag force profile.....	61
5.7	Missile 2 trajectory - Final version.....	67
5.8	Missile 2 drag forces - Final version.....	68
5.9	Subsystems arrangement.....	68
10	Co-authorship density visualization.....	79
11	Risk index: combination of severity and likelihood.....	97

LIST OF TABLES

3.1	Example of a severity-of-consequence scoring scheme [1]	21
3.2	Example of a likelihood score scheme [1].....	21
4.1	Engine performance comparison	50
4.2	Aerobee 150A mass breakdown	51
5.1	Missile refinement process	58
5.2	Missiles comparison	61
5.3	Baseline missile parameters.....	63
5.4	Missile 2 refinement process.....	65
5.5	Missile 2 final parameters	66
5.6	Missiles comparison	67
7	Risk identification (Technical and External).....	100
8	Risk identification (Organisational, Project Management. and Cost).....	101
9	Risk assessment [1]	102

Chapter 1

Introduction

The Brazilian coastal line is roughly 8.5 thousand kilometers in length and houses 80% of its population [2]. In the narrow strip of the territory, which runs along all shore lengths, there are sixteen out of twenty-seven state capitals, vital ports and airports, two spaceports, and a large oil and gas complex consisting of pipelines, offshore drilling, and refineries. The majority of the Brazilian infrastructure for maritime routes supported international commerce in the region.

This scenario imposes a challenging surveillance and defense tasks to the Brazilian Navy, requiring the development of a state-of-the-art anti-ship weapons capable to deny any action against the Brazilian interest.

Brazil has extensive experience in developing rockets based on solid propellant propulsion. [3]. The Brazilian company AVIBRAS is currently testing a long-range gas turbine jet missile ranging around 300 km. [4].

Regarding propulsion systems, deserve attention the efforts of the Institute of Aeronautics and Space - IAE and the Institute for Advanced Studies - IEAv on studies to develop hypersonic technology (Martos et al. 2017). The country, however, has limited experience in supersonic missile technology and incipient academic studies on ramjet propulsion systems.

For tactical supersonic missile development, the next logical step is an research effort in ramjets propulsion system due to its substantially superior energetic performance to that of rockets [5].

The development cycle of paraffin-based propulsive systems is presumably faster and of lower cost when compared to engines similar to liquid fuel-based. Such systems are less complex than liquid-fueled state-reactors [5], however, they present similar performance [6], [7].

The Chemical Propulsion Laboratory at UnB has been pushing forth new studies on the development of supersonic long-range missiles based on solid and liquid propulsion reactors [8].

Although solid-fuel ramjet provides a variety of solutions for supersonic flight regimes, this know-how is not available for commercialization or technology transfer between countries. The Missile Technology Control Regime limit the proliferation of such capability [9].

To start up the project development of a supersonic ramjet missile, we present a methodology for the conceptual phase based on project design standards supported by a computational tool to solve the equations referring to the missile's mission profile covering the flight's ascending, cruising, and descending phases.

This proposal takes advantage of a significant apparatus developed by the University of Brasilia to research a broad range of fuels, including those used for ramjet propulsion, with high-temperature air streams [10].

We propose to address the following motivating question: **Is it feasible to design a paraffin-fuel-based ramjet missile in the Brazilian universities from the grounds to the Technology Readiness Level 3 - TRL 3 ?**

1.1 General objective

This research aims to develop and present a methodology accompanied by a comprehensive suite of numerical tools for the preliminary design of solid-fueled ramjet missiles.

1.2 Specific objectives

1. Formulate the conceptual design of a supersonic tactical missile propelled by a solid-fuel-based ramjet engine (Phase 0).
2. Commence Phase A of the project.
3. Develop computational tools to support the performance simulations in the conceptual design activity.

Chapter 2

Literature review

Initially, we underwent bibliometric network research to identify and rank countries and authors that present significant works in this research field. For this purpose, a survey is available in Appendix A.

On the other hand, the following sections focus on a comprehensive analysis of aspects relevant to further discussions.

2.1 Solid fuel ramjet main characteristics

Solid fuel ramjets are the simplest air breathing engines and can provide propulsion solutions for high speed long-range missions [5]. Figure 2.1 shows a generic solid-fuel ramjet missile subsections.

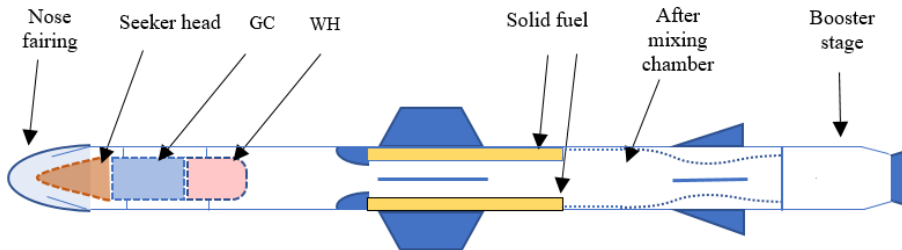


Fig. 2.1: Solid-fuel ramjet missile.

Ramjet air-breathing propulsion is particularly efficient at the supersonic flight regimes, beyond the operating range of turbojet engines, and its energetic performance is substantially superior to that of rockets [5].

The author presented the main aspects of solid fuel ramjets propellants based on comprehensive theoretical and experimental studies as follow [5]:

1. The overall solid fuel ramjet system are much simpler and most likely of a lower cost compared to liquid fuel ramjet or scramjet systems.

2. Since, in general, the solid fuel contains no oxidizer; it cannot sustain combustion in quiescent atmosphere. Its storage as a bulk does not allow mixing with surrounding air. The result is that SFRJs exhibit excellent safety properties and very low fire and explosion hazards compared to liquid fuel ramjets.
3. Thermal protection of the combustion chamber is a lot easier than in the case of a liquid fuel, because the solid fuel itself provides good insulation for the combustor walls.
4. The overall fuel-to-air ratio cannot be controlled directly because of the dependence of the fuel regression rate on the port flow characteristics with major effects of: Reynolds number, Re ; mass flow rate, \dot{m} ; mass flux, G ; inlet air temperature, T ; and port diameter, d . A bypass regulation concept may be applied for the regular SFRJ.
5. The characteristic gas-phase diffusion flame over the solid-fuel surface in SFRJs may result in low combustion efficiency because of incomplete mixing of the fuel gases emerging from the wall and the oxygen diffusing from the core flow. The supersonic flow characteristics in the scramjet combustor further worsen the situation.

Regarding the heating values per unit mass of hydrocarbon-type propellant used in liquid and solid ramjet rockets, these parameters are essentially the same (approximately around 44 MJ/kg). [11].

The density of solid fuel used is generally 15 - 20 % higher than liquid fuels. Adding metallic fuel powders such as aluminum or boron to solid propellants can enhance their characteristics (regression rate and mechanical properties).

2.2 Solid fuel ramjets studies overview

The literature review conducted in 1994 identified certain topics that garnered more interest than others. One such topic is metalized fuel-rich propellant (FRP), which continues to be a focal point of study to the present day. The review within the field of FRP concentrated on assessing the limitations and merits of various potential metals (Al, Mg, B, Be, or Zr) as components of propellants. The work highlights that the current systems based on Al and B face challenges in achieving ideal performance due to low combustion efficiency. This issue becomes particularly critical at the low pressures used in upper-stage motors. It has been observed that detailed research is necessary to develop FRP with all three crucial attributes: ease of ignition, stable combustion under operating conditions, and high-performance specific impulse (I_{sp}) within a single composition. [12].

Boron is a metal with the highest volumetric specific energy in nature. For this reason, there is a considerable number of investigations on boron's performance as a fuel additive. [13].

Considering the significant higher energetic performance of metalized fuels in bi-propellant systems in comparison to non-metalized hydrocarbons fuels, the authors conducted a parametric investigation of the effect of boron concentration, boron particles diameter and size distribution, and bypass air ratio on the performance of the ramjet. They also described the model governing equations and boundary conditions [13].

Tests with the addition of 5% nano-Aluminum to the hydroxyl-terminated polybutadiene - HTPB in hybrid rockets demonstrate an increase in the regression rate and the mass loss rate of the fuel [14].

Gel propellants are also a field of study that drives researchers' attention. DISKIN and NATAN (2017) described gel propellants as liquid fuels or oxidizers whose rheological properties are modified by adding gelling agents. The gel is a substance containing a continuous solid skeleton enclosing a continuous liquid phase. The continuity of the solid structure gives elasticity to the gel. Its characteristics also enable the addition of metal particles to the gel fuel.

Metalized gel fuel used in ramjet engine has potential for higher performance and increased safety in comparison to the conventional Liquid Fuel Ramjets, Solid Fuel Ramjets or Ducted Rockets [13].

Studies also indicate that the non-Newtonian flow behavior of gel propellants offers the possibility to built throttleable engines with easy handling and storage capabilities [15].

The researchers identified a declining interest in gels in the mid of the '70s of the last century. In the '80s, the stake increased again due to new demands on the performance of future propulsion systems like thrust and energy management, insensitive munitions (IM) criteria, fuels with high energy density, low toxicity, improved handling and storage safety, low overall life costs, etc [15].

Significant progress has been made in the last years in basic research as well as in work on propulsion system development and demonstration. This can be seen on the one hand in the increasing number of publications and in the conduction of whole sessions about gel propulsion at several international conferences in the last years [15].

The authors concluded that up to now the understanding of basic as well as of technology processes of gel propulsion has significantly been increased. The basic process relevant areas are mainly related to rheology and the flow, spray and combustion behavior of gelled energetic fluids [15].

The technology important areas cover mainly combustor process control and engine development. Nevertheless there are still open gaps to close [15]. Only the initial analysis of parameters such as bypass ratio, the boron content and the particle diameter distribution was studied [13].

With regards to paraffin wax as a hybrid rocket fuel, an extensive literature review was carried out. The analyses performed demonstrated that paraffin wax-based fuels have not

been comprehensively characterized, especially regarding the structural feasibility of the material in launch applications. Preliminary structural testing has shown paraffin wax to be a brittle, low-strength material, and at risk of failure under launch loading conditions [16].

Structural enhancing additives have been identified but their effect on motor performance has not always been considered, nor has any standard method of testing been identified between research institutes [6]. Additives such as metal hydrides, aluminum, and boron could enhance paraffin wax's viscosity and structural properties. However, there is very little analysis of these additives' structural effects on the wax grain [16].

There is evidence that hybrid fuels, particularly liquefying fuels, have potential as an applicable form of chemical propulsion. Despite the advances in this technology, no detailed review of the existing performance and structural test results or methods is available for paraffin wax in particular [16].

The regression rate data presented indicates a strong link between regression rate improvements in paraffin wax with the addition of metalized additives. Unfortunately, very little testing has been conducted in the structural performance of the grains with these additives [16]. The data available also indicates a gap in the development and use of paraffin wax hybrid fuels for launch applications.

Complementary research on the mechanical characteristics of paraffin-based fuel identifies a strengthening of the fuel by adding ethylene vinyl acetate copolymer (EVA). Additionally, paraffin exhibits a high fuel regression rate, approximately 3 to 4 times greater than that of a conventional hybrid fuel [6]. In a different strategy, a survey on a specific class of paraffin-based fuel shows an increasing rate of fuel mass transfer without the use of oxidizer additives [17].

An investigation into combustion performance, involving the alteration of the ram airflow inlet interface position combined with a powder feed system providing aluminum fuel particles, demonstrated a combustion efficiency of 73.05% [18]. Analysis on combustion characteristics of star solid fuel for ramjet, allow the developed of a code that can predict the effect of fuel configuration on the regression rate. In this process was observed that turbulent viscosity is a critical parameter affecting the regression rate [19]. The use of a three-dimensional scanner and scanning electron microscope (SEM) to obtain the local regression rate and morphology of paraffin and polyethylene blend fuel after combustion revealed that decreasing the inlet diameter enhances performance [20]. Investigations regarding a fixed geometry combustor have resulted in the comparative optimization of solid fuel ramjet candidates to maximize total impulse in relation to the interactions between impulse, fuel regression rate, and stoichiometric air-to-fuel ratio [21].

Significant research efforts have led to the development of equations for thrust-to-drag, net specific impulse, impulse density, and the definition of a new performance parameter: momentum density. The work also explores the optimization of fuels for the maximum thrust-to-drag ratio or specific impulse and establishes the linkage of geometric restraints on

the selection of fuel materials. For a fixed inlet, the regression rate equations show that the required regression rate is a function of the air-to-fuel (AF) ratio and material density [17].

In a 2017 study, it was confirmed that increasing the inlet pressure ratio of the ramjet leads to a non-linear variation in specific thrust. The research also highlighted critical factors influencing the performance output of the ramjet, namely the air-fuel ratio and the area of the nozzle throat. The study additionally defined the utilization of thermogravimetric data as a method for determining fuel regression rates. It demonstrated that high-density fuels with lower regression rates and lower stoichiometric air-fuel ratios yield the highest values of normalized total impulse within a fixed geometry [22].

In the field of swirling turbulent flows, experimental and numerical investigations in a solid fuel ramjet engine demonstrated that swirl flow enhances the regression rate.

An increase of swirl number and air inlet temperature also raise mass transport at the solid fuel surface [23].

In a pertinent study conducted in 2017, challenges associated with the numerical modeling of swirling flow with combustible gases were examined. The study provided an overview of turbulence modeling for swirling flow and various numerical approaches. Emphasizing the significance of the solid fuel regression rate as a key parameter in the design of Solid Fuel Ramjet (SFRJ) due to its direct impact on performance, the researchers noted that the regression rate is primarily influenced by convective heat transfer to the solid fuel surface rather than radiation. The mathematical determination of this phenomenon was outlined by the researchers [23]:

$$\dot{r} = \frac{q_{con}}{(\rho_s h_v)} \quad (2.1)$$

Where h_v is the latent heat of decomposition or gasification of condensed fuel and ρ_s is the solid fuel density. Since the convective heat transfer q_{con} is a function of the heat transfer coefficient h_c , then Eq. 2.1 can be written as:

$$\dot{r} \propto h_c \quad (2.2)$$

With some mathematical deviations, the final relation of the dependency of regression rate on other parameters is given by:

$$\dot{r} \propto G_{air}^a \cdot d_p^b \cdot T_{air}^m \cdot P_c^n \quad (2.3)$$

Where G_{air} , d_p , T_{air} and P_c^n are constant, the mass flux, port diameter, air inlet temperature, and chamber pressure. a, b, m and n are the exponents that affect the average regression rate which are suggested by experiments through average procedure.

The authors also developed a multi-physic code and unsteady simulation with swirling

flow and chemical reactions which demonstrated a positive impact of swirling flow on SFRJ.

2.3 Trajectory

In the field of missile design and development, a significant contribution comes from a work in 2012, where key drivers in aerodynamics, propulsion, flight performance, weight, sizing, and other relevant aspects are thoroughly addressed. This work also proves valuable during the conceptual and preliminary development phases, providing insights into defining various measures of merit and conducting comparisons of missile performance [24].

Another relevant work for sizing and weight prediction uses empirical statistical regression to estimate missiles and their subsection's weight. The method groups missiles logically, like short-range air-to-air, air-to-surface, and surface-to-surface missiles, to find statistical relationships.

The regression analysis conducted in 1992 not only provides valuable input for project design in the preliminary phase but also holds significant relevance for the definition of a baseline missile. By establishing correlations with existing missiles, this statistical analysis aids in identifying key parameters and performance characteristics essential for shaping the baseline model. The insights gained from the regression analysis contribute not only to a nuanced understanding of the project design but also facilitate informed decision-making by leveraging the relationships identified through comparisons with established missile systems [25].

In the context of engineering-level codes utilized in preliminary aerodynamic design for missiles, it is asserted that many developers leverage extensive databases from entities such as NASA, the US Army, USAF, and the US Navy to validate their codes. Typically, these investigations involve enhancements to existing codes aimed at improving their capabilities. Additionally, comparisons were made among three widely used computer programs in the industry: the DATCOM (MD99), the Naval Surface Weapons Center Aeroprediction Code (AP98), and the Nielsen Engineering and Research Missile Analysis Program (M3FLR) [26].

Aerodynamic analysis should consider drag characterization at speed varying from subsonic to supersonic flight in different altitudes, linear wing theory, slender theory, and Newtonian impact theory to predict the normal coefficient [27].

The numerical method often provides the required results for rocket trajectory calculations [28].

Another field for missile design studies is the optimization procedures to improve the aerodynamic characteristics of a missile. The primary effort, in this case, is to maximize the lift-to-drag ratio, mainly at supersonic speeds, by increasing the lift coefficient c_l and reducing the drag coefficient c_d . These results are possible through enhancements in the shape and size of the nose, body, canard, wing, and tail-fin. Besides, the location of the last

three surfaces also contributes to profile optimization [29].

In contemporary discussions on fluid dynamics, it is emphasized that the utilization of sophisticated computer programs, notably Computational Fluid Dynamics (CFD) software packages, has addressed the fluid flow challenges in intricate geometries within a manageable timeframe. These advanced tools employ numerical solution techniques, enabling a more efficient and effective resolution of complex fluid dynamics problems [29].

Many available techniques propose to solve the complex turbulent flow at supersonic speeds and different angles of attack, optimizing surface efficiency and increasing maneuverability, range, and speed. To attain the validation of these methods, the results are confronted with experimental data.

Optimization methods evolved through time from classical computer programs such as Missile DATCOM and CFD to evolutionary algorithms, commonly known as genetic algorithms (GA's).

GA's imply a computational process where individuals with desired characteristics are compared. After removing the less qualified from the population, the strongest remain in reproducing and developing better specimens [30].

In general, the application of genetic algorithms depends on the execution of the following steps: problem coding for computational use, use of initial population selection techniques, use of strategies for qualitative assessment of individuals, application of selection methods of genitors in a similar way to natural selection, use of techniques for comparing competitors and application of population and elitism methods [10].

A 2012 study explored the benefits of employing steady-state genetic algorithms (GAs) and highlighted the distinction from binary GAs: 'In steady-state GAs, only the worst performer is replaced by a new member in each generation. In contrast, generational GAs replace all members of the population (except in elitist mode, where the best member remains in the next generation) using a similar tournament routine' [30].

In Brazil, there are few studies focusing on optimizing missile profiles through the application of genetic algorithms. A Matlab program was developed in 2016 to evolve the characteristics or "genes" of subsonic missiles, employing the genetic algorithm for both ballistic and cruise missiles operating at subsonic or supersonic speeds. The research addresses the optimization demands of in-service missiles, utilizing algebraic equations to achieve their objectives. The current study takes a step back to define the conceptual project design of a new supersonic missile, involving the development of phase 0 procedures complemented by a program capable of solving the differential equations associated with the missile trajectory [10].

Chapter 3

Preliminary design

Figure 3.1 demonstrates the synthesis of the conceptual missile design adopted in this work.

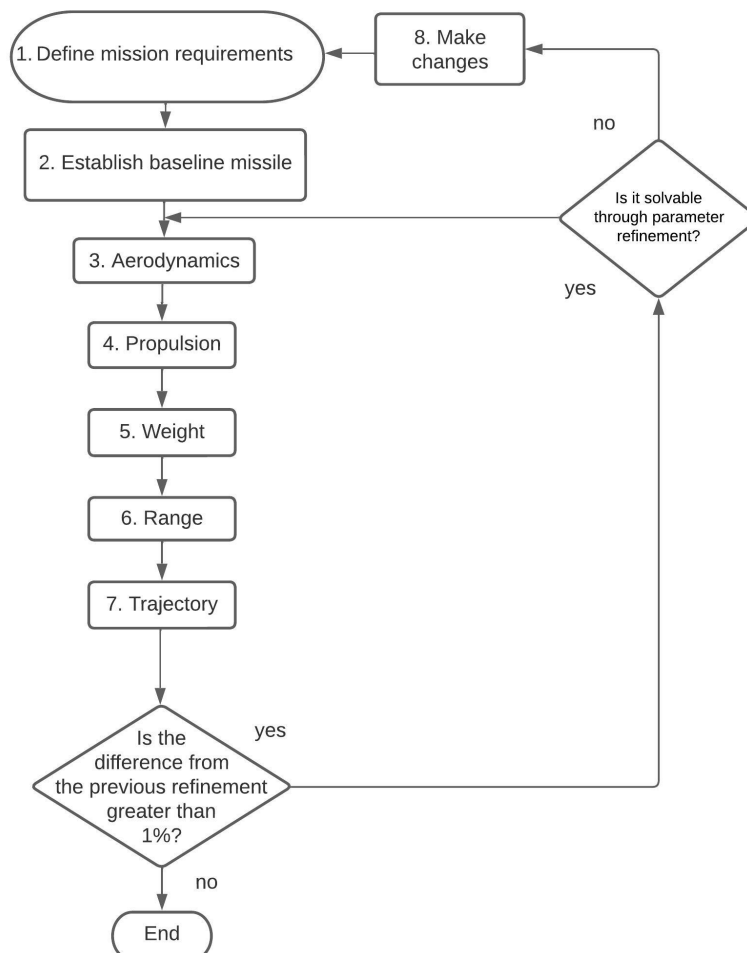


Fig. 3.1: Conceptual missile design.

Step 1 gathers information from project phase 0 as a guideline for the development process. For this study we adopt the the European Cooperation for Space Standardization -

ECSS as a reference for missile design development.

Step 2 requires the definition of a reference missile as the initial parameter from which a convergence process will lead to the desired objectives.

Steps 3, 4, 5, and 6 allow modifications focused on enhancements to achieve the final missile version, which meets the design requirements. In addition, the interactions between propulsion and aerodynamics will guide the missile sizing process.

After that, flight trajectory simulations will demonstrate the missile's ability to meet the project requirements such as range, payload, maneuverability, mass etc. Following this phase, the model is resized if necessary and reiterated if the intermediate missile version fails to meet the desired performance.

Finishing the process, step 8 regards final refinements and comparisons against mandatory or desirable attributes such as cost [24].

3.1 Project design reference

This study follows the conceptual project activities encompassing the entire project phase 0, which represents the fulfillment of step 1 (mission requirements definition).

Phase A is initialized but not concluded since there are demands which can only be defined at the industrial level. Therefore, Phase A should be revisited in the future and completed.

To elaborate on conceptual step, we will observe the life cycle of space projects defined by the European Cooperation for Space Standardization - ECSS [31].

The ECSS divide the life cycle of space projects into 7 phases as follow:

- Phase 0 - Mission analysis/needs identification
- Phase A - Feasibility
- Phase B - Preliminary Definition
- Phase C - Detailed Definition
- Phase D - Qualification and Production
- Phase E –Utilization
- Phase F – Disposal

Considering the objective of starting up the project, the priorities of this study are concepts, theory, and preliminary assessment that precedes the industrial stage. For this reason, the proposal is to maintain the activities described in ECSS-M-ST-10C for phase 0 and adapt the project phase A.

According to the standard, phase 0 aims to identify the needs and perform the mission

analysis. The following tasks characterize this phase [31]:

1. Identify possible mission concepts.
2. Elaborate the mission statement in terms of identification and characterization of the mission needs, expected performance, dependability and safety goals and mission operating constraints with respect to the physical and operational environment.
3. Develop the preliminary technical requirements specification.
4. Perform preliminary assessment of programmatic aspects supported by market and economic studies as appropriate.
5. Perform preliminary risk assessment.

The standard also defines that phase A seeks to refine the issues raised in the previous phase and starts responding to the needs.

Considering that the tasks defined by the European Cooperation for Space Standardization of phase A are not in the binding order, the author organized a new sequence of activities to present a coherent line of ideas.

For this reason, the phase A sequence of tasks changed as follows.

1. Elaborate possible system and operations concepts and system architectures and compare these against the identified needs, to determine levels of uncertainty and risks.
2. Establish the function tree.
3. Identify critical technologies and propose pre-development activities.
4. Propose the system and operations concept(s) and technical solutions, including model philosophy and verification approach, to be further elaborated during Phase B.
5. Assess the technical and programmatic feasibility of the possible concepts by identifying constraints relating to implementation, costs, schedules, organization, operations, maintenance, production and disposal.
6. Quantify and characterize critical elements for technical and economic feasibility.
7. Establish the preliminary management plan, system engineering plan and product assurance plan for the project.
8. Elaborate the risk assessment.

According to the mentioned ECSS standard, the conduction of these tasks is the responsibility of the top-level customer and one or several first-level suppliers. Nevertheless, it is possible at this stage of the project the development of task 1 and 3.

The other tasks can only be elaborated on and implemented at the industrial level.

In the next phase, tasks are mainly dedicated to identifying activities and resources needed for the ground segment and the initiation of pre-development actions.

After a preliminary requirement review, all specifications, conceptions, requirements, management, and control information from the conceptual phase will be necessary as input in the preliminary project phase. At this point, systems, components, pieces, and materials are detailed [32].

As a contribution to support the activity regarding phase B, we propose a computer-based simulation program developed to allow an analysis on flight trajectories

This numerical code tool could provide useful data to conduct "trade-off" studies, for the selection of the preferred system concept, together with the preferred technical solutions for this concept, and for the model philosophy.

All tasks cited in this section as feasible at this time use as reference ECSS' Standard parameters, the mission concept, the operational performance described in section 2, and the author's expertise.

For test and evaluation purposes, we adopt the United States Department of Defense Standard practice and the Standardization Agreement (STANAG) used by North Atlantic Treaty Organization members, both applicable to defense material as technical guides accepted worldwide.

3.1.1 Phase 0

3.1.1.1 Mission concept

Due to its geographic position in the South Atlantic, Brazil plays a strategic role, being capable of influencing this region in political and economic terms.

Brazil's coast extends approximately 4,600 miles from the Amazon region to the border with Uruguay, passing by the Middle Atlantic narrow [33], a key zone of interest for allied forces in the Second World War.

Brazil has an exclusive economic zone (ZEE) area, corresponding to 4.5 million square kilometers, which is more than half of the Brazilian continental mainland. Considering the equivalence to the Amazon forest in dimension and resources, the ZEE is called "Blue Amazon" [34].

More than 95% of Brazilian commerce occurs in this area, with intense maritime routes linking this country to Europe and the United States. Besides the way to the Middle East, crossing the Cape of Good Hope is also crucial for oil supply [35].

Brazil keeps an extensive oil and gas infrastructure and significant oil reserves in the South Atlantic. Recent discoveries of sizeable pre-salt oil fields could lead the country to shift from a traditional buyer to a major oil exporter.

The economic relevance of the South Atlantic is noticeable to other countries, mainly from outside the region and their growing interest is clear. For instance, the US decision

to reactivate the 4th Fleet after 60 years on standby, the military presence of the United Kingdom in Falklands/Malvinas and Ascension Islands, the dramatic increase of Chinese political, military, and economic cooperation in this zone, and the Russian investments in Venezuela and seabed mineral prospecting [36].

In terms of military threats, Brazil faced many attacks coming from the sea. Two Dutch invasions in the 16th century, two French invasions in the 16th and 17th centuries, a Spanish attack on the Anhatomirim Fortress in 1777 (State of Santa Catarina), and hundreds of casualties as a consequence of German U-Boats action against Brazilian merchant ships in World War II, and more recently a dispute between Brazil and France due to fishery rights in the Atlantic Ocean, involving both navies. This conflict is known as Lobster War [37].

Concerned with the importance of the South Atlantic for the country, the Brazilian Ministry of Defense released the National Defence Strategy (NDS) in 2008 and the White Paper in 2012, bringing up extensive analyses and directives.

The general guidelines of the NDS for the South Atlantic could be summarized as reinforcing sovereignty, security thinking, international defense cooperation, and naval build-up. Since then, Brazil has been following these orientations systematically.

On the international stage, Brazil's agenda counts on a peer action between the Brazilian International Affairs Minister and the Brazilian MOD, supported by the Brazilian Navy, aiming to strengthen international cooperation.

As such, Brazil cooperates with many countries in continental shelf mapping, supporting the build-up of the Namibia Navy, and strengthening ties with São Tomé and Príncipe, Equatorial Guinea, Cape Verde, Guinea-Bissau, Nigeria, Angola, and South Africa. The country also reiterates claims on its sovereignty through the international legal regime [36].

Complementary to the actions mentioned above, the NDS (2008) established for the internal stage the build-up capacity to answer any threat through a Naval power able to detect, identify, and neutralize actions that could harm the Brazilian interests in its jurisdictional waters. The Brazilian Navy should also be capable of keeping adequate operational readiness.

For detection and control the country seeks to develop a new satellite and radar-based surveillance system (SisGAAz). The system will integrate different technologies and platforms, such as software-defined radios, satellite communications, long-range radar, and a submarine acoustic sensing system. In addition, Brazil recently started to operate two satellites (Synthetic Aperture Radar - SAR) that will increase the awareness level in the South Atlantic.

Following the NDS (2008) directives, the Brazilian Navy has been acquiring new warships, such as the new carrier Atlântico and the construction of four multi-mission frigates, combined with the international cooperation for developing four conventional submarines (Scorpène) and one nuclear-powered attack submarine [34].

According to the NDS (2008), these actions aim to provide the Brazilian Navy with the

capability to control maritime areas and for dissuasive purposes.

The defense of such vast jurisdictional waters poses a challenging defensive scenario.

Protecting Brazilian strategic infrastructure in this area during crises requires the activation of exclusion zones along with the associated military apparatus to control them.

At this point, the Falklands war brings a crucial lesson. The use of modern missiles almost changed the war's end in favor of the Argentinians. Since that conflict, the warship's defensive systems have evolved, effectively increasing the ability to react against the anti-ship missile threat. Therefore, this scenario requires the deployment of weapons with specific characteristics such as reduced radar detection and high-speed profile[38].

The Brazilian Navy operates short and middle-range subsonic missiles, but for better accomplishment of the mission defined in the Brazilian National Strategy of Defense, an additional effort to provide the Brazilian Navy with a long-range supersonic missile is crucial [39].

3.1.1.2 Mission statement

Missiles are self-propelled guided weapons classified as tactical or strategic. Tactical missiles generally carry conventional warheads, have a relatively short range and low cost, and are used at relatively high frequency.

On the other hand, strategic missiles carry a nuclear warhead, reach targets at long distances, and are costly. This weapon is rarely used [24]. In this study, the focus is on the conceptual development of tactical missiles.

Researchers believe that the advanced features of air-defense and anti-missile weapon systems make the penetration probability of a single anti-ship missile significantly reduced[40].

Missile defence systems effectiveness depends upon specific factors such as detection probability, anti-ship cruise missile (ASCM) maneuverability, multiple-layered defence, multi-platform defence scenarios, multiple defensive missiles engagement etc [41].

The ASCM survivability technics, on the other hand, must consider the long exposure time to threat defenses, their long flight duration, and heavily defended targets. Enhancements could increase the chances of success. Improvements include low detectability, high altitude navigation, high speed, and maneuverability.

It is worth mentioning that any change in route or low altitude flight brings as disadvantage a loss in range, which requires a tradeoff analysis of enhanced survivability versus the loss in range [24].

In this study, we will analyse the characteristics of the cornerstone scenario which leads to an infinity of attack and defense tactics in the anti-ship warfare. This fundamental scenario

consists of a single ship firing multiple interceptors against a single non-maneuvering missile threat which is helpful to understand the core principles.

For the defined conditions presented, the anti-ship missile defense (ASMD) ability to engage and destroy an ASCM is considered the measure of effectiveness of the ASMD.

The measure of lethality effectiveness could be expressed as $p = p_d p_{k/d}$, where p is kill probability, p_d is detection probability of ASMD and $p_{k/d}$ is kill probability of ASMD after detection [41]. Notice that $p_{k/d}$ is intrinsic to the interceptor and p_d is the result of interceptor and threat characteristics combined.

After the definition of the effectiveness of an interceptor against a threat the next step is the determination of the number of interceptors to be fired to achieve the desired level of kill probability.

The total amount of interceptors that can be fired depends upon available engagement duration and the time between two successive interceptor launches. The engagement time is calculated considering maximum and minimum effective firing range, **ASCM Velocity** (V_{ASCM}) and **target detection range** as shown in the equation below [41].

$$T_D = \frac{r_{LI} - r_{min}}{V_{ASCM}} \quad (3.1)$$

In the engagement time equation, r_{LI} represents the initial interceptor launch range and r_{min} denotes the denial range, i.e. the range beyond which the Anti-Ship Cruise Missile (ASCM) would not be permitted to cross.

Logically, shorter engagement time entail less time available for further firings, considering a shot-look-shot (S-L-S) firing policy.

Considering a shot-shot firing policy where n interceptors are fired against a threat without assessing outcome, it is supposed that each interceptor is statistically independent with identical kill probability p_k . For this reason, the lethality of ASMD (p_l) can be defined as [41]:

$$p_l = p_d (1 - (1 - p_k)^n) \quad (3.2)$$

Regarding this expression, it is possible to infer that ASMD depends on **detection probability** - p_d , kill probability of an interceptor - p_k and number of interceptors fired - n . Once more, the number of interceptors - n - that can be fired depends upon the available engagement time.

Considerations presented in this subsection demonstrate the relevance of speed and detectability to raise the ASCM probability of success. To that extent, the maximum radar detection range - R_{max} depends upon radar characteristics, target characteristics and environment factors. R_{max} can be determined using radar equation [41]:

$$R_{max} = \alpha \left(\frac{\sigma}{SNR} \right)^{\frac{1}{4}} \quad (3.3)$$

In the previous equation, SNR is signal to noise ratio and σ is radar cross section. This equation demonstrates that R_{max} measure is directly proportional to the radar cross-section.

Using the physical optics method - PO and assuming that the body of an ASCM is similar to a circular cylinder, the total Radar Cross Section - RCS results from the vectorial summing of contributions in the following equation [42].

$$\sigma_{\theta_n} = \frac{2\pi H^2 r}{\lambda} \quad (3.4)$$

In this equation, H is the height of the cylinder, r is the radius, Θ_n is the aspect angle (degrees) and λ the wavelength.

Based on a typical engagement situation where the threat is viewed in zero degree aspect angle it is possible to consider the height of the missile and fins area negligible in the previous equation, remaining the radius as the main factor building the radar cross-section. Therefore, r is directly linked to the maximum radar detection range.

All in all, if the objective is to enhance the probability of success in an anti-ship missile attack, then it seems to be mandatory to undergo efforts to maximize the velocity and minimize the Radar Cross-Section of the ASCM in the conceptual project's phase.

A lower RCS is obtained by reducing the missile diameter and wings thickness, adding a faceted seeker dome, body chines, or graphite composite structure that absorbs radar energy[24].

All these aspects concerning the operational conception will play an essential role in the requirement specification phase.

3.1.1.3 Preliminary Technical Requirements Specification

In a broad sense, a Technical Requirements Specification is a means to define the type of system designing and its implementation. It lists the system's attributes as it conforms to a specific metric and mirrors the stakeholder's expectations on what the system is supposed to provide.

The ECSS' Standard states that project planning requirements apply to all project actors, from the top-level customer down to the lowest level supplier. The ECSS' Standard asserts the overall scope made applicable reduces, down through the customer-supplier chain.

We also highlight that it is not objective of this study to outline the functioning of guidance technology employed in cruise missiles.

Regarding general requirements, the following parameters define the missile design

scope.

- A two-stage configuration that uses solid fuel booster in the first stage and a ramjet motor in the second stage is acceptable.

- The system should allow ship launching.

- Priorities include lower drag in supersonic flight, increased range seeker, higher signal-to-noise, and adequate radar cross-section. For this reason, the missile diameter trade-off should be searching within the fineness ratio (l/d =length-to-diameter ratio) presented next[24]:

$5 < l/d < 25$, where l is the length and d is the diameter of the missile.

- The requisite kinetic energy for an anti-ship missile at the impact point is subject to variability, contingent upon multiple factors such as the target ship's dimensions, armor, and structural composition, alongside the missile's design and intended functionality. In the context of this study, we adopt the maximum speed of the AGM-84D Harpoon missile as an acceptable parameter, recognizing the need for further refinement in subsequent project phases. Consequently, the speed at the impact point should surpass Mach 0.85, indicative of a requisite penetration effect.

- In comparison with missiles of the same category, the operational parameters must remain within the following limits:

1. Range - from 80 km to 300 km;
2. Speed - from Mach 2.0 to Mach 3.0;
3. Launch weight - less than 3,000 kg;
4. Cruise altitude - from 10,000 m to 14,000 m;
5. Length - less than 9 m;
6. Diameter - less than 600 mm; and
7. Warhead - from 100 Kg to 300 Kg.

Based on the ECSS' Standard recommendations and the author's expertise, a list of detailed technical requirements is accessible in Appendix B of this study, implying any claim to completeness.

3.1.1.4 Programmatic aspects supported by the market and economic studies

Regarding the market and economic aspects, the analysis considers the following findings.

Firstly, it is worth mentioning that the development cycle of paraffin-based propulsive systems is presumably faster and of lower cost when compared to liquid fuel-based engines. Solid fuel ramjet is less complex while it does not incorporate pumps, moving parts, injectors, and pressurized tanks. Notwithstanding, both types of machines present similar performance.

For the same reasons, a solid fuel ramjet's development and operational cost should be lower than the liquid fuel technology.

The project's operational and logistic simplicity and low-cost characteristics are relevant features for insertion in the Brazilian defense market.

The defense market is monopsony in general, and budget restrictions in Brazil have impacted military procurements [43]. However, due to the National Defense Strategy (NDS), the Brazilian defense companies benefit from the military effort to keep strategic weaponry production as independent as possible from international suppliers.

To implement this objective, incentives are available for the national defense companies, such as a special tributary regime, submission of commercial considerations to the strategic imperatives, and priority to developing independent technological capacities [34].

The Brazilian defense companies' master's the technology of development and manufacture of rocket engines with solid propulsion, such as sounding rockets, and also dominate the know-how for long-range subsonic missile propelled by an aeronautical turbine.

In addition, the country counts on a rising capability in the space sector based in industrial and academic effort to develop orbital rockets.

This scenario leads to the existing opportunity to develop the tactical solid-fuel ramjet missile in the national industry. Such a project fits the demand for enhancement in the operational capability to execute the mission of protecting the Brazilian infrastructure close to the coastal line.

3.1.1.5 Preliminary risk assessment

According to ECSS-M-ST-10C Rev. 1, the initial assessments of a project's technical and programmatic risks are carried out by the customer, based on the project initiator's inputs concerning the project's objectives, together with the identified technical and programmatic constraints applied to the project. Comprehensive risk assessments occur at each significant project review. The risk management process requires information exchange among all project domains, and provides visibility over risks, with a ranking according to their criticality for the project; these risks are monitored and controlled according to the rules defined for the domains to which they belong [44].

In this study, we follow the risk management process described in the ECSS-M-ST-80C, which is one of the series of ECSS standards [45].

In a broad sense, the risk management process assesses undesirable events for their severity and likelihood of occurrence. The assessments of the alternatives for mitigating the risks are iterated, and the resulting measurements of performance and risk trends result in optimization of the tradable resources.

The proposed method comprise a iterative four-step risk management process of a project, detailed in the ECSS-M-ST-80C, which is illustrated in Figure 3.2.

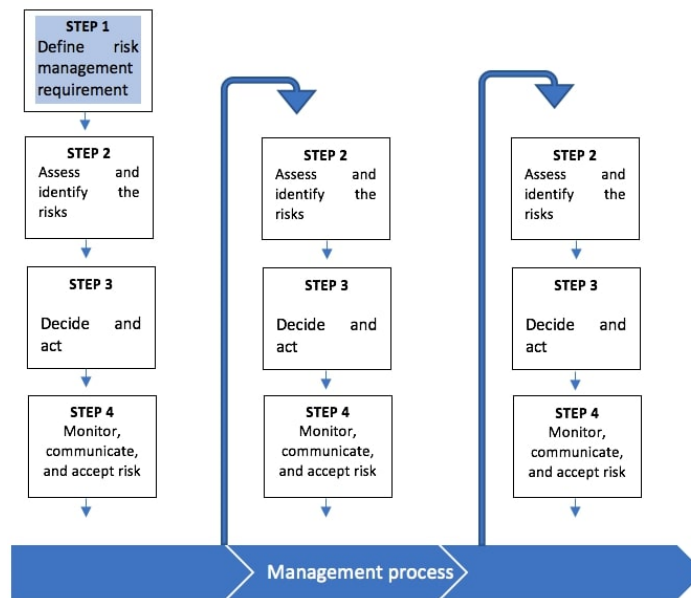


Fig. 3.2: The steps and cycles in the risk management process

Step 1 comprises establishing the risk management policy (Task 1) and risk management plan (Task 2). These tasks occur at the beginning of a project. For that reason, the contribution of this study on project risks is limited to steps 1 and 2. Besides, the last steps 3 and 4 demand the participation of other stakeholders not present at this time [1].

Step 2 identifies each risk scenario to determine then, based on the outputs from Step 1, the magnitude of the individual risks and, finally, rank them. This step comprises tasks 3 and 4, risk scenarios identification and risk assessment, respectively.

Step 1: Risk management implementation

The starting point for risk management shall be the formulation of the risk management policy at the beginning of the project.

The Risk Management Policy (Task 1) includes the following activities [1]:

- Identification of the set of resources with impact on risks.
- Identification of the project goals and resource constraints. For this study, the project goal is to develop the conceptual design of a supersonic tactical missile propelled by a solid-fuel-based ramjet engine.
- Description of the project strategy for dealing with risks, such as the definition of margins and the apportionment of risk between customer and supplier. This description is pro-

vided in figure 3.3.

E	LOW	MEDIUM	HIGH	VERY HIGH	VERY HIGH
D	LOW	LOW	MEDIUM	HIGH	VERY HIGH
C	VERY LOW	LOW	LOW	MEDIUM	HIGH
B	VERY LOW	VERY LOW	LOW	LOW	MEDIUM
A	VERY LOW	VERY LOW	VERY LOW	VERY LOW	LOW
	1	2	3	4	5

Fig. 3.3: Risk magnitude designations and proposed actions

- Definition of scheme for ranking the risk goals according to the requirements of the project [1]. This definition is provided in Figure 11 (See Appendix C).

- Definition of scoring scheme for the severity of consequences for the relevant resources. This scoring scheme is defined in table 3.1.

Table 3.1: Example of a severity-of-consequence scoring scheme [1]

Score	Severity	Severity of consequence: impact on (for example) cost
5	Catastrophic	Leads to termination of the project
4	Critical	Project cost increase > 11-15 %
3	Major	Project cost increase > 6-10 %
2	Significant	Project cost increase > 1-5 %
1	Negligible	Minimal or no impact

- Definition of a risk index scheme to denote the magnitudes of the risks of the various risk scenarios [1]. The index scheme for this project is available in Figure 3.3.

- Table 3.2 exemplify the scoring scheme for the likelihood of occurrence for the relevant resources.

Table 3.2: Example of a likelihood score scheme [1]

Score	Likelihood	Likelihood of occurrence
E	Maximum	Certain to occur, will occur one or more times per project
D	High	Will occur frequently, about 1 in 10 projects
C	Medium	Will occur sometimes, about 1 in 100 projects
B	Low	Will seldom occur, about 1 in 1000 projects
A	Minimum	Will almost never occur, 1 of 10 000 or more projects

A complete risk management process comprising technical, external, organizational, management, and cost risk categories is available in Appendix C.

3.1.2 Phase A

3.1.2.1 System and Operations Concepts

In accordance with a work released in 2012, we have curated a comprehensive yet not exhaustive list of concepts. This list encompasses key aspects demanding specific attention from project designers. Subsequently, these concepts serve as guiding principles for the computational trajectory program, as elucidated in a subsequent chapter of this research~[24].

- As asserted by the author, for a long circular cylinder (e.g., $l/d=10$) at $\alpha = 90^\circ$, the drag coefficient varies from approximately 1.2 to 1.5 times l/d , depending on the Mach number. The cross-flow drag coefficient is greatest ($C_{D\alpha = 90^\circ}$) for transonic Mach number ($0.8 < M < 1.2$). For subsonic ($M < 0.8$) and supersonic Mach number ($M > 1.2$) an average value of ($C_{N\alpha = 90^\circ} = 1.3 l/d$) is usually of sufficient accuracy for conceptual design.

- The normal force prediction is based on combining slender body theory [46] and body cross flow theory [47].

- Wing, tail, and canard surfaces may be characterized by their location relative to the center-of-gravity, cg.

- Weight and balance conditions must provide a safe flight pattern from launch to maximum range, considering the constant moving or shifting weight.

- Tail surfaces size should comprise just the necessary area to provide a stable flight. Special attention is required to infer the possible wing downwash effect on the tail.

- For flight conditions with a laminar boundary layer over much of the body (e.g. $M < 0.2$ or $H > 80,000$ ft), the body boundary layer thickness at the tails may blanket a significant portion of the tails, reducing its effectiveness.

- If the nozzle exit area is nearly as large as the missile base area, the base drag may be negligible during the powered flight.

- For supersonic missiles the drag due to the shock wave on the nose may be comparable to or even larger than skin friction drag and base drag. The body wave drag is driven by nose fineness and Mach number and it decreases with the increasing nose fineness ratio.

- For aspect ratio $A > 2$, increasing wing sweep significantly decreases the normal force.

- Aerodynamic surfaces are more effective at subsonic Mach number if they are high aspect ratio.

- Doubling the aspect ratio (A) doubles the normal force at a subsonic Mach number.

- The advantage of low aspect ratio is there is less change in the aerodynamics with Mach

number.

- The body normal force coefficient is a function of angle of attack, fineness ratio, and cross section geometry.

- The normal force prediction is likely to be optimistic for very low Mach number (*e.g.*, $M > 2$) and for very high altitude (*e.g.*, $h > 80,000$). For these conditions, boundary layer transition from laminar to turbulent is delayed, resulting in a thicker boundary layer.

- For an aspect ratio more prominent than 2 ($A > 2$), increasing wing sweep significantly decreases normal force.

- The rocket baseline missile wing is limited to a maximum local angle of attack of $\alpha_w = 22$ deg, because of stall of the wing. For a typical cg location, this results in an angle of attack of the body and tail of $\alpha = 9,4$ deg for a maximum wing control deflection of $\delta = 12,6$ deg.

- Due to the considerable advantages in weight reduction, manufacturing flexibility, and reduced cost, at least 10% of the airframe components or missile subsystems should incorporate high-temperature organic composites such as aromatic polyimides, and related polymers.

- For RCS analysis, consider a typical threat fire control radar having the following characteristics:

a. transmitted power of 50.000 W;

b. lookup angle of 20 deg;

c. X-band;

d. mono-static radar; and

e. circular polarization.

- Enhancements in the missile's RCS characteristics should consider:

a. priority in reducing the frontal aspect;

b. swept wing and tail leading edge; and

c. avoid large flat surfaces facing the threat radar.

3.1.2.2 Critical technologies

First, to avoid misunderstandings, we assert that the criticality of a specific technology does not keep any relation to the idea of national security, regional stability, chemical, and biological weapons proliferation, nuclear nonproliferation, or missile technology control regime.

For research's sake, critical technologies refer to the scientific and technological know-

how needed to enable a ramjet project. This assessment is an important cost and schedule driver when dimensioning the required resources and risk analysis.

The assessment presented should be refined by the customer and suppliers to investigate the availability of know-how and components needed to implement the project and explore alternatives to overcome constraints.

For this reason, the following technologies can be used or not in the project depending on the requirements regarding the mission performance:

1. External duct - To modulate thrust of solid fuel ramjets. This technology improves lift in the final stage of the attack, maximizing the kill probability against aircraft maneuvers. It is adequate just for surface-to-air and air-to-air missiles.[48]
2. Intake design - To meet the best performance over the required Mach and Reynolds number ranges while overcoming constraints imposed by the missile, and its mission. [49]
3. Ceramic Matrix Composites - Lightweight and high-temperature resistant materials to withstand the operation loads.
4. Diffusion-controlled combustion process - This system is responsible for releasing energy to the combustor, providing combustion stability.
5. Numerical modeling of swirling flow - Required for investigations on the impact of swirling flow on solid-fuel ramjet.
6. Fuel geometry - Direct impact on flammability and performance improvement.
7. High-speed aerodynamics analysis. The complex effects of High-speed external and internal flow acting on a missile frame demand Computational fluid dynamics (CFD) for evaluations. [50]
8. Air induction system technology - This device requires perfect integration to the airframe, analysis of geometry granting subsonic flow internally, and development of unique materials. [50]
9. Combustor technology - Mainly regarding thermal insulation, heat transfer distribution, flame holding, and combustion ignition.[50]
10. Ramjet fuels - [50] Regarding the thermodynamic properties when burning inside the combustor chamber, regression rate, stability, use of additives to improve solid fuel characteristics, etc.
11. Propulsion/airframe integration, materials, and thermal management - These sensitive areas demand efforts in CFD, thermal resistant alloys and structures, and cooling systems. [50]

12. Solid propellant booster technology - Imply a variety of solid propellant choices and grain configurations for evaluation and definition, and the use of aerodynamics prediction code for axisymmetric configuration analysis. [50]
13. Fixed and variable geometry nozzle technology - Necessary for achieving optimum thrust efficiency. [50]
14. Thermochemical modeling and simulation development - Relevant to predicting the transition from subsonic to supersonic combustion, downstream mixing and combustion at lower Mach number, pre-combustion shock train, and the level of turbulent mixing.[50]
15. Processing capability - Application of processors providing near to real-time trajectory optimization. [24]
16. Ground-test methodologies - This infrastructure is required to validate performance predictions, and operability prior to flight testing.

The test apparatus should comprise distinct facilities such as but not limited to a direct-connect combustor test, complete engine test facilities (free jet and semi-free jet test), high-temperature tunnel, etc.

The ground test techniques and data analysis procedures will be useful for the adjustments of technical decisions, evaluation of service life and reliability, Validation of mathematical models, and revision of technical decisions [50].

In a broad sense, it is believed that the Brazilian Industrial Base has the necessary knowledge and expertise to develop all the systems and subsystems of the proposed missiles. For instance, the guidance and control subsystem of MAA-1 (Piranha) missile was developed by national institutions. The successful operation of the missile implies the system reached technology readiness level 9 (TRL) and, therefore, all of its subsystems.

On the other hand, Avibras company has produced surface-to-surface medium-range missiles, for the national and international markets, for more than 30 years. Therefore, the company has a family of missiles with TRL = 9, and as such, the propulsion (solid fuel booster) and different warheads.

Regarding solid-fueled ramjet, the Chemical Propulsion Laboratory (University of Brasilia) successfully fired such engines with different combinations of fuel composition (PE and paraffin). Therefore, the propulsion system is in TRL = 6, with a low risk for development. The biggest challenge in the ramjet engine operation is integrating the engine with the intake diffuser. Risks associated with developing long-range missiles based on solid-fueled ramjet technology are of low concern, given the ample expertise available in both the Brazilian academic sector and the industry, encompassing each missile subsystem.

Chapter 4

Physical and computational models

4.1 Physical model

This section presents the physical model regarding the auxiliary numeric code proposed to support analysis at the preliminary project phase.

4.1.1 Flight dynamic

Considering the ECSS recommendations, we assumed that the Brazilian Navy is the primary client for the proposed project. Therefore, dealing with the operational scenario previously detailed in this work, it is expected that the Brazilian Navy requires a missile capable of flying at long distances, at high speed, carrying a heavy warhead to discouraging the action of threatening vessels.

Addressing these assumptions, the flight dynamic equations and parameters will make it possible to understand and predict the forces acting on a missile and their influences on the trajectory, contributing to reach the project design requirements.

For the operational concepts and system architecture, we will follow the aerodynamic, propulsion, and trajectory set of equations proposed by Fleeman (2012).

4.1.2 External ballistics

This subsection presents the physical models applied to the project design. Figure 4.1 illustrates the forces acting with the missile trajectory.

In the following figure, α is the angle of attack, γ represents the flight path angle, and ϕ is the thrust angle concerning the missile axis.

The flight performance relies on force balance applied to the object, including thrust, drag, lift, and weight, representing a two-degree of freedom system.

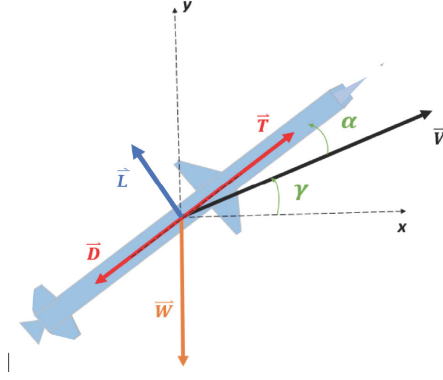


Fig. 4.1: Forces acting on flight.

System architecture and operational concepts follow the propulsion, aerodynamic, and trajectory equations proposed in the literature [24]. We assume that flight trajectory changes with the help of control surfaces, maintaining phi equal to zero and alpha values reaching as high as 40 degrees (Lesieutre et al., 1987). The gamma angle, hence, alters accordingly.

The equations of motion in the Frenet-Serret orthogonal plane are given by

$$m(t) \frac{dv}{dt} = -w \sin(\gamma) - D \cos(\alpha) - L \sin(\alpha) + T \cos(\alpha + \phi) \quad (4.1)$$

$$m(t) V \frac{d\gamma}{dt} = -w \cos(\gamma) - D \sin(\alpha) - L \cos(\alpha) + T \sin(\alpha + \phi) + m(t) V K \quad (4.2)$$

The computational code developed in this study for trajectory estimation relies on a two-degree-of-freedom system, enabling rapid adjustments in pitch angle by assigning suitable values to the constant K in the equation (4.2).

The following equation expresses the variation in time of mass due to propellant consumption (booster and ramjet) and booster separation.

$$\frac{dm_p}{dt} = \frac{dm_{pb}}{dt} + \frac{dm_{pr}}{dt} \quad (4.3)$$

Equation (4.4) provides the rocket booster mass flow rate in kilograms per second, wherein $m_{p,bi}$ represents the initial booster's propellant mass, and δt_{bb} stands for the total burning time of the booster's propellant.

$$dm dt_{bi} = \frac{m_{p,bi}}{\delta t_{bb}} \quad (4.4)$$

Equation (4.5) provides the ramjet mass flow rate in kilograms per second, wherein $m_{p,ri}$ represents the initial booster's propellant mass, and δt_{br} denotes the total burning time of the

ramjet propellant.

$$dm_{dr} = \frac{m_{p,ri}}{\delta t_{br}} \quad (4.5)$$

The total missile mass at any specific time is defined by the equation:

$$m(t) = m_{db} + m_{dr} + m_{pb} + m_{pr} \quad (4.6)$$

Eq. 4.6 delineates the dry masses of both the booster (m_{db}) and the ramjet (m_{dr}), as well as the propellant masses of the booster (m_{pb}) and the ramjet (m_{pr}). The booster stage separates from the missile at the booster's propellant burnout time, denoted as $t_{f,b}$.

The missile range and altitude prediction are given, respectively, by:

$$\frac{dh}{dt} = V \cdot \sin(\gamma) \quad (4.7)$$

$$\frac{dx}{dt} = V \cdot \cos(\gamma) \quad (4.8)$$

In the equations of motion, weight, drag and lift are obtained respectively by:

$$W = m(t) \cdot G \quad (4.9)$$

$$D = m(t) \cdot \frac{1}{2} \cdot cd(\alpha) \cdot A_{ref} \cdot \gamma_{air} \cdot P_h \cdot M^2 \quad (4.10)$$

$$L = m(t) \cdot \frac{1}{2} \cdot cn(\alpha) \cdot A_{ref} \cdot \gamma_{air} \cdot P_h \cdot M^2 \quad (4.11)$$

In the previous equations, $cd(\alpha)$ and $cn(\alpha)$ are the drag and lift coefficients, respectively, A_{ref} is the missile reference area, γ_{air} and P_h are the air's specific heat ratio and static pressure, respectively, and M is the missile Mach number.

$$h = \left(h_0 + \int_0^{time} \frac{dh}{dt} dt \right) \quad (4.12)$$

The preceding integral predicts the missile altitude at any point along the trajectory, with h_0 representing the altitude of the launch site.

$$m_{p,b} = c_3 \cdot \left(m_{p,bi} - \int_0^{time} \frac{dm}{dt} dt \right) \quad (4.13)$$

The previous equation forecasts the rocket booster's fuel consumption, with the initial

value of c_3 set to 1 and transitioning to zero after the propellant burnout time.

$$m_{p,r} = c_4 \cdot \left(m_{p,ri} - \int_0^{time} \frac{dm}{dt} dt \right) \quad (4.14)$$

The earlier equation forecasts the ramjet's fuel consumption, initially setting the value of c_4 to 1, which subsequently transitions to zero after the propellant burnout time.

$$x = x_0 + \int_0^{time} \frac{dx}{dt} dt \quad (4.15)$$

This integral predicts the distance covered at any point in the trajectory, where x_0 is zero at the launch site.

Short maneuvers can be executed by assigning a value to the constant 'k' in Equation(4.2). Drag and lift calculations are performed for the missile body, wings, and tail. The integrated external ballistic code provides values for each stage of the missile trajectory. The Engineering Equation Solver employs an equation-based integral function directive to solve this set of equations.

$$F(t) = F(0) + Integral(integrand; dFdt; LowerLimit; UpperLimit; StepSize) \quad (4.16)$$

4.1.3 Gravity and aerodynamic model

We have employed Newton's Law of Gravity, as expressed in Eqs. 4.17, for our gravity model [51]:

$$F = G \cdot \frac{m_1 \cdot m_2}{r^2} \quad (4.17)$$

In this equation, F is the gravitational force acting between two objects, G is the gravitational constant ($G = 6.672 \cdot 10^{-11} \cdot Nm^2/kg^2$), m_1 and m_2 denote the masses of the respective objects, and r denotes the distance between these objects.

The aerodynamic forces are presented in Eqs. 4.18, and 4.19.

$$L = c_n \cdot A_{ref} \cdot q \quad (4.18)$$

$$D = c_d \cdot A_{ref} \cdot q \quad (4.19)$$

Here, c_d is the drag coefficient, q is the dynamic pressure, and A_{ref} is a reference area of the vehicle.

Regarding the zero-lift coefficient of drag for the body, the value results from the addition of skin friction drag, base drag, and wave drag. Equations 4.20, 4.21, 4.22, 4.23, and 4.24 give it [24].

The Maximum value for the drag coefficient of a rocket baseline missile occurs at Mach 1, and, at supersonic regime, the shock wave on the nose may be equal or even higher than skin friction [24].

The equation for the body wave drag coefficient is given by [52]:

$$C_{d,body\ wave} = (1.586 + \frac{1.834}{M^2}) \cdot (\tan^{-1} \cdot (\frac{0.5}{\frac{l_n}{d}}))^{1.69} \quad (4.20)$$

For coasting flight at supersonic regime, the base drag can be approximately expressed by the following equation [24]:

$$C_{d,base\ coast} = \frac{0.25}{M} \quad (4.21)$$

where M is the Mach number. For subsonic regime the equation changes to:

$$C_{d,base\ coast} = 0.12 + 0.13 \cdot M^2 \quad (4.22)$$

During the powered flight, the base drag equations declines by the following factor F_d [24]:

$$F_d = (1 - \frac{A_r}{S_{Ref}}) \quad (4.23)$$

Here, A_r is the aspect ratio of the exposed planform. The base drag is negligible if the nozzle exit area has nearly the size of the missile base area.

The base drag can significantly contribute to body total drag in coasting flight due to the low pressure formed at the missile's base area, caused by flow separation [24].

Lastly, in the subsonic flight regime the major contributor to total body drag is friction, and it is consequence, primarily, of the fineness ratio design.

The equation for body skin friction drag coefficient is given by [24]:

$$C_{d,body\ friction} = 0.053 \cdot (\frac{l}{d}) \cdot (\frac{M}{q \cdot l})^{0.2} \quad (4.24)$$

Assumptions regarding the above equation are [24]:

a. the wetted body area of a non-circular lifting body is, approximately, the same as of an equivalent circular cross-section cylinder;

b. the free stream speed of sound and viscosity variation with altitude is small;

c. there is no boattail; and

d. the flow over the body has a turbulent boundary layer, which is least applicable for short-length missiles and at high altitudes.

For planar surfaces such as wings, canards, tails, at subsonic and supersonic Mach numbers, the main contributors to the surface total drag coefficient are the skin friction and wave drag, respectively [24].

The base drag for the planar surface in most supersonic missiles is negligible due to the sharp trailing edge and low flow separation [24].

The equation 4.25 gives the surface skin drag ($C_{DSurfacefriction}$) [24]:

$$C_{d, Surface\ friction} = n_{Surface} \cdot \left(0.0133 \cdot \left(\frac{M}{q \cdot c_{mac}} \right)^{0.2} \right) \cdot \left(2 \cdot \frac{S_{Surface}}{S_{Ref}} \right) \quad (4.25)$$

In this equation, $n_{Surface}$ is the number of surface planforms, and c_{mac} is the length of the mean aerodynamic chord.

For the drag wave ($C_{DSurfacewave}$) contribution, a modified Newtonian theory gives the equation based on the pressure across the normal shock as a function of Mach number [24].

$$C_{dSurface\ wave} = n_{Surface} \cdot \left(\frac{2}{\gamma_{air} \cdot M_{\Delta LE}^2} \right) \cdot \left(\frac{(\gamma_{air} + 1) \cdot M_{\Delta LE}^2}{2} \right)^{\frac{\gamma_{air}}{\gamma_{air} - 1}} \cdot \left(\left(\frac{\gamma_{air} + 1}{(2 \cdot \gamma_{air} \cdot M_{\Delta LE}^2) - (\gamma_{air} - 1)} \right)^{\frac{1}{(\gamma_{air} - 1)}} - 1 \right) \cdot \sin^2 \delta_{LE} \cdot \cos \Delta_{LE} \cdot t_{mac} \cdot \frac{b}{S_{ref}} \quad (4.26)$$

In this equation, variable Δ_{LE} signifies the leading-edge sweep angle, δ_{LE} is the leading-edge section total angle, t_{mac} denotes the maximum thickness of mean aerodynamic chord, 'b' represents the surface span length, and γ_{air} is the specific heat for air.

The normal force coefficient for a slender body is a function of angle of attack and body geometry, and it is not dependent on the Mach number and Reynolds number [24].

At low angle of attack, the slender body theory drives the results. When the angle of attack approximates to 90 degrees, the cross-flow theory is the main driver [24].

The equation 4.27 expresses the normal force coefficient (C_N) of the body [24].

$$|c_n| = \left(\left(\frac{a}{b} \right) \cdot \cos^2 \phi \right) + \left(\frac{a}{b} \cdot \sin^2 \phi \right) \cdot (|\sin(2 \cdot \alpha) \cdot \cos\left(\frac{\alpha}{2}\right)|) + 1.3 \cdot \left(\frac{l}{d} \right) \cdot \sin^2 \alpha \quad (4.27)$$

Where ϕ is the missile bank angle, α is the angle of attack, and 'a' and 'b' are the elliptical cross-section major and minor axis, respectively.

This equation is applicable for a body fineness ratio higher than 5 and is the result of combining the slender body theory [46] and the cross-flow theory [47].

For missile surfaces, the same methodology to predict the normal force coefficient on the wings is valid for tail and canard. Normal force is a function of Mach number, angle of attack, aspect ratio, and the surface planform area.

Slender wing theory provides excellent accuracy for low aspect ratio $A_r = 1$, Mach number lower than 0.5, and no wing sweep, but over-predicts the influence of aspect ratio when it goes around $A_r = 3$. At transonic flight regimes, the compressibility tends to compensate for this error [24].

The slender wing theory does not account for the influence of wing sweep and taper ratio. The normal force decreases with an increasing wing sweep for an aspect ratio higher than 2.

A high aspect ratio is more efficient for subsonic flight conditions; however, a low aspect ratio provides less aerodynamic changes with Mach number. At a high Mach number, the effect of the aspect ratio on normal force is negligible.

The decision criterion for selecting the better-fitted equation within the Mach number profile range is determined by the parameter expressed by [24]:

$$\left(1 + \left(\frac{8}{\pi \cdot A_r}\right)^2\right)^{0.5} \quad (4.28)$$

If the Mach number falls below this reference value, then the recommended choices are the slender wing theory combined with Newtonian impact theory equations. Conversely, if the Mach number exceeds this threshold, the suitable option is the linear wing theory in conjunction with Newtonian impact theory[24].

Within this criteria, the following equation gives the values of surface normal forces when the Mach number is under the parameter previous mentioned:

$$|c_{n, Surface}| = \left(\left(\pi \cdot \frac{A_r}{2}\right) \cdot |\sin\alpha \cdot \cos\alpha| + 2 \cdot \sin^2\alpha\right) \cdot \left(\frac{S_{Surface}}{S_{Ref}}\right) \quad (4.29)$$

In equation (4.29), A_r is the aspect ratio of exposed planform and $S_{Surface}$ represents the area of exposed planform.

When the Mach number is above the parameter, the linear wing theory plus Newtonian impact theory lead to the Eq.4.30:

$$|c_{n, Surface}| = \left(\frac{4 \cdot |\sin\alpha \cdot \cos\alpha|}{(M^2 - 1)^{0.5}} + 2 \cdot \sin^2\alpha\right) \cdot \left(\frac{S_{Surface}}{S_{Ref}}\right) \quad (4.30)$$

The normal force (N) and the parasite drag force (D) are identified as follow:

The equations 4.31, 4.32, and 4.33 present the body normal force (N_{body}), wing normal force (N_{wing}), and tail normal force (N_{tail}) [24]:

$$N_{body} = |c_{n,body}| \cdot S_{Ref} \cdot \frac{1}{2} \cdot \gamma \cdot P_h \cdot M^2 \quad (4.31)$$

$$N_{wing} = |c_{n,wing}| \cdot S_{Ref} \cdot \frac{1}{2} \cdot \gamma \cdot P_h \cdot M^2 \quad (4.32)$$

$$N_{tail} = |c_{n,tail}| \cdot S_{Ref} \cdot \frac{1}{2} \cdot \gamma \cdot P_h \cdot M^2 \quad (4.33)$$

In these equations, P_h is the static pressure at a given altitude.

The set of equations for the normal force considers the body cross-sectional reference area even for the surface area [10].

The equations 4.34, 4.35, and 4.36 give the parasite drag force on the body ($D_{p,body}$), wing ($D_{p,wing}$), and tail ($D_{p,tail}$) respectively [24]

$$D_{p,body} = |c_{d,body}| \cdot S_{Ref} \cdot \frac{1}{2} \cdot \gamma \cdot P_h \cdot M^2 \quad (4.34)$$

$$D_{p,wing} = |c_{d,wing}| \cdot S_{Ref} \cdot \frac{1}{2} \cdot \gamma \cdot P_h \cdot M^2 \quad (4.35)$$

$$D_{p,tail} = |c_{d,tail}| \cdot S_{Ref} \cdot \frac{1}{2} \cdot \gamma \cdot P_h \cdot M^2 \quad (4.36)$$

The governing equations 4.37, 4.38, and 4.39 give the body (L_{body}), wing (L_{wing}), and tail (L_{tail}) lift respectively [10]:

$$L_{body} = N_{body} \cdot \cos\alpha_{body} - D_{body} \sin\alpha_{body} \quad (4.37)$$

$$L_{wing} = N_{wing} \cdot \cos\alpha_{wing} - D_{wing} \sin\alpha_{wing} \quad (4.38)$$

$$L_{tail} = N_{tail} \cdot \cos\alpha_{tail} - D_{tail} \sin\alpha_{tail} \quad (4.39)$$

The governing equations 4.40, 4.41, and 4.42 express the body (D_{body}), wing (D_{wing}), and tail (D_{tail}) drag respectively:

$$D_{body} = N_{body} \cdot \sin\alpha_{body} - D_{p,body} \cdot \cos\alpha_{body} \quad (4.40)$$

$$D_{wing} = N_{wing} \cdot \sin\alpha_{wing} - D_{p,wing} \cdot \cos\alpha_{wing} \quad (4.41)$$

$$D_{tail} = N_{tail} \cdot \sin\alpha_{tail} - D_{p,tail} \cdot \cos\alpha_{tail} \quad (4.42)$$

The addition of these drags components expresses the missile's total drag.

The Eq.4.43 gives the vertical component of thrust that contribute to lift [10]:

$$F_{y,thrust} = T \cdot (\sin\alpha_{body}) \quad (4.43)$$

4.1.4 Atmosphere model

The aerodynamic forces are directly influenced by the atmosphere's density, temperature, and pressure, which vary with altitude. To determine these atmospheric characteristics, this study employs a mathematical model based on a set of established atmospheric equations [53]:

The Eqs. 4.44, 4.45 and 4.1.4 give the static pressure concerning the altitude. [54].

For altitudes higher than 25,000 m (upper stratosphere):

$$P_h = 2.488 \cdot \left(\frac{T + 273.1}{216.6} \right) \quad (4.44)$$

$$T = -131.21 + 0.00299 \cdot h \quad (4.45)$$

For altitudes between 11,000 m and 25,000 m (lower stratosphere):

$$P_h = 22.65 \cdot e^{(1.73 - 0.000157 \cdot h)}$$

$$T = -55.46 \quad (4.46)$$

For altitudes below 11,000 m (troposphere):

$$P_h = 101.29 \cdot \left(\frac{T + 273.1}{288.08} \right)^{5.256} \quad (4.47)$$

$$T = 15.04 - 0.00649 \cdot h \quad (4.48)$$

For all equations used in the atmospheric model, pressure P_h is in Kilopascal, the temperature T is in Celsius, and the altitude h in meters.

The Eq. 4.49 provides the dynamic pressure.

$$q = 1/2 \cdot \gamma_{air} \cdot P_h \cdot M^2 \quad (4.49)$$

4.1.5 Missile geometry

There are drivers toward large and small missile diameters. Lower drag (D) and small lateral dimensions are examples of drivers that require small diameter. On the other hand, seeker increased range, higher resolution, better tracking, higher signal-to-noise, warhead increased effectiveness, body structure bending increased, etc., are characteristics that impose a higher diameter [24].

The missile diameter trade-off should remain within the typical range for missile body fineness ratio (l/d =length-to-diameter ratio) of $5 < l/d < 25$. This scale reflects a variety of in-service missiles from subsonic to supersonic performances [24].

In a supersonic flight regime, drag is a relevant parameter impacting range. Therefore, the ideal missile's diameter remains from the middle to the upper part of the fineness ratio scale [24].

4.1.5.1 Nose fineness

There are several designs for missile noses. The final configuration is a matter of optimum compromise among aerodynamic, structural, guidance, and mission requirements.

One of the critical factors when designing the missile nose is drag which is generally the result of three components: drag directly related to the cross-sectional of the missile, skin-friction drag, wave drag as a result of the shock wave, and base drag as a result of bluntness and diameter of the base [55].

The general shape, fineness ratio, and bluntness ratio are the main factors influencing the pressure drag along the flight path. Below Mach 0.8, the pressure drag is almost zero for all shapes. The drag pressure increases significantly for the transonic region and beyond, where the nose shape plays an important role. In that situation, the minimum drag fineness will be a trade-off between increasing friction drag and decreasing wave drag.

By and large, high fineness ratio, such as $l_n/d = 5$ (nose length-to-diameter ratio) is ideal for low radar cross-section and low supersonic drag. In opposition, a low fineness

ratio as $l_n/d = 0.5$ is ideal for increasing the seeker characteristics, offering more space for subsystems. Supersonic drag is usually more sensitive to nose fineness ratio than nose geometry [24].

4.2 Internal ballistic

Considerations regarding missile propulsion addressed in this section emphasize the parameters, concepts, and equations related to solid propellant rockets and ramjet engines.

Considering an ideal gas behavior as a working fluid and solving the conservation of mass and energy equation is the way to find the engine's main characteristics. In the equations used for internal ballistics, the variable 'i' refers to the engine station, ranging from 1 to 5. The use of symbols like ρ , V , T , and h represent the properties at a specific section of the engine, while T_0 and P_0 denote stagnation properties. Letters such as h and e subscript to properties symbols express the condition at a given altitude and condition at nozzle exit section, respectively. The ramjet engine control volume depicted in Figure 4.2 presents the ramjet main stations and mass and energy transfer.

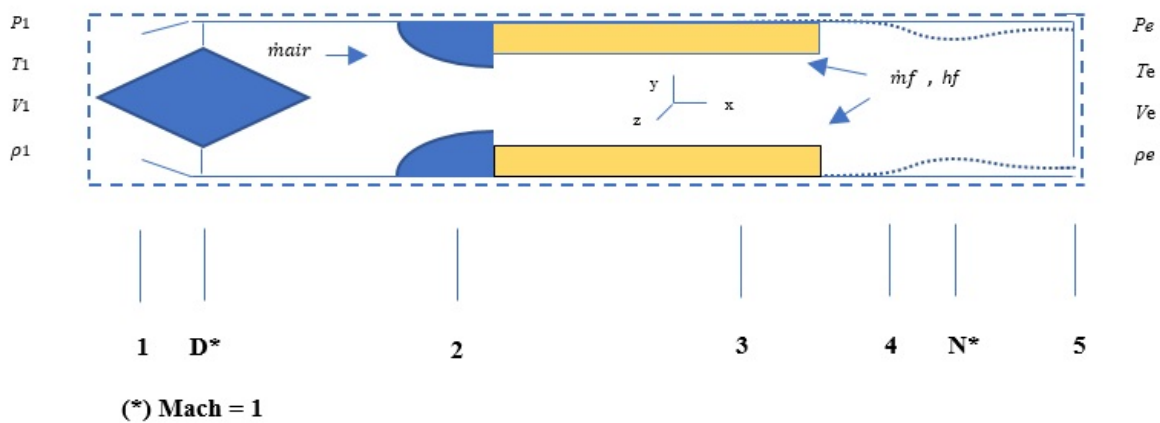


Fig. 4.2: Control volume

The following equations determine the engine main parameters:

$$\dot{m} = \rho_i V_i A_i \quad (4.50)$$

$$\sum q + \sum w = (h_{i+1} - h_i) + \frac{1}{2}(V_{i+1}^2 - V_i^2) \quad (4.51)$$

$$P_i = \rho_i R_{gas} T_i \quad (4.52)$$

The flow velocity interactions with local speed of sound provides the Mach number using the equation:

$$M_i = \frac{V_i}{\sqrt{V_i R_{gas} T_i}} \quad (4.53)$$

Mass balance in the region of diffuser and nozzle considering stagnation properties and area could be found using (Struchtrup, 2014):

$$\dot{m} = \rho_0 \sqrt{\frac{2\gamma R_u T_0}{\gamma - 1}} A_i \left[\frac{P_i^{\frac{1}{\gamma}}}{P_0} \sqrt{1 - \left(\frac{P_i}{P_0}\right)^{\frac{\gamma-1}{\gamma}}} \right] \quad (4.54)$$

The equation delimited by brackets represents the flow function $\psi = (P_0, P_i, \gamma)$. The ratio at each station pressure P_i limit the flow function to the maximum pressure (P_0), which occurs where the flow is choked (ψ^*) at the system critical section.

The following expression defines this condition:

$$\psi^* = \left(\frac{2}{\gamma + 1} \right)^{\frac{1}{\gamma-1}} \sqrt{\frac{\gamma - 1}{\gamma + 1}} \quad (4.55)$$

and the critical pressure:

$$\frac{P^*}{P_0} = \left(\frac{2}{\gamma + 1} \right)^{\frac{1}{\gamma-1}} \quad (4.56)$$

The condition of constant mass flow, as illustrated next, is used to comprehend converging and converging-diverging nozzle flows.

$$A\psi \cdot \left(\frac{p}{p_0} \right) = const \quad (4.57)$$

4.2.1 Diffuser

The calculation of exit ($i = 2$) condition and diffuser intake air critical (D^*) depends on the flight altitude and Mach number ($i=1$).

For station $i=1$, flight altitude, speed, and atmospheric conditions determine temperature and pressure.

For diffusers, the stagnation temperature T_{D0} is derived from the thermodynamic first law, specifically the adiabatic deceleration, while the corresponding stagnation pressure p_{D0} is determined by the isentropic relation [56].

$$T_{D0} = \frac{c_p \cdot T_{in} + \frac{1}{2} \cdot V_{D0}^2}{c_p} \quad (4.58)$$

$$p_{D0} = p_{in} \left(\frac{T_{D0}}{T_{in}} \right)^{\frac{\gamma_{air}}{\gamma_{air}-1}} \quad (4.59)$$

The stagnation temperature could be calculated assuming that flow velocity is zero at station=2, and there is no heat and work interaction through the diffuser's walls. The efficiency of the isentropic intake was configured to 90%, resulting in a stagnation pressure recovery of 72.8% at station 2.

The incoming flow at diffuser inlet is at temperature T_i , static pressure p_i , and Mach number M_i conditions. In these circumstances, the inlet density (ρ_i), and velocity (V_i) are:

$$\rho_i = \frac{p_i}{RT_i} \quad (4.60)$$

$$V_i = M_i \cdot a_i = M_i \cdot \sqrt{R\gamma_{air}T_i} \quad (4.61)$$

The following equation gives the mass flow:

$$\dot{m} = \rho_i \cdot V_i \cdot A_R \quad (4.62)$$

In the previous equation, A_R is the diffuser cross section.

For the diffuser at the critical state, the pressure (P_{D^*}), temperature (T_{D^*}), mass flow (ψ_d^*), and cross section (A_{D^*}) are given by, respectively:

$$P_{D^*} = P_2 \left(\frac{2}{\gamma_{air} + 1} \right)^{\frac{\gamma_{air}}{\gamma_{air}-1}} \quad (4.63)$$

$$T_{D^*} = T_2 \left(\frac{P_2}{P_{D^*}} \right)^{\frac{\gamma_{air}-1}{\gamma_{air}}} \quad (4.64)$$

$$\psi_d^* = \left(\frac{2}{\gamma_{air} + 1} \right)^{\frac{\gamma_{air}}{\gamma_{air}-1}} \cdot \left(\sqrt{\frac{\gamma_{air} - 1}{\gamma_{air} + 1}} \right) \quad (4.65)$$

$$A_{D^*} = \frac{\dot{m}}{\rho_{D^*} \cdot V_{D^*}} \quad (4.66)$$

$$\rho_{D^*} = \frac{P_{D^*}}{RT_{D^*}} \quad (4.67)$$

In the preceding equations, the constant R is equal to $0.287 \frac{kJ}{kgK}$, and the gas heat capacity ratio γ_{air} is 1.4.

Considering the ideal gas law, critical temperature and pressure are necessary to determine the critical specific volume.

The diffuser's exit area is dictated by the constant mass flow relation, $A\psi = const$, and is expressed by the following equation:

$$\psi_d = \psi_d^* \frac{A_{D^*}}{A_R} \quad (4.68)$$

4.2.2 Burner

The analysis of the combustion process takes into account an isobaric condition, with the exit gas temperature (T_3) constrained by material limitations. In the regime of solid fuel combustion, heat transfer is primarily convective, playing a crucial role in determining the combustor exit area (A_3). A flame-out condition may arise under circumstances involving a high mass flux coupled with an excess of oxidizer, resulting in a hard lean combustion. Alternatively, it can occur when the chemical reaction significantly outpaces the transport of reactants or products within the system, as indicated by a Damkohler number (Da) much smaller than 1 [57].

The overall equivalent ratio of the combustor is an outcome of the total heat provided by the combustor and the exit burner temperature. The definition of the fuel grain length relies on factors such as solid fuel mass flux, density, and the average regression rate. These parameters collectively influence the combustion dynamics, emphasizing the intricate interplay between heat transfer, chemical reactions, and material constraints within the combustor system.

$$\phi = \frac{(O/F)_{stoic}}{(O/F)_{act}} \quad (4.69)$$

$$(O/F)_{act} = \frac{\dot{m}_{air}}{\dot{m}_{fuel}} \quad (4.70)$$

$$\dot{m}_{fuel} = \dot{r} A_{fg} \rho_{fg} \quad (4.71)$$

The combustion heat transfer to the fuel grain and the mass transfer from the grain to the burning zone define the fuel regression rate. This process should be solved by numerical method. There are many models for liquefying (paraffin) and non-liquefying (polyethylene) fuels for hybrid propulsion, but the relation between mass flux of the oxidizer and the regression rate is the most known for practical application [17] as described in the following equation:

$$\dot{r} = \frac{dr}{dt} = a \cdot G_o^n \quad (4.72)$$

In this equation, the empirical constants $a > 0$ and $n > 0$, and $G_o = \frac{\dot{m}_{air}}{A_{port}}$ is the oxidizer mass flux average through the transverse section of the grain port (A_{port}). As the grain's port area increases during flight, the regression rate decreases.

The thermodynamic condition at station 3 defines the state at station 4 (nozzle) and the stagnation temperature at station 4 is a consequence of the conservation of energy. The same steps used to define the diffuser's geometry are adequate to obtain the thermodynamic condition at N^* and station 5.

The burner geometry is governed by the fuel-burning regime when using solid-fuel grain. During the flight, as the fuel burns, the engine's port area increases while the gas mass flux decreases keeping the gas speed constant. This is a condition for high engine performance.

Considering this engine operation system, integrating the \dot{r} function along the engine, the operation determines the final grain thickness and the engine.

Fuel and oxidizer compositions, flow structure, and the temperature of the hot air flow through the ramjet's diffuser strongly impact constants a and n [8].

Tests at UnB's laboratories with three types of solid fuel grains define a broad range of their regression rates for multiple flight regimes, by controlling the mass flow rates and heating levels. The fuels of interest in these tests were paraffin, high-density polyethylene (HDPE), and paraffin-polyethylene blends. The experiments demonstrate that for typical mass flux from 3 to 15 g/cm²/s, the regression rate of HDPE approximates to 0.05 mm/s, and for pure paraffin reaches 1.5 mm/s [58].

For polyethylene and air, stable flames could be held even in higher mass fluxes, such as 36 g/cm²/s. The simulations in the laboratory reveal that doping polyethylene in paraffin causes a relevant impact on the regression rate. Droplet size and the grain's mechanical integrity [11].

The test results also demonstrate that polyethylene positively enhances the paraffin grain characteristic, leading to higher accelerations compared to pure paraffin fuel.

The regression rate of blended fuels can efficiently be controlled by the fuel composition from 0.05 to 1.5 mm/s according to the missile flight profile. Flexibility in fuel grain design simplifies ramjet integration and overall flight vehicle optimization. For simplicity, when executing Project Phase-0, the solid fuel regression rate is kept constant over the burning time.

In 1986, a study provided values for constants $a = 0.031$ and $n = 0.37$, focusing on a propellant composed of air and 100% polyethylene [59]. Jumping to 2019, another research effort introduced the regression rate equation for a propellant made from air and 100% paraffin, revealing $a = 0.279$ and $n = 0.34$ [60]. In our innovative proposal, we recommend a new

material combination, specifically utilizing air along with a blend of paraffin and 30 to 50% polyethylene. This unique combination yields empirical constants (ballistic coefficients) $a = 0.069$ and $n = 0.34$. It is noteworthy that this blend exhibits a combustion rate slightly faster than pure polyethylene but significantly slower than pure paraffin [61].

4.2.3 Laval nozzle

A Laval nozzle is a specially designed nozzle that converts the thermal energy of a high-pressure gas into kinetic energy by accelerating the gas to supersonic velocities. The design of a Laval nozzle is based on the principle of conservation of energy and mass, and it involves creating a converging-diverging nozzle that gradually increases in cross-sectional area from its narrow throat to its exit.

The nozzle is named after Gustaf de Laval, who first developed the concept in the late 19th century. The design of the nozzle is based on the principle of supersonic flow and the Bernoulli equation, which relates the velocity, pressure, and density of a fluid flowing in a pipe.

The narrower cross-sectional area of this subsystem is called the nozzle throat, which increases the velocity of the gas flowing through it and is designed to achieve sonic velocity of the gas. The diverging section of the nozzle has an increasing area, which reduces the velocity of the gas and allows the pressure to equalize with the surrounding pressure at the nozzle exit. The internal gas pressure can be controlled by adjusting either the length of the nozzle or the exit area. [62].

Our focus will be on isentropic flows, and to facilitate analytical calculations, we limit our analysis to ideal gases characterized by constant specific heats.

The inlet state of the nozzle (station 4) is determined by the thermodynamic conditions at the burner exit (station 3). Through an energy balance, the stagnation temperature at station 4 is derived. Extending the same methodology employed in defining the diffuser's geometry, the remaining thermodynamic conditions at N^* and station 5 are established [56],

The ramjet post-combustion chamber and main nozzle dimensions incorporate a conical exit nozzle with a 22° half-angle and a contraction area ratio of two. A post-combustion section was included to enhance the residence time of flue gases for improved combustion efficiency, with a diameter-to-length ratio of two.

The primary equations pertaining to the Laval nozzle are described as follows:

1. Nozzle throat cross-sectional area (A_t).

$$A_t = \frac{\dot{m}_*}{P_0} \sqrt{\frac{RT_0}{\gamma}} \cdot \left(\frac{\gamma + 1}{2} \right)^{\frac{\gamma + 1}{2 \cdot \gamma - 2}} \quad (4.73)$$

In the preceding equation, R represents the gas constant, and γ denotes the gas specific heat.

2. Gas temperature at the nozzle throat (T_t).

$$T_t = T_c \left[\frac{1}{1 + \frac{\gamma_{air}-1}{2}} \right] \quad (4.74)$$

In the equation (4.74), the variable T_c represents the chamber temperature.

3. Gas pressure at the nozzle throat.

$$P_t = P_c \left[1 + \frac{\gamma_{air}-1}{2} \right]^{\frac{-\gamma_{air}}{\gamma_{air}-1}} \quad (4.75)$$

In the equation (4.75), the variable P_t denotes the the gas pressure at the nozzle throat, and P_c represents the gas pressure at the combustion chamber.

4. Mach number at the nozzle exit (M_e).

$$(M_e)^2 = \frac{2}{\gamma_{air}-1} \left[\left(\frac{P_c}{P_h} \right)^{\frac{\gamma_{air}-1}{\gamma_{air}}} - 1 \right] \quad (4.76)$$

5. Nozzle exit area.

$$A_e = \frac{A_t}{M_e} \left[\frac{1 + \frac{\gamma_{air}-1}{2} M_e^2}{\frac{\gamma_{air}+1}{2}} \right]^{\frac{\gamma_{air}+1}{2(\gamma_{air}-1)}} \quad (4.77)$$

6. Nozzle throat diameter (D_t).

$$D_t = \sqrt{\frac{4A_t}{\pi}} \quad (4.78)$$

7. Nozzle exit diameter (D_e).

$$D_e = \sqrt{\frac{4A_e}{\pi}} \quad (4.79)$$

Isentropic flow equation: This equation describes the change in pressure and density of a gas flowing through a Laval nozzle in an isentropic process.

$$\frac{P_2}{P_1} = \left(\frac{\rho_2}{\rho_1} \right)^{\gamma_{air}} \quad (4.80)$$

4.2.4 Thrust

Rocket engines carry their oxygen (oxidizer) and fuel and produce thrust by transmitting energy and momentum while accelerating the exhaust gases to supersonic velocities through a nozzle. In other words, thrust results from the distribution of tensions on the surfaces inside and outside the exhaust chamber.

For a stationary motor with one-dimensional steady flow, the equation 4.81 expresses the rocket thrust (F_t) prediction at the nozzle exit plane [63]:

$$F_t = \frac{(\dot{m}_{air} + \dot{m}_{fuel}) \cdot V_e - (\dot{m}_{air}) \cdot V_h + A_e \cdot (p_e - p_h)}{p_h \cdot A_1} \quad (4.81)$$

The condition where $P_e = P_h$ is known as optimum expansion and corresponds to the maximum thrust for combustion chamber given characteristics.

The thrust equation for ramjets contain three terms: gross thrust, ram drag, and a pressure correction.

$$F_t = \dot{m}_e \cdot V_e - \dot{m}_h \cdot V_h + (p_e - p_h) \cdot A_e \quad (4.82)$$

In the phase of steady-state level flight, commonly referred to as cruise, and at a low angle of attack, the lift (L) is roughly equivalent to the weight (W), while the thrust (F_t) is approximately balanced with the drag (D).

4.2.5 Specific impulse

The specific impulse is the thrust that an engine produces and how fast the fuel is burned to deliver that thrust. This parameter is helpful to compare the performance of rocket motors and is highly dependent on exhaust-product mass-flow, nozzle exit exhaust velocity and pressure, and nozzle exit area [63].

It allows the sizing of an engine during preliminary analysis.

The impulse (I) and the specific impulse (I_{sp}) is given by:

$$I_{sp} = \frac{F_t}{\dot{m} \cdot G}$$

or

$$I_{sp} = \frac{I}{m_{fuel} \cdot G} \quad (4.83)$$

The impulse I is expressed by the following equation:

$$I = F_t \cdot \delta t$$

As the propellant is a considerable part of the rocket's total weight, the higher is the specific impulse, the better is the engine.

4.3 Power and Efficiency

In the following equations we present isentropic efficiencies for nozzles, diffusers, and adiabatic combustion.

Nozzles:

Ignoring the inflow velocity, in the context of a nozzle expanding from pressures p_{ini} to p_e the outflow velocity (V_{out}) is given by:

$$V_{out} = \sqrt{2 \cdot (h_{ini} - h_e)} \quad (4.84)$$

Here, the variables p_{ini} and h_{ini} correspond to the pressure and enthalpy conditions at the initial section of the nozzle, where the expansion process starts.

The nozzle efficiency (η_N) is given by:

$$\eta_N = \frac{\frac{1}{2} \cdot V_{out}^2}{\frac{1}{2} \cdot V_{rev}^2} \quad (4.85)$$

In this equation, "rev" stands for reversible process.

Diffusers:

A reversible diffuser capable of achieving the end pressure p_2 from an irreversible diffuser has the ability to convert kinetic energy, represented as $\frac{1}{2}V_x^2 = h_x - h_x$, where $h_x = h(T_x)$. Here T_x is the temperature at the end of an isentropic compression occurring between the initial state (p_1, T_1) and the final state $((p_2, T_x))$. This conversion allows for the definition of isentropic diffuser efficiency, denoted as [56]:

$$\eta_D = \frac{h_x - h_1}{h_2 - h_1} \quad (4.86)$$

Combustion:

The combustion efficiency (η_b) could be expressed through the given equation [11]:

$$\eta_b = \frac{T_{04} - T_a}{T'_{04} - T_a} \quad (4.87)$$

In the given equation, T_{04} represents the stagnation temperature at the exit of the aft mixing chamber, T'_{04} is the adiabatic flame temperature, and T_a denotes the stagnation temperature of ambient air corresponding to Mach number M.

Propulsion efficiency:

The following equation provides the thermal propulsive efficiency (η_P):

$$\eta_P = \frac{\dot{W}_P}{\dot{Q}_B} \quad (4.88)$$

In the preceding equation, \dot{W}_P is the propulsive power, and \dot{Q}_B ($\dot{Q}_B = F_t \cdot V_1$) is the total heat supplied [56].

4.4 Miscellaneous equations

$$M = \frac{abs(V)}{SS} \quad (4.89)$$

This is the equation for the missile Mach number, where V is the missile velocity in kilometers per hour and SS is the speed of sound.

The speed of sound in an ideal gas (a_{ss}) is provided by:

$$a_{ss} = \sqrt{\gamma RT} \quad (4.90)$$

In the preceding equation, R represents the gas constant, T denotes the temperature, and the variable γ (specific heat ratio) is temperature-dependent [56].

$$S_{Ref} = 0.25 \cdot \pi \cdot d^2 \quad (4.91)$$

Equation (4.91) provides the missile's transverse body section area.

$$F_{drag} = -c_d \cdot q \cdot S_{Ref} \quad (4.92)$$

The previous equation provides the total drag force on the missile.

$$F_{grav} = -m_t \cdot G \cdot \sin(\gamma) \quad (4.93)$$

The preceding equation provides the component of gravitational force.

4.5 Algorithm

In completing this study, we present a design tool to solve the equations referring to the missile's aerodynamic and propulsive parts, allowing analysis of various mission profiles.

As a tool to support the development of the conceptual project optimization techniques for an operational reference missile, we present a code developed in the Engineering Equation Solver - EES software.

EES is an equation-solving program that can numerically solve thousands of coupled non-linear algebraic and differential equations. EES also incorporates a high accuracy thermodynamic and transport property database providing hundreds of substances, allowing it to work with the equation solving capability. The program enables simulations in the software and quickly determines the optimal design parameters maximizing the missile's trajectory performance [64].

Basically, to manage variables EES uses functions, that is a code segment that accepts inputs and returns a single result or procedures, which are similar to a function, but it can return one or more results[64].

The program combined slender body theory and body cross flow theory to precisely reflect flight conditions. For this purpose, conditional parameters trigger a shift from one approach to another, returning the best performance of each one.

The model allows for various input possibilities, such as rocket booster characteristics, desired maneuver levels, launch angle, cruise altitude, and final path speed, among others. The code generates important information for each defined profile, including range and payload. An additional advantage is that the code incorporates subroutines that provide precise data on static pressure and dynamic pressure up to an altitude of 70 km. Furthermore, the code also includes a wide range of thermodynamic constants that can be easily integrated and follows the international unit system for introducing variables.

The proposed code aims to simplify the analysis during the conceptual phase. As a result, it enables the introduction and testing of multiple variables to meet the demands of the development team. The primary code features are available in Appendix D, excluding the drag and lift equations library and the atmospheric model.

4.6 Cost assessment

For the assessment of development and fabrication costs, we adopted the TRANSCOST model, assuming that the calculations for space solid rocket motors provide a reasonable

estimate for missiles propelled by solid fuel [65].

The following parameters are necessary for cost definition:

- Cost of one Work-Year in Brazil - 102,000 USD.
- System engineering integration factor (f_0). This factor is related to the number of stages and is equal to 1.06 [65].
- Technical development status factor (f_1). Considering that Baseline 2 is the first generation development of the proposed missile, this factor is defined as 1.3.
- Technical quality factor (f_2). This factor is not applicable for solid rocket engine.
- Team experience factor (f_3).
- Cost reduction factor for series production (f_4). This factor varies from 0.25 to 1.0. Lower mass and high production rate reduce the factor value [65]. We assumed (f_4) as 0.5.
- Deviation from the optimum time schedule (f_6). This factor is assumed as 1.0.
- Cost growth for development by parallel contractors (f_7). This factor is assumed as 1.0.
- Correction for productivity (f_8). This factor varies from 0.7 to 1.4 [65]. The Brazilian industry has considerable experience in similar projects; therefore, we assumed (f_8) as 1.0.
- Engine fabrication cost (f_E).
- Stage fabrication cost (f_s).
- Engine development cost (H_E).
- Number of engines (N_e).
- Fabrication cost (C_{fab}).
- Booster mass.
- Ramjet engine mass.

Equation 4.94 presents the development cost for the solid rocket engine [65]:

$$H_{ES} = 16.3 \cdot m_{ES}^{0.54} \cdot f_1 \cdot f_3 \quad (4.94)$$

where H_{ES} is the solid booster cost and m is the mass of booster or ramjet engine.

Equation 4.95 shows the stage development cost formed on solid propellant rocket engines. [65]:

$$H_{SS} = 0.05 \cdot H_E \cdot N_e \quad (4.95)$$

Equation 4.96 gathers factors such as solid rocket and stage development cost to provide the total development cost.

$$C_{dev} = f_0 \left(\sum_{n=1}^{N_S} H_S + \sum_{n=1}^{N_e} H_E \right) \cdot f_6 \cdot f_7 \cdot f_8 \quad (4.96)$$

For engine fabrication cost assessment, equation 4.97 and 4.98 specifies the value of solid propellant rocket and stage respectively [65].

$$F_{ES} = 2.3 \cdot m_E^{0.399} \cdot f_4 \quad (4.97)$$

$$F_{SS} = 0.05 \cdot F_{ES} \quad (4.98)$$

Equation 4.99 gathers factors such as system engineering integration and production correction and provides the total fabrication cost.

$$C_{fab} = f_0^{N_S} \left(\sum_{n=1}^{N_S} F_S + \sum_{n=1}^{N_e} F_E \right) \cdot f_8 \quad (4.99)$$

4.7 Numerical solution and code validation

As a contribution to the advancement of missile development in Brazil, this study introduces a computational model that incorporates equations capable of simulating a two-degree-of-freedom system. The model encompasses the simulation of lift force, drag, thrust, and weight.

An engineering equation-solving program (EES) serves as a valuable computational resource, enabling the integration of numerous interconnected nonlinear algebraic, differential, and integral equations crucial for trajectory prediction. Additionally, this program facilitates unit conversion, ensures unit consistency, and incorporates extensive thermodynamic and transport property databases for a wide range of substances[64].

The EES also has a unique feature to enhance results using a built-in genetic algorithm [64]. This Characteristic could be relevant to optimize parameters such as missile range and speed.

The models in the present study account for eight effects regarding the missile trajectory in the atmosphere:

1. The mass variation due to propellant consumption;
2. The variation of thrust over time;
3. The aerodynamic drag, which is significant at lower altitudes;
4. The aerodynamic lift, which is significant for winged vehicles, generating important

forces to the flight path;

5. The dependence of aerodynamic forces (lift and drag) on supersonic and subsonic regimes;

6. The atmospheric mass density variation and its impact over aerodynamic forces;

7. The effect of discarded mass at a multi-stage missile;

8. The alpha angle (α) variation and consequences for lift and drag forces components;

9. The gamma angle (*gamma*) and its influence on the range, altitude, and velocity.

The auxiliary design tool detailed in this research is suitable for the conceptual and preliminary phases of the missile project. For that reason, some effects are not prioritized at this time, such as:

1. The variation of thrust due to throttling;

2. The thrust vectoring;

3. Non-uniform gravity;

4. The Coriolis force;

5. Wind speed across the flight path;

6. The centrifugal force;

7. The use of flare stabilizer to increase the static stability.

Regarding the equations used in this model, most of them are suggested by Fleeman, covering thrust, the body and surfaces drag prediction, the body and surfaces normal prediction, the influence of wing and tail geometry, and the center of gravity [24].

The model developed in this study employs a one-dimensional solution method to determine altitude, velocity, and range as functions of time. The trajectory profile consists of a vertical climb at the desired angle, during which a booster rocket accelerates the missile to the optimal altitude and velocity for activating the ramjet engine. Subsequently, the missile maintains propelled cruise at a specific altitude level before executing a final dive towards the objective at the desired velocity.

The Engineering Equation Solver (EES) utilizes functions within the main program and employs procedures that store essential database information in the library for solving equations. These procedures can store data related to dynamic and static pressure, for example, and provide this information to the main program during calculations.

To realistically represent the missile's flight profile, certain approximations are introduced for specific parts of the trajectory. When considering thrust performance curves, each rocket engine exhibits a distinct shape in the plot. The thrust generated by a rocket engine depends on the speed and volume of hot exhaust gas passing through the nozzle, which, in turn, is determined by the area of the flame front. Typically, there is an incremental rise in

thrust, occurring within a fraction of a second, before reaching the maximum thrust. This characteristic varies for each type of solid rocket propellant.

The governing equations regarding missile performance were then inserted in the Engineering Equation Solver (EES) platform, allowing the calculation of coupled non-linear algebraic and differential equations and the use of high accuracy thermodynamic and transport property library for many substances, facilitating the researcher’s work.

The adjunct equations related to the thermodynamic state of the gases are obtained from the NASA polynomials for ideal gases stored in the internal function library of the EES platform.

All drag and lift coefficient equations were programmed as external functions and procedures stored in the EES external library. The drag and lift coefficients’ value is obtained from call statements anywhere in the main code. We took the same approach for air density, static pressure, speed of sound, and temperature as a function of flying altitude. The atmospheric earth model infers thermodynamic properties with high accuracy up to 70,000 m altitude.

For code validation purposes, we use two different methods. First, the ramjet engine internal ballistics estimations are compared to a multi-platform tool designed for rocket engine analysis [66]. The latter process minimizes the Gibbs free energy for a broad range of operating conditions to obtain the equilibrium composition of the combustion products. Table 4.1 compares the results considering the combustion of paraffin wax (C₃₂H₆₆) with hot air. Deviations between the two methods remained below 2%. The chamber geometries are similar, with differences of less than 6.5%. Therefore, the internal ballistics code was deemed adequate for the preliminary design of solid fuel ramjet missiles.

Table 4.1: Engine performance comparison

Input/output	RPA	RAMJET	Diff.
Ambient pressure (bar)	0.2644	0.2644	
Chamber pressure (bar)	4.465	4.465	
Inlet air temperature (bar)	500.4	500.4	
O/F ratio (bar)	26.1/1	26.1/1	
Gross Thrust (kN)	11.89	11.71	+ 1.52%
Nozzle throat diameter (mm)	156.2	164.76	- 5.2%
Nozzle exit diameter (mm)	259.5	276.94	- 6.3%
Effective exhaust velocity (m/s)	1,400	1,379	+ 1.54 %

To validate the code for external ballistic calculations, we utilized the mission profile of the Aerobee 150A sounding rocket [67]. The Aerobee 150A is a four-fin sounding rocket with dimensions of approximately 9.0 meters in length and 38 cm in diameter. It consists of a solid rocket booster as the first stage and a liquid propellant rocket engine serving as the second stage or sustainer. Detailed information on this rocket can be found in the NASA Technical Report R-226 (NASA, 1966), supplemented by additional data available on specialized rocketry websites [68]. Table 4.2 outlines the specific features of the Aerobee 150A

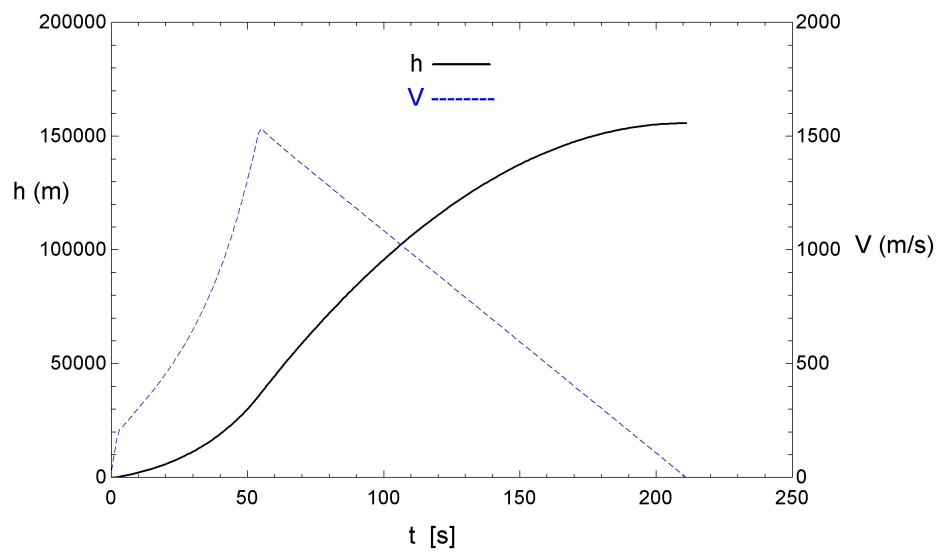
rocket [69].

Table 4.2: Aerobee 150A mass breakdown

Description	Mass [kg]	Note
2.5 KS-18,000 Booster		
Booster body	153 .31	with fins
Propellent	118.84	-
Total - Booster	272.15	-
Sustainer		
Nosecone	7 .71	-
Payload	136.07	Maximum
Nose Extension	6 .35	-
Tank Shroud	3 .0	-
Head end plumbing	1 .81	-
Tank assembly	74.15	-
Propellant	478.26	-
Aft Shroud	7.03 kg	-
Thrust chamber assembly	14.56	-
Misc. (fasteners, etc.)	5.62	-
Reserve Propellent	6.35	
Fins	12.70	Four fins
Total - Sustainer	753.63	-

The Aerobee project is designed to achieve a nominal peak altitude of approximately 163 km when carrying a payload weighing 136 kg. Utilizing the proposed code, the maximum predicted altitude for the Aerobee 150A rocket, fired at an elevation angle of 85 degrees, is 155.7 km, as illustrated in Figure 4.3. This demonstrates an error of less than 5% when compared to the nominal performance, thereby validating the effectiveness of the proposed program testing. These results establish the preliminary missile design code as a valuable tool for supporting phases zero and A in the development of missile projects.

Figure 4.3: Code validation



Source: External ballistic code

Chapter 5

Results and discussion

This chapter focuses on the preliminary design of two tactical ramjet missiles. The first missile aims to utilize commercially available off-the-shelf space-qualified systems already produced in the Brazilian industry. By leveraging these existing systems, the production process can be expedited cost-effectively while also significantly reducing the risks associated with the development and integration of ramjet technology. Given the absence of any available sources on the industry's development expenditure for FTI development, we applied the TRANSCOST methodology to gauge the value. The approximated cost savings resulting from avoiding booster development (weighing 360 kg) amount to approximately 54 million US dollars.

The second missile will be defined from the ground up, and both processes will adhere to the conceptual missile design steps outlined in Chapter 3.

The primary contribution of this chapter lies in the determination of the booster and sustainer volumes and weights for testing during the project's preliminary phase. This crucial step will provide valuable insights and data necessary for further development.

5.1 Baseline missile development

Following the ECSS standard definitions regarding the conceptual project phase (phase 0), the proposed missile should meet the general guidelines summarized in this section by example. To complete phase 0, the top-level customer must provide all required information, studies, and definitions. A proposition for these activities is detailed in Chapter 3.

The mission concept analysis demonstrates that low detectability and reduced engagement time are crucial to success. These characteristics imply supersonic speed and low radar cross-section (RCS). Completing the main parameters required, a variety of operational anti-ship missiles provides feasible limits for the Baseline missile's mission profile:

Launcher platform – warships;

Range - from 80 km to 300 km;

The minimum range adheres to the classification proposed in the literature for long-range missiles [25], while the maximum limit complies with the restrictions of the Missile Technology Control Regime (MTCR).

Flight regime – supersonic, exceeding Mach 2.5.

Terminal velocity – high speed providing adequate kinetic energy for penetration and high kill probability (P_K);

Launch weight - up to 3,000 kg;

Cruise altitude – from 10 to 20 km;

Length – up to 9 m;

Diameter – less than 600 mm;

Warhead mass within 100 kg to 300 kg of High Explosive (HE); and

Configuration - two stages (solid-fuel booster plus solid-fuel ramjet as a sustainer).

The preliminary technical requirements and risk assessment were broadly presented in Chapter 3. Regarding the economic studies for the development and fabrication process defined in the ECSS Phase-0, we adopted cost projection applied to space launch systems (TRANSCOST), to overcome the scarcity of related data.

The methodology was based on a work-year metric, which refers to the annual company budget divided by its total full-time employees. The correlations analysis with work-year criterion considers the system and subsystem masses as the main parameters [65]. The related equations provide a good estimation for solid propellant booster; nevertheless, there is no correlation for ramjet. The feasible alternative was the use of the same correlations applied for booster.

To establish the baseline missile characteristics, this study utilized statistical regression analysis with an R-square value exceeding 90% [25]. The results are valuable correlations as they capture significant interactions between subsystem weights and volumes with the operational range, the dependent variable. The study covers overall missile characteristics and surface-to-surface mission profiles, enabling the prediction of subsystem characteristics such as propulsion, guidance and control, and warhead. The missile mass results from the sum of each subsystem's weight multiplied by 1.22 (body structure factor) [24]. However, this factor is smaller for predicting the weight of an intercontinental ballistic missile case. A preliminary total mass approximation is obtained by averaging overall missile weights. The initial prediction for guidance and control mass considers the average of overall missile weights.

The process starts by selecting an operational supersonic missile similar in diameter to the desired baseline. The reference missile provides the mission profile characteristics, initial range, and warhead mass necessary for external ballistic calculations. The propulsion corre-

lations [25] are helpful for the first baseline missile configuration and are refined in further interactions. An auxiliary equation allows wing mass and area predictions. The wing mass is negligible compared to the missile's total mass, but the geometry and area are significant for drag estimation.

Figure 5.1 shows a step-by-step process for preliminary missile development, adequate to Phase-0 requirements.

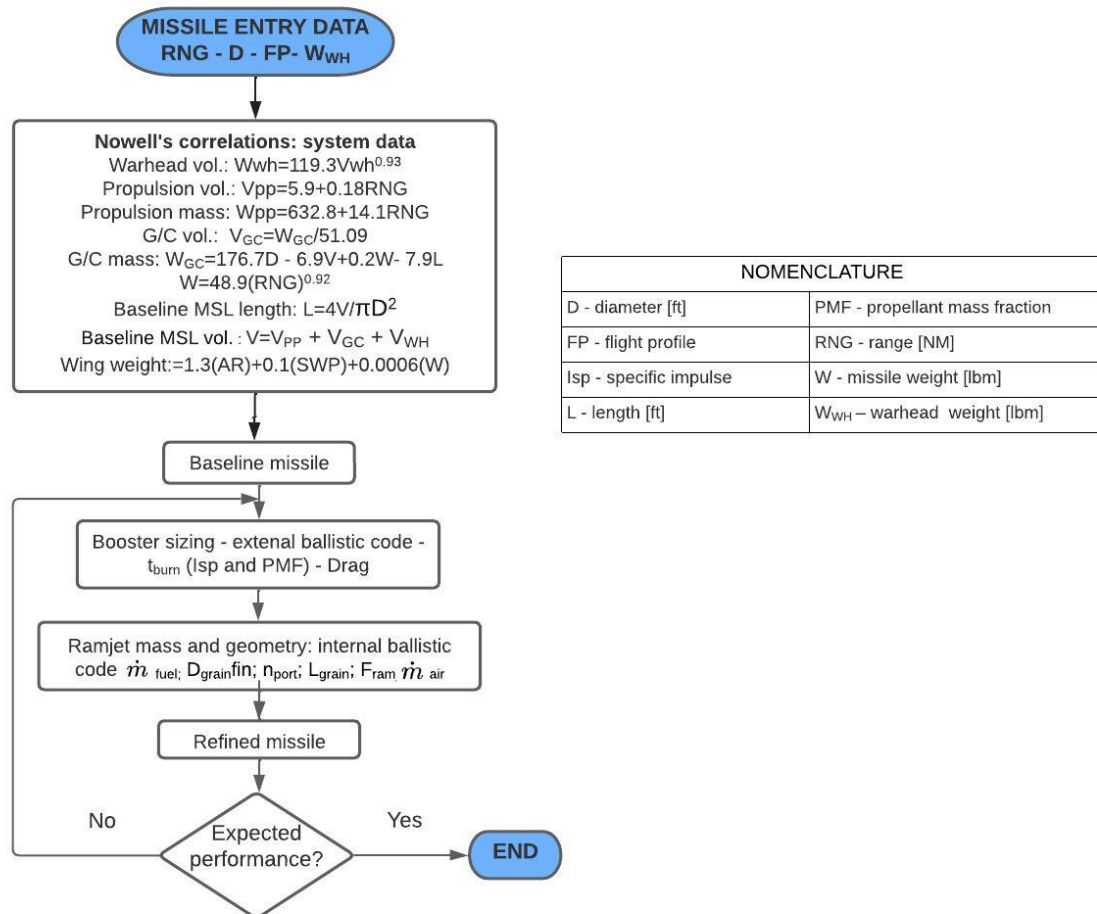


Fig. 5.1: Successive process for preliminary missile design.

Complementary and relevant correlations are available in Appendix F to facilitate the researchers' future analysis and comparisons.

Based on the cruise phase speed and altitude, the solid-fueled ramjet engine volume and mass are defined using another EES code running internal ballistic equations. The code provides nozzle geometry, initial and final grain diameters, and lengths. In the next step, considering the mass and geometry of the baseline missile, specific impulse, and propellant mass fraction, adjustments on booster thrust and impulse occurs [61]. The warhead and guidance and control subsections are accommodated in 90% of the missile reference diameter.

The flight profile comprises a fast ascension to cruise altitude, booster cold separation,

cruising phase, and parabolic trajectory toward the target. Achieving the initial configuration is a consequence of satisfactory system performance. Otherwise, the system and subsystem are refined and code-checked until mass variation becomes negligible. After this first step, most effort is focused on optimizing the sustainer volume and mass [61]. Since the code is based on two degrees of freedom, rapid changes in pitch angle are accomplished by setting proper values to the constant K in Equation 4.2.

Based on the previous rationale, we developed the first missile design by adopting a booster available in the Brazilian industry.

5.2 Missile 1 development

The proposed ramjet missile combined with a solid booster produced by Avibras Brasil (Fig. 5.2) aims to reduce development costs.

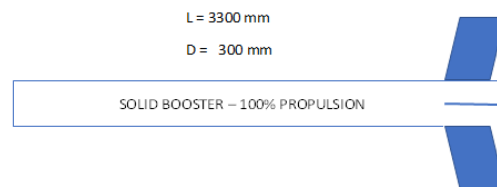


Fig. 5.2: FTI training rocket solid motor.

The selected booster powers the FTI sounding rocket for the Alcantara Launch site operational training program. The FTI system is already space-qualified, reducing the development risk and integration cost with the ramjet[65].

For preliminary prediction, the RIM-66B/C supersonic medium-range missile [70] furnished the initial parameters approach for range (minimum 74 km) and 100 kilograms warhead.

At this range, Nowell's correlations yield a guidance and control weight of 57 kg, a payload length of 900 mm capable of accommodating 100 kg of high-explosive material in a cylinder casing with a diameter of 270 mm. The estimated density of the warhead subsection is $1,825 \text{ kg/m}^3$. Regarding the propulsion subsystem, the overall weight prediction amounts to 581 kg. The total Baseline missile mass prediction is 750 kg. Additionally, we estimate a missile length of 9.6 meters and a total wing and tail area of 0.26 m^2 . For the wing and tail sweep angles, we have adopted 37 and 25 degrees, respectively.

The FTI delivers 64.5 kN thrust burning during 10.5 sec. For the ramjet engine, We suggest a solid-fueled ramjet for the sustainer based on a blend of paraffin and polyethylene. This fuel composition provides good strength and regression rate for long burning regimes in the range of 0,05 to 0,5 mm/s with a good relation between fuel grain length and initial

port diameter [8].

In the first run of the simulation code, the booster accelerates the Baseline to Mach 2.4, reaching 10,000 m. After burnout, the 1st stage separates from the sustainer. At these conditions, the code predicts drag forces of around 12.1 kN at the cruise phase.

The total length and weight of the missile depend on the required sustainer thrust and the operational time of the engine. The geometry of the nozzle and the mass of the fuel grain are determined by the engine thrust, impulse, oxidizer-to-fuel ratio, and fuel regression rate. Therefore, apart from the diameter, the main dimensions of the missile must be obtained through an iterative design process.

For the first refinement attempt, the internal ballistic code establishes the following conditions:

1. The fuel's initial and final port diameters are 180 mm and 290.2 mm, respectively, with a burning time of 130 s.
2. The ramjet engine operates at a maximum temperature of 1,388 K.
3. The weights of the propellant and the dry engine are 34 kg and 15 kg, respectively.
4. The lengths of the solid fuel and the ramjet are 1.3 meters and 2.0 meters, respectively.
5. The air intake area is $0.20m^2$.

Based on the information obtained from the Baseline version, we initiated the refinement process by multiplying the sum of the warhead weight (100 kg), guidance and control (G/C) weight (57 kg), and ramjet engine weight (49 kg) by a factor of 1.22 to predict the body structure weight.

After correcting the length and weight of the solid fuel ramjet and ensuring that the port diameter does not exceed 292 mm, as well as adjusting the body structure, the range has been improved to reach 166 km. These improvements were achieved after three rounds of refinement processing, as indicated in Table 5.1. Although further refinements are possible, their impact on the range is considered negligible.

The length of the solid fuel grain (1,000 mm) was determined during the final refinement phase, considering the suggested fuel composition, a regression rate of 0.35 mm/s, and a maximum flame temperature of 1388 °K in lean combustion mode (OF = 14.8). With a burning time of 139 s, the initial and final diameters of the fuel port were 180 mm and 291.4 mm, respectively. Furthermore, the combustion chamber experienced an initial mass flux of $294.4 \text{ kg}/m^2/s$, which reduced to $114.8 \text{ kg}/m^2/s$ by the end of combustion. For comparison, studies demonstrate stable combustion of high-density polyethylene with mass flux ranging from 360 to $250 \text{ kg}/m^2/s$ [11]. The post-combustion chamber and main nozzle dimensions were obtained for a conical exit nozzle with a 22° half-angle and contraction

area ratio of two. A 150 mm post-combustion section ($D/L = 2$) was added to improve combustion efficiency. The conical nozzle throat diameter and length were estimated as 151.2 mm and 176 mm, respectively, with a 276.7 mm exit diameter.

Table 5.1: Missile refinement process

Data	Baseline	1st ref.	2nd ref.	3rd ref.
Total missile mass (kg)	750	611	605	599
Total missile length (m)	9.6	7.7	7.6	7.5
Missile density (kg/m³)	1,078	1,175	1,163	1,130
Inlet length (m)	0.3	0.3	0.3	0.3
Warhead length (m)	0.9	0.9	0.9	0.9
Warhead mass (kg)	100	100	100	100
Warhead density (kg/m³)	1,825	1,825	1,825	1,825
G/C length (m)	1.2	1.2	1.2	1.2
G/C mass (kg)	57	57	57	57
G/C density (kg/m³)	818	818	818	818
Booster mass (kg)	-	360	360	360
Booster propellant mass (kg)	-	253	253	253
Ramjet engine mass (kg)	-	49	44	39
Ramjet fuel mass (kg)	-	34	28	25
Ramjet engine length (m)	3.7	2.0	1.9	1.8
Propulsion mass (kg)	581	409	404	399
Propulsion length (m)	7.0	5.3	5.2	5.1
Body structure mass (kg)	12	45	44	43
Burning time (sec) Booster/sustainer	10.5/-	10.5/130	10.5/137	10.5/139
Range (km)	74	158	163	166
Speed (Mach)	2.4	2.9	2.9	2.9
Total flight time (sec)	-	207	216	219
Cruise level (m)	10,000	12,000	13,000	13,000
F_{drag} at cruise level (kN)	12.1	11.6	10.1	9.8

Table 5.1 depicts the preliminary system development of the baseline missile parameters.

The guidance, navigation and control unit has a density of 818.4 kg/m³ and occupies a 1,200 mm length and 270 mm in diameter (payload bay).

Ramjet's total weight estimation is 239 kg, distributed in 3,900 mm length, and its engine delivers around 10.0 kN thrust necessary to beat the drag forces at the cruising step.

The propellant and dry engine weights were 25 kg and 14 kg, respectively. The sub-

sections, booster, and sustainer weight and size are 599 kg and 7,500 mm with 300 mm of external diameter. The ramjet propellant mass fraction and specific impulse were around 63% and 1967 s.

Table 5.1 presents the initial predicted masses and geometries using Nowell’s correlation, compared to the final refined solution. Nowell’s correlation results in a bulkier and heavier missile. However, through the refinement process, a solution (Missile 1) was found with a reduced total length (22% decrease) and a 20% lighter version. This reduction in weight is primarily attributed to the lower ramjet propellant mass fraction (PMF) compared to solid propellant rockets, which require carrying the oxidizer.

Figure 5.3 illustrates the volume breakdown of the missile subsections, excluding the booster. These subsections include guidance and control, warhead (payload), and propulsion, and occupy 25%, 29%, and 46% of the total missile volume, respectively. They are accommodated within a length of 3.9 mm (without diffuser) and a missile diameter of 300 mm.

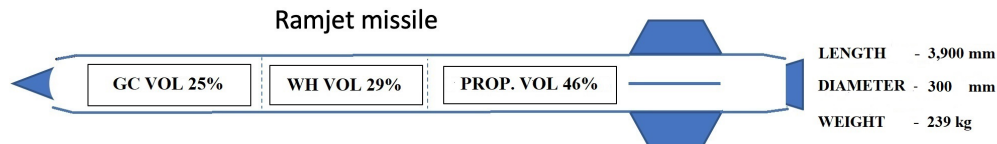


Fig. 5.3: subsystems volume arrangement without the booster.

The density of Missile 1 is 27% lower than the average density (1,554 kg/m³) identified in a study released in 1992 [25]. Furthermore, the length of Missile 1 maintains the fineness ratio (length-to-diameter) within the recommended limits ($5 < l/d < 25$).

Figure 5.4 shows the missile flight altitude and velocity during ascending (0 - 24 s), cruise (24 – 166 s), and coasting (166 – 219 s) stages. The peak speed reaches around Mach 3.8 in the ascending phase. During the cruise pattern, the Mach number remained at 2.9. The missile impact occurs 3.7 min after launch at Mach 1.6, at a steep angle of -42 degrees, and ranging more than 166 Km.

The initial angle (gamma) was set to 85 degrees for fast ascension to cruising conditions at about 11 km from the launch site, where the ramjet engine must deliver at least 9.8 kN of thrust. The maximum missile speed occurs at 11 s after takeoff when booster engine burnout. Booster cold separation follows, and the pitch angle is adjusted for near-horizontal cruising flight, after which the missile ramjet engine is fired up and burns for 139 s.

During the cruise phase, lift counterbalanced gravitational forces by adjustments in the angle of attack, as shown in Fig. 5.5. Lift forces vary from about 2,300 to 2,000 N, with an angle of attack average of 0.137 rad (7.8° degrees). Considering that Lift increases drag, requiring more thrust, thus, near-constant flight altitude resulted from forces compensation.

Figure 5.6 depicts the drag force profile over flight time. The maximum observed drag,

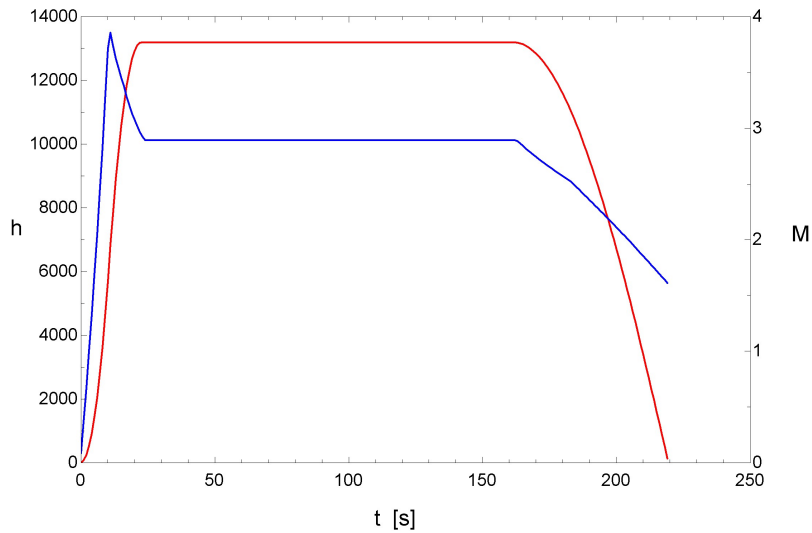


Fig. 5.4: Missile 1 flight altitude and velocity profile.

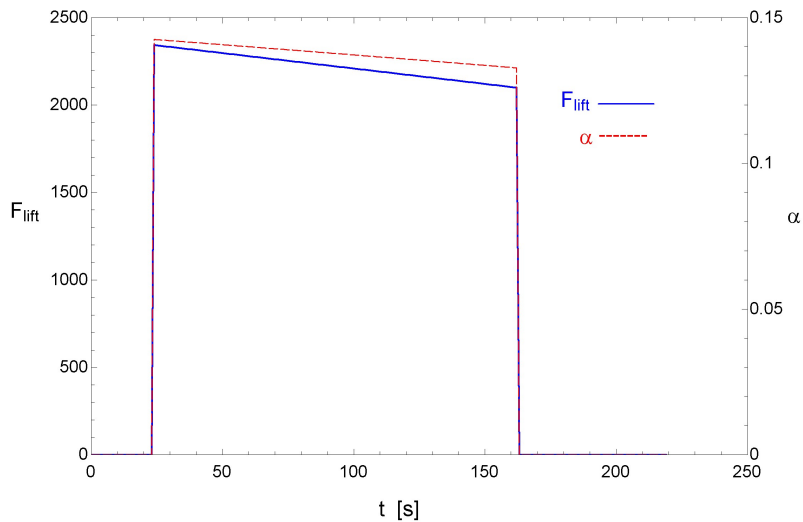


Fig. 5.5: Missile 1 lift force and angle of attack during the flight.

over 13.0 kN, occurs near 10 seconds, decaying to about 3.1 kN. In the cruising stage, the drag forces range from 9.8 to 9.5 kN, with the most considerable contribution from the missile angle of attack.

Table 5.2 summarizes the main parameters of Missile 1 after refinements compared to the MGM 140 - BLK B (solid propellant) [71] and the Harpoon (RGM-84) missile (turbojet engine) [72]. The proposed SSM performs better in radar signature (lower diameter) and total mass. Missile 1 also exceeds RGM-84 performance and has a similar profile to MGM-140 in range and speed parameters.

The reduced mass of Missile 1 compared to the solid propellant motor (MGM-140) results from the higher specific impulse (sustainer) and better efficiency at high operational altitudes. Compared to the subsonic Harpoon missile, the Missile 1 counterpart carries around

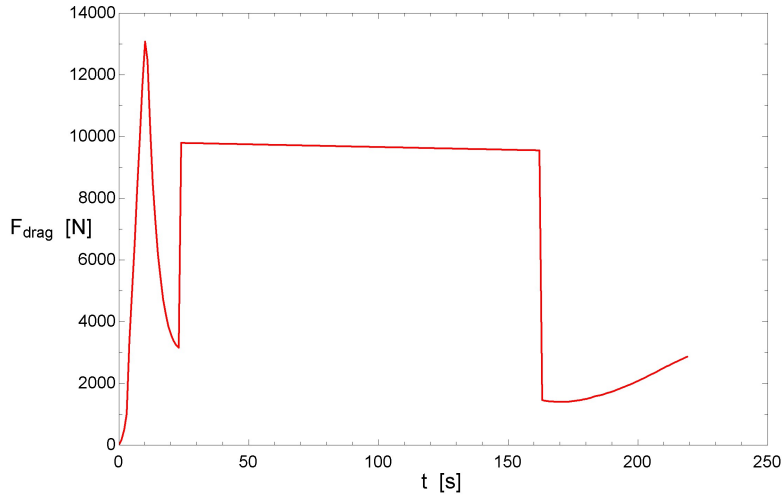


Fig. 5.6: Missile 1 drag force profile.

Table 5.2: Missiles comparison

PARAMETER	Missile 1	MGM-140 (BLK B)	RGM-84
Mass	599 kg	1,670 kg	683 kg
Length	7.5 m	4.0 m	4.6 m
Diameter	300 mm	610 mm	340 mm
Density	1,130 kg/m ³	1017 kg/m ³	1025 kg/m ³
Speed	2.9 M	3.0 M	0.7 M
Warhead	100 kg	160 kg	221 kg
Range	166 km	300 km	130 km

half of the payload at a greater distance and a significantly higher speed. The turbojet engine has a higher specific impulse which, for the same distance, can carry higher payload mass.

Missile 1 is the longest of the three missiles; nevertheless, the trade-off is favorable compared to the sectional area since the proposed missile has a smaller radar cross-section, still carrying the necessary payload mass.

5.3 Missile 2 development

In the previous section, we used a booster available in the market and detailed the ramjet section to reduce cost and expedite development. Seeking a comprehensive development methodology, we will now provide a step-by-step procedure that guides the definition of the total mass, dimensions, booster, and sustainer thrust, as well as the flight performance of a baseline missile, from its initial conception to the development of a feasible missile concept.

This method will ensure that all crucial aspects of the missile are considered, resulting in an efficient design process.

The process also adheres to the definitions and equations available in the literature regarding the correlation between missile variables based on the statistical method [25].

Following the sequence presented in figure 5.1, we conducted the preliminary analysis to obtain the geometry and mass of a baseline missile.

The warhead mass was defined as 200 kg, and the range follows the MTCR range restriction of 300 km for those countries that adhered to this regime, including Brazil [73], cruise flight at 14,000 m altitude, and Mach 3.0.

To obtain a realistic reference for speed, warhead weight, and transversal reference area diameter, we used maximum parameters from the P-800 Oniks missile (Russia) [74] and the Brahmos missile - block I (India) [75], considering that both missiles apply the same technology proposed for Baseline 2. Therefore, the new weapon will cruise at Mach 3.0, carrying a 200 kg warhead and having a 600 mm diameter of transversal area. The choice of a smaller diameter aims for better furtive quality.

We also considered the Brazilian airspace motor S-44 for the booster mass fraction estimations guide. This rocket stage applies a steel propellant casing, the same technology expected for the Baseline 2 missile. The S-44 propellant mass fraction is 83 % [65].

The wing and tail aerodynamic surface weight is based on Nowell's correlations. [25]. Complementary parameters were defined empirically by the author as follows:

$TR (ramjet) = 0.25$ - taper ratio;

$AR (ramjet) = 1,5$ - Aspect ratio;

$Swp (ramjet) = 20\ degree$ - Sweep angle;

Wing weight (ramjet)=4.7 lbm (total);

$NW = 4$ (number of wings);

$TR (booster) = 0.13$ - taper ratio;

$AR (booster) = 1.54$ - Aspect ratio;

$Swp (booster) = 35\ degree$ - Sweep angle;

Wing weight (booster)=28 lbm (total);

$NF = 4$ - (number of fins).

The missile uses a cruciform wing attached to the ramjet and a cruciform tail connected to the booster totaling 14.83 kg weight.

The baseline missile characteristics are calculated with the initial parameters defined and applying the proposed methodology, and the results are presented in table 5.3.

Table 5.3: Baseline missile parameters

Section	Weight kg	Volume m ³	Length m	Density kg/m ³
Missile (complete)	2,401	3.02	7.4	1,144
Propulsion	1,479	1.12	4.9	1,324
Warhead	200	0.12	0.50	1,732
GC	289	0.35	1.54	818.4

The initial data is now used to determine the booster characteristics. Based on an airspace project like the Avibras FTI, we guessed the initial missile acceleration to around 8 G and defined the initial thrust as approximately 188,000 N. The definition of the specific impulse and propellant mass fraction are inferred using the motor S-44 parameters.

Inserting the mentioned information in the trajectory program and fixing the missile launch elevation at gamma equal to 85 degrees, seeking a fast ascension to the desired flight level, the calculations indicate the booster burns for 14.4 seconds, delivering the ramjet at 14.000 meters and speeding Mach 3.0 after cold and nose cone separation. The external ballistic code estimates the drag force at 33.5 kN at cruise level. At this initial guess, the booster parameters are:

- booster propellant mass - 1022 kg;
- booster dry mass - 209 kg;
- total booster mass - 1,231 kg;
- booster volume - 0.93 m³
- booster density - 1,324 kg/m³
- $\dot{m} = 71$ kg/sec; and
- booster length - 3.3 m.

The refinement starts by considering the drag at 14,000 meters, the ramjet engine burning time at cruise level, and applying the proposed computational code for external and internal ballistics. Table 5.4 presents the entire refinement sequence. Notice that drag reduction leads to a series of weight adjustments. The new missile size and weight then return to the trajectory code for data adjustments. We tested a slightly longer missile length due to the necessity of harmonizing the nose cone to the missile dimension, fitting drag to acceptable limits.

For the body structure weight-to-launch-weight fraction, we adopt a measure-of-merit intermediate between the approaches used for middle and long-range missiles [24]. This structure houses and fixes the ramjet components.

The accepted general mass fraction for missiles is[24]:

$$\left(\frac{W_{BS}}{W_L}\right) = 0.2 \quad (5.1)$$

where W_{BS} is the weight of body structure (motor case + airframe) and W_L is the launch weight.

For long-range strategic intercontinental ballistic missile (ICBM), the mass fraction is [24]:

$$\left(\frac{W_{BS}}{W_L}\right) = 0.1 \quad (5.2)$$

For the baseline missile, we assumed the mass fraction equal to 0.15, disregarding booster weight.

Applying the equations presented in Chapter 4, we find the following refined parameters for ramjet engine operation at 14,000 ft altitude:

- Number of ports - 5;
- Fuel grain weight - 157 kg;
- Ramjet engine m_{dry} - 60 kg;
- Fuel grain length - 1.57 m;
- Air intake area - 0.112 m^2 ;
- Thrust - 29.8 kN;
- Port initial diameter - 0.350 m;
- Port final diameter - 0.56 m;
- Ramjet engine volume - 0.79 m^3 ;
- Ramjet engine total weight - 217 kg;
- ramjet length - 2.8 m (sum of grain length, combustor chamber length, and nozzle length); and
- PMF - 0.72;
- ISP - 1,943.

The calculations for finding the ramjet engine weight observe the following rationale. We used the pressure vessel theory for a carbon steel class material in cylinder shape (the material name is A-283-GR.C), measuring 3.0 mm nominal thickness and density of 7.8 g/cm³, with heated walls. This cylinder houses the solid fuel grain and forms the combusting chamber, the convergent and divergent nozzle [76]. The outside cylinder diameter is 600 mm, 2,973 mm long, the corrosion allowance is 0.1 mm, and the tolerance is 0.5mm.

The select yield stress and specific gravity from the material database are 206.8 N/mm^2 ,

Table 5.4: Missile 2 refinement process

Data	Baseline	1st ref.	2nd ref.	3rd ref.
Total missile mass (kg)	2,401	2,107	1,970	1,932
Total missile length (m)	7.4	9.0	8.3	8.3
Missile density (kg/m³)	1,144	878	895	878
Inlet length (m)	0.5	0.5	0.5	0.5
Total ramjet length (m)	-	5.2	5.0	4.8
Warhead length (m)	0.5	0.5	0.5	0,5
Warhead density (kg/m³)	1,732	1,732	1,732	1,732
G/C length (m)	1.5	1.5	1.5	1.5
G/C mass (kg)	289	289	289	289
G/C density (kg/m³)	818	818	818	818
Booster dry mass (kg)	209	211	196	190
Booster propellant mass (kg)	1022	1029	958	930
Ramjet engine mass (kg)	248	273	221	217
Ramjet fuel mass (kg)	-	202	160	157
Total propulsion mass (kg)	1,479	1504	1375	1,337
Booster/ramjet eng. length (m)	3.3/1.6	3.3/3.2	3.0/2.8	3.0/2.8
Body structure mass (kg)	-	114	106	106
Burning time (sec)	14.4/-	13.5/306	13.1/309	13.0/309
Range (km)	300	324	324	326
Speed (Mach)	3.0	3.0	3.0	3.0
Total flight time (sec)	-	386	389	389
Cruise level (m)	14,000	14,000	14,000	14,000
F_{drag} at cruise level (kN)	33.5	30.4	29.8	29.8

7000 kg/m³ [76] respectively, and the ramjet maximum operational limits are 1,231.85 °C and 4.97 bar. Using these parameters, we found 1.447 mm for the Nominal required thickness. The calculation does not consider the stress caused by acceleration and maneuvers in the axial and transversal axis, but just the pressure inside the cylinder with a conservative approach [76].

With the same launch conditions, the booster's operating time decreases by around 1.4 seconds during the process, resulting in the ramjet being delivered at 14,000 meters with a speed of M 3.0. The optimized ramjet engine begins its cruise flight, requiring 309 seconds of operating time and covering a range of 326 kilometers. A thrust of 29.8 kilonewtons is needed to maintain flight level and speed. The entire flight lasts for a total of 389 seconds.

Table 5.5: Missile 2 final parameters

Subsection	Weight kg	Volume m ³	Length m	Density kg/m ³
Booster	1,120	0.85	3.0	1,317
Ramjet engine	217	0.79	2.8	275
G/C	289	0.353	1.5	818
Warhead	200	0.11	0.5	1,732
body structure	106	-	-	-
Total	1,932	2.103	7.8	878

Regarding the ramjet engine length, 2.79 meters includes the grain length (1.583 m), the combustor chamber, and the nozzle.

Table 5.5 further shows the refined data obtained from the trajectory code computing the new parameters and the accommodation of warhead and Ground and Control subsystems in 90 % of the missile reference diameter.

The newly adjusted parameters now permit the missile to cruise flight at 14,000 meters with a missile speed exceeding Mach 3.0. Upon ramjet burnout, the missile initiates a ballistic descent towards the target at high kinetic energy, reaching Mach 1.9 upon impact. Missile 2 geometry also keeps the fineness ratio (length-to-diameter) within the recommended limits ($5 < l/d < 25$).

Figure 5.7 shows the missile flight altitude and velocity during ascending (0 - 25 s) cruise (26 – 334 sec), and coasting (335 – 389 s) stages. The maximum speed occurs at booster engine burnout, around 14 s after takeoff, and the cold separation starts. After that, the cruising stage begins approximately 11 km from the launch platform. From this point on, the ramjet engine delivers no less than 29,800 N burning its propellant for 309 s.

Fig. 5.8. illustrates the drag force profile during the flight trajectory. The maximum drag force of 57.6 kN occurs 13 seconds after launch and then decays to around 14 kN. In the cruising stage, the drag forces range from 29.8 to 28.3 kN due to variations in the missile's angle of attack.

Figure 5.9 shows the final booster and ramjet missile dimensions and subsystems arrangement.

Table 5.6 summarizes the main parameters of Baseline 2 after a sequence of refinements, comparing the result to P-800 (Oniks) and Brahmos (BLK 1) missiles. The conceptual missile performs better in some system parameters and characteristics, particularly the furtivity (diameter), and weight. The performance is similar in density, range and speed. The difference in length and weight could be explained considering different operational altitudes and that both reference missiles present export versions and other profiles for the manufacturing country purchases; however, the differences between these missile types are unclear in the

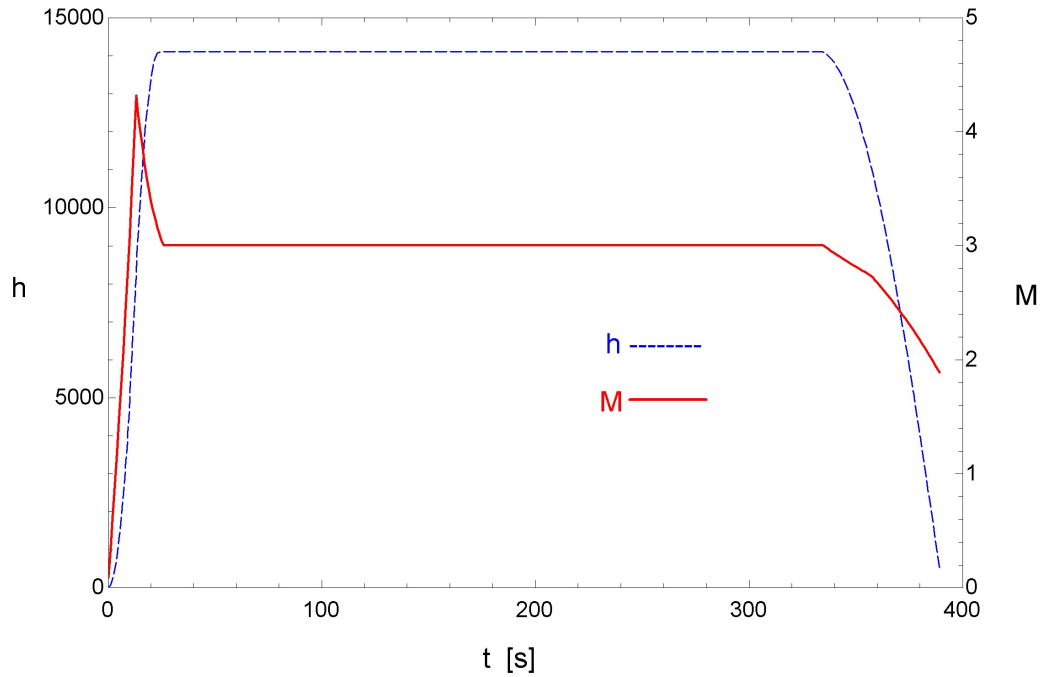


Fig. 5.7: Missile 2 trajectory - Final version.

available literature.

The comparison demonstrates that Missile 2 performs a trajectory profile compatible with missiles of the same category, providing reliability to the design process in the conceptual phase.

Table 5.6: Missiles comparison

PARAMETER	MISSILE 2	P-800 (ONIKS)	BRAHMOS/BLK 1
Mass	1,932 kg	3,000 kg	3,000 kg
Length	7.8 m	8.6 m	8.6 m
Diameter	600 mm	670 mm	670 mm
Density	878 kg/m ³	992.39 kg/m ³	992.39 kg/m ³
Speed	M 3.0	M 2.6	M 2.8
Warhead	200 kg	250 kg	200 kg
Range	326 km	300 km	300 km
Development cost	322 MM (USD)	-	250 MM (USD)

The TRANSCOST model estimates that the project development would cost USD 322 million. This estimation is based on a booster mass of 1,231 kg and a Ramjet engine mass of 217 kg. According to the model, the project would require 2,432 workers dedicated to the development for one year, or approximately 486 specialists working for five years.

The cost prediction did not include the integration between stages because this interface

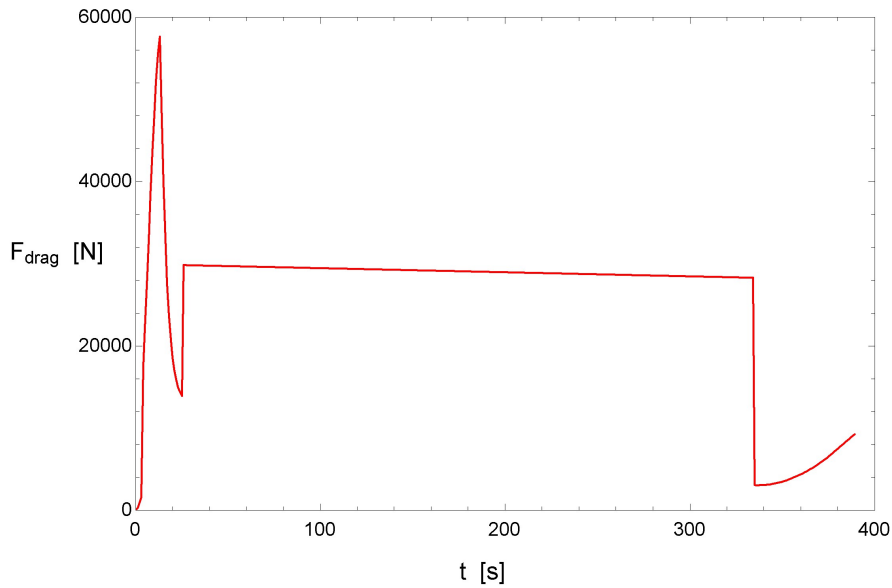


Fig. 5.8: Missile 2 drag forces - Final version.

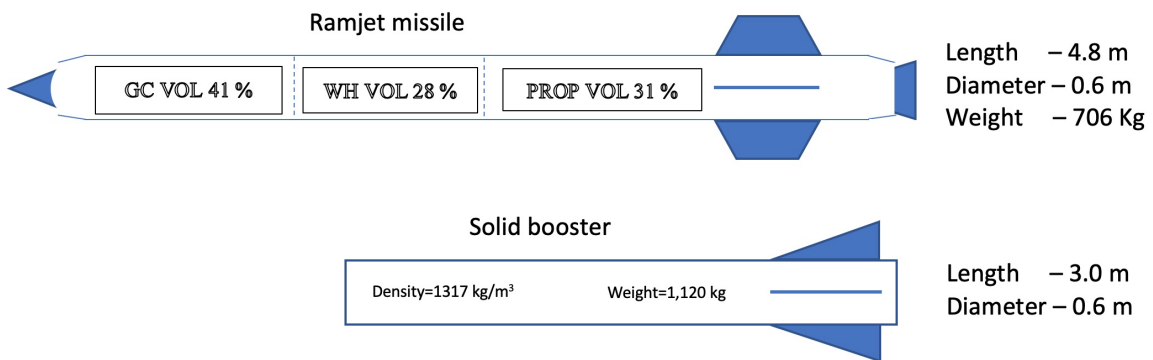


Fig. 5.9: Subsystems arrangement.

development is simpler for a missile than for a rocket. Additionally, we excluded the costs of the diffuser, payload, and guidance/control (G/C) development, as these subsystems require further technical refinement and extensive market research. Regarding fabrication, the cost per unit of Missile 2 is estimated at 1,930,043.30 USD, requiring approximately 17 work-years.

For comparison, BrahMos BLK 1 had a development cost of 250 million USD. Given its similarity to Russian missiles with the same technology, there is a possibility of using off-the-shelf systems and subsystems [77].

Time is a scarce and valuable resource in project design and development. As a contribution to planning activities, the assessment of weight and size estimation, integration of the findings into the new trajectory computational code, and the simulations were completed in less than one working day for thoroughness.

Conclusion

This research highlights the importance of Brazil incorporating a supersonic cruise missile into its defense sector inventory and proposes the necessary foundations to initiate and guide the development processes. The Brazilian Exclusive Economic Zone presents complex surveillance and defense challenges for the Brazilian Navy, necessitating advanced anti-ship weaponry to effectively address potential conflicts in the region. Based on the characteristics of naval warfare and the Brazilian strategic defense scenario, we focus on the academic development of the conceptual phase of an anti-ship missile system. The outcome is a set of tools for the conceptual design phase of a supersonic anti-ship missile propelled by a solid fuel ramjet engine. Additionally, the study introduces a design tool that enables various mission profiles for preliminary analysis, determining the system's basic configuration to accommodate key missile subsections such as propulsion, guidance and control, and warhead. Considering the European Cooperation for Space Standardization (ECSS) and the current constraints regarding industrial activities definitions, we advocate for adopting ECSS phase 0 and adapting project phase A concepts to expedite the development process while providing a foundation for subsequent steps. By aligning with aerodynamic theory and developing a user-friendly computational code, it becomes possible to predict crucial aspects of missile design studies, including range, endurance, and payload. The computational code proposed in this work, validated through simulation with the extensively documented NASA Aerobee 150A, supports the development of a missile with significant capabilities. This missile, weighing 599 kilograms, flying at an altitude of over 13,000 meters, at a speed of Mach 2.9, and carrying 100 kilograms of high explosive material, can engage targets at 166 kilometers. The system achieves operational speed through the utilization of a space-qualified solid rocket booster manufactured by Avibras Company. This approach reduces system development costs, estimated at 54 million US dollars for the proposed ramjet missile. In conclusion, this research presents a comprehensive method for missile development, starting from scratch and progressing towards a conceptual missile for design planning. The step-by-step approach facilitates the definition of parameters for missile subsections, and the computational tools created to support the design process streamline data refinement, resulting in a reliable final version. Considering all the efforts conducted in this academic work and the availability of adequate laboratories and skilled personnel at the University of Brasília, we can confidently assert that achieving TRL 3 in this project, including the construction of a proof of concept, is indeed feasible in the Brazilian academic sector.

Future works should explore system optimization based on genetic algorithms to enhance the proposed missile (Missile 2). Additionally, detailed cost estimations for development and fabrication, as outlined in ECSS Phase A, will assist the Brazilian Navy in formulating their Request for Information and Proposals for long-range surface-to-surface supersonic missiles. Overall, this proposal serves as a stepping stone that facilitates and guides the development of subsequent project phases. Furthermore, the following fields of study, not addressed in this work, require continued research:

1. The effect of wind speed on missile trajectory.
2. Automatic selection of the optimal launch angle.
3. Expanding the system to include three or more degrees of freedom.
4. Surfaces sizing optimization.
5. Completion of Project Phase A.

Bibliography

- [1] STANDARD, E. *Space Project Management-Risk Management (ECSS-M-ST-80C)*. 2008. <https://ecss.nl/standard/ecss-m-st-80c-risk-management/>. Accessed: 2022-09-17.
- [2] WIESEBRON, M. Blue amazon: thinking about the defence of the maritime territory. *Austral: Brazilian Journal of Strategy & International Relations*, v. 2, n. 3, p. 107–132, 2013.
- [3] GARCIA, A. et al. Vsb-30 sounding rocket: History of flight performance. *Journal of Aerospace Technology and Management*, v. 3, n. 3, p. 325–330, 2011. Cited By 15.
- [4] DEFENSE Industry Dayly. 2014. <https://www.defenseindustrydaily.com/astros-2020-brazil-moves-to-revive-avibras-07069/>. Accessed: 2022-08-30.
- [5] GANY, A. Accomplishments and challenges in solid fuel ramjets and scramjets. *International Journal of Energetic Materials and Chemical Propulsion*, v. 8, n. 5, p. 421–446, 2009. Cited By 3.
- [6] MARUYAMA, S. et al. Study on mechanical characteristics of paraffin-based fuel. In: *47th AIAA/ASME/SAE/ASEE Joint Propulsion Conference & Exhibit*. [S.l.: s.n.], 2011. p. 5678.
- [7] HASHIM, S. A. et al. Regression rates and burning characteristics of boron-loaded paraffin-wax solid fuels in ducted rocket applications. *Combustion and Flame*, Elsevier, v. 191, p. 287–297, 2018.
- [8] SHYNKARENKO, O. et al. Experimental investigation of hydrocarbon based fuels in solid fuel ramjet propulsion. In: . [S.l.: s.n.], 2019. v. 2019-October. Cited By 0.
- [9] SIDHU, W. P. S. Looking back: The missile technology control regime. *Arms Control Today*, Arms Control Association, v. 37, n. 3, p. 45, 2007.
- [10] NEIVA, R. Q. Técnica de otimização aplicada em projeto conceitual de mísseis táticos. 2016.

- [11] KRISHNAN, S.; GEORGE, P. Solid fuel ramjet combustor design. *PROGRESS IN AEROSPACE SCIENCES*, v. 34, p. 219–256, 1998. Cited By 37.
- [12] ATHAWALE, B.; ASTHANA, S.; SINGH, H. Metallised fuel rich propellants for solid rocket ramjet: A review. *Defence Science Journal*, Defence Scientific Information & Documentation Centre, v. 44, n. 4, p. 269, 1994.
- [13] DISKIN, D.; NATAN, B. Numerical simulation of a boron loaded gel fuel ramjet combustor. *Proc. of EUCASS*, p. 2017–268, 2017.
- [14] THOMAS, J. C. et al. Enhancement of regression rates in hybrid rockets with htpb fuel grains by metallic additives. In: *Proceedings of the 51st AIAA/SAE/ASEE Joint Propulsion Conference, Orlando, FL, USA*. [S.l.: s.n.], 2015. p. 27–29.
- [15] CIEZKI, H. K.; NAUMANN, K. W.; WEISER, V. Status of gel propulsion in the year 2010 with a special view on the german activities. *Deutscher Luft-und Raumfahrtkongress 2010*, 2010.
- [16] VEALE, K. et al. A review of the performance and structural considerations of paraffin wax hybrid rocket fuels with additives. *Acta Astronautica*, v. 141, p. 196–208, 2017. Cited By 19.
- [17] KARABEYOGLU, A. et al. Scale-up tests of high regression rate paraffin-based hybrid rocket fuels. *Journal of propulsion and power*, v. 20, n. 6, p. 1037–1045, 2004.
- [18] LI, C. et al. Experimental study on the operation characteristics of aluminum powder fueled ramjet. *Acta Astronautica*, v. 129, p. 74–81, 2016.
- [19] GONG, L. et al. Combustion characteristics of the solid-fuel ramjet with star solid fuel. *Journal of Aerospace Engineering*, v. 31, n. 4, 2018.
- [20] LI, W. et al. Combustion characteristics of paraffin-polyethylene blends fuel for solid fuel ramjet. *Journal of Aerospace Engineering*, v. 33, n. 4, 2020.
- [21] MCDONALD, B.; RICE, J. Solid fuel ramjet fuel optimization for maximum impulse-density with respect to air to fuel ratio and relative fuel regression rates derived from thermogravimetric analysis. *Aerospace Science and Technology*, v. 86, p. 478–486, 2019. Cited By 3.
- [22] OU, M. et al. Thermodynamic performance analysis of ramjet engine at wide working conditions. *Acta Astronautica*, v. 132, p. 1–12, 2017.
- [23] MUSA, O. et al. Effect of inlet conditions on swirling turbulent reacting flows in a solid fuel ramjet engine. *Applied Thermal Engineering*, v. 113, p. 186–207, 2017.
- [24] FLEEMAN, E. *Missile design and system engineering*. [S.l.]: American Institute of Aeronautics and Astronautics, Inc., 2012.

- [25] JR, J. B. N. *Missile total and subsection weight and size estimation equations*. [S.l.], 1992.
- [26] PACKARD, J.; MILLER, M. Assessment of engineering-level codes for missile aerodynamic design and analysis. In: *Atmospheric Flight Mechanics Conference*. [S.l.: s.n.], 2000. p. 4590.
- [27] SETHUNATHAN, P.; SUGENDRAN, R.; ANBARASAN, T. Aerodynamic configuration design of a missile.
- [28] CAMPOS, L. M.; GIL, P. J. On four new methods of analytical calculation of rocket trajectories. *Aerospace*, MDPI, v. 5, n. 3, p. 88, 2018.
- [29] ŞUMNU, A.; GÜZELBEY, İ. H.; ÖĞÜCÜ, O. Aerodynamic shape optimization of a missile using a multiobjective genetic algorithm. *International Journal of Aerospace Engineering*, Hindawi, v. 2020, 2020.
- [30] DYER, J. D. et al. Aerospace design optimization using a steady state real-coded genetic algorithm. *Applied Mathematics and Computation*, Elsevier, v. 218, n. 9, p. 4710–4730, 2012.
- [31] EUROPEAN Cooperation for Space Standardization. <https://ecss.nl/>. Accessed on December 7, 2023.
- [32] GAMAL, Y. E.; KRIEDTE, W. European cooperation for space standardisation (ecss). In: *Product Assurance Symposium and Software Product Assurance Workshop*. [S.l.: s.n.], 1996. v. 377, p. 43.
- [33] KELLY, P. L. Geopolitical themes in the writings of general carlos de meira mattos of brazil. *Journal of Latin American Studies*, Cambridge University Press, v. 16, n. 2, p. 439–461, 1984.
- [34] GOVERNO, L. F. Decreto n. 6.703, de 18 de dezembro de 2008. *Aprova a Estratégia Nacional de Defesa, e dá outras providências*, v. 1, 2008.
- [35] ABDENUR, A. E.; NETO, D. M. d. S. Brazil's maritime strategy in the south atlantic: The nexus between security and resources. South African Institute of International Affairs (SAIIA), 2013.
- [36] ABDENUR, A. E.; NETO, D. M. de S. Brazil in the south atlantic: growing protagonism and unintended consequences. *Policy Brief, Oslo Norwegian Peacebuilding Resource Centre*, 2013.
- [37] AZZAM, I. The dispute between france and brazil over lobster fishing in the atlantic. *International & Comparative Law Quarterly*, Cambridge University Press, v. 13, n. 4, p. 1453–1459, 1964.

- [38] MISHRA, S. Cruise missiles: Evolution, proliferation and future. *Journal of Defence Studies*, v. 6, n. 3, p. 139–142, 2012.
- [39] (BRAZIL), M. O. D. B. National strategy of defense: Peace and security for brazil. 2008.
- [40] GANG, L. et al. Research status and progress on anti-ship missile path planning. *Acta Automatica Sinica*, Elsevier, v. 39, n. 4, p. 347–359, 2013.
- [41] DUTTA, D. Probabilistic analysis of anti-ship missile defence effectiveness. *Defence Science Journal*, v. 64, n. 2, 2014.
- [42] RAO, G. S. et al. Monostatic radar cross section estimation of missile shaped object using physical optics method. In: *IOP Conference Series: Materials Science and Engineering*. [S.l.: s.n.], 2017. v. 225, n. 1, p. 012278.
- [43] SCHMIDT, F. de H.; ASSIS, L. R. Soares de. *A dinâmica recente do setor de defesa no Brasil: análise das características e do envolvimento das firmas contratadas*. [S.l.], 2013.
- [44] ECSS, S. Space engineering: System engineering general requirements. *ESA-ESTEC Requirements Standards Division, Noordwijk, The Netherlands*, 2017.
- [45] ECSS, S. Risk management. *ESA-ESTEC Requirements Standards Division, Noordwijk, The Netherlands*, 2008.
- [46] PITTS, W. C.; NIELSEN, J. N.; KAATTARI, G. E. *Lift and Center of Pressure of Wing Body Tail Combinations at Subsonic, Transonic, and Supersonic Speeds*. [S.l.]: US Government Printing Office, 1957.
- [47] JORGENSEN, L. H. *Prediction of Static Aerodynamic Characteristics for Space-shuttle-like and Other Bodies at Angles of Attack from 0 O to 180 O*. [S.l.]: NASA, 1973.
- [48] KOTHARI, V. et al. Enhancement in the lift force of the solid fuel ducted ramjet (sfdr) with an increase in the controlling surface. *Materials Today: Proceedings*, Elsevier, v. 50, p. 1878–1882, 2022.
- [49] CAIN, T. *Ramjet Intakes*. [S.l.], 2010.
- [50] FRY, R. A century of ramjet propulsion technology evolution. *JOURNAL OF PROPULSION AND POWER*, v. 20, n. 1, p. 27–58, JAN-FEB 2004. ISSN 0748-4658.
- [51] VERLINDE, E. On the origin of gravity and the laws of newton. *Journal of High Energy Physics*, Springer, v. 2011, n. 4, p. 1–27, 2011.
- [52] BONNEY, E. A.; ZUCROW, M. J.; BESSERER, C. W. *Aerodynamics, propulsion, structures and design practice*. [S.l.]: Van Nostrand, 1956.

- [53] JOHNSON, D. et al. Atmospheric models for engineering applications. In: *41st Aerospace Sciences Meeting and Exhibit*. [S.l.: s.n.], 2003. p. 894.
- [54] EARTH Atmosphere Model: Metric units. <https://www.grc.nasa.gov/www/k-12/airplane/atmosmet.html>. Accessed: 2022-09-30.
- [55] SAW, A. S.; AL-OBAIDI, A. S. M. Drag of conical nose at supersonic speeds. *EUREKA Annual Report, Department of Mechanical Engineering, Taylor's University, Malaysia*, 2013.
- [56] STRUCHTRUP, H. *Thermodynamics and energy conversion*. [S.l.]: Springer, 2014.
- [57] PASTRONE, D. Approaches to low fuel regression rate in hybrid rocket engines. *International Journal of Aerospace Engineering*, Hindawi, v. 2012, 2012.
- [58] AZEVEDO, V. et al. Experimental investigation of high regression rate paraffin for solid fuel ramjet propulsion. In: . [S.l.: s.n.], 2019. Cited By 0.
- [59] SCHULTE, G. Fuel regression and flame stabilization studies of solid-fuel ramjets. *Journal of Propulsion and Power*, v. 2, n. 4, p. 301–304, 1986.
- [60] AZEVEDO, V. A. et al. Experimental investigation of high regression rate paraffin for solid fuel ramjet propulsion. In: *AIAA Propulsion and Energy 2019 Forum*. [S.l.: s.n.], 2019. p. 3984.
- [61] CRUZ, R. L.; VERAS, C. A.; SHYNKARENKO, O. Paraffin-based ramjet missile preliminary design. *Advances in Aircraft and Spacecraft Science*, Techno-Press, v. 10, n. 4, p. 317, 2023.
- [62] PATTERSON, T. How to design, build and test small liquid-fuel rocket engines. *Rocketlab, USA*, 1971.
- [63] MILLER, W. H. *Solid rocket motor performance analysis and prediction*. [S.l.]: National Aeronautics and Space Administration, 1971.
- [64] KLEIN, S. A.; NELLIS, G. *Mastering EES*. [S.l.]: f-Chart software, 2013.
- [65] CÁS, P. L. da et al. A brazilian space launch system for the small satellite market. *Aerospace*, MDPI, v. 6, n. 11, p. 123, 2019.
- [66] PONOMARENKO, A. Tool for rocket propulsion analysis. *www.propulsion-analysis.com Cologne*.
- [67] BUSSE, J. R.; LEFFLER, M. T. *A Compendium of Aerobee Sounding Rocket Launchings from 1959 Through 1963*. [S.l.]: National Aeronautics and Space Administration, 1966.

- [68] AEOROBEE 150: A Classic Sounding Rocket. <https://open-aerospace.github.io/Aerobee-150/>. Accessed: 2022-09-17.
- [69] JR, P. B. et al. *A compendium of NASA Aerobee sounding rocket launchings for 1966*. [S.l.], 1967.
- [70] DIRECTORY of U.S. Military Rockets and Missiles. <https://designation-systems.net/dusrm/m-66.html>. Accessed: 2023-02-13.
- [71] MGM-140 ATACMS: Short-range ballistic missile. <https://www.military-today.com/missiles/atacms.htm>. Accessed: 2022-09-17.
- [72] RGM-84 Harpoon: Overview. <https://weaponsystems.net/system/583-RGM-84+Harpoon>. Accessed: 2022-09-17.
- [73] MISSILE Technology Control Regime (MTCR): Annex handbook 2017. <https://mtcr.info/wordpress/wp-content/uploads/2017/10/MTCR-Handbook-2017-INDEXED-FINAL-Digital.pdf>. Accessed: 2022-09-18.
- [74] MISSILES of the world: P-800 Oniks/Yakhont/Bastion (SS-N-26 Strobile). <https://missilethreat.csis.org/missile/ss-n-26/>. Accessed: 2022-09-18.
- [75] MISSILES of the world: Brahmos. <https://missilethreat.csis.org/missile/brahmos/>. Accessed: 2022-09-18.
- [76] SHELL Thickness Calculation. <https://www.red-bag.com/shell-thickness-calculation.html>. Accessed: 2022-09-30.
- [77] HISTORY of BrahMos. <https://www.brahmos.com/content.php?id=1&sid=2>. Accessed: 2022-10-12.
- [78] 20+RISK Management Techniques. <https://simplicable.com/new/top>. Accessed: 2022-09-26.
- [79] ADALSTEINSSON, G. *The liquidity risk management guide: From policy to pitfalls*. [S.l.]: John Wiley & Sons, 2014.
- [80] WHAT Is Pure Risk? <https://www.investopedia.com/terms/p/purerisk.asp>. Accessed: 2022-09-25.
- [81] LEMKE, F.; PETERSEN, H. L. Teaching reputational risk management in the supply chain. *Supply Chain Management: An International Journal*, Emerald Group Publishing Limited, 2013.
- [82] LANCASTER, J. The financial risk of airline revenue management. *Journal of Revenue and Pricing Management*, Springer, v. 2, n. 2, p. 158–165, 2003.

[83] MCCORMICK, R. *Legal risk in the financial markets*. [S.l.]: Oxford University Press on Demand, 2010.

[84] WU, T.; BLACKHURST, J.; CHIDAMBARAM, V. A model for inbound supply risk analysis. *Computers in Industry*, v. 57, n. 4, p. 350–365, 2006. ISSN 0166-3615. Disponível em: <<https://www.sciencedirect.com/science/article/pii/S016636150500179X>>.

Appendix A: Bibliometric Networks

The process uses text mining to construct and visualize co-occurrence networks based in keywords such as ramjet, paraffin, solid fuel, and regression rate extracting related information from a body of scientific literature.

All the information for analysis was obtained using the metrics, tools, and database available on the Web of Science site.

The survey is divided into two fields of interest. In the first step, the objective is to bring up the main field of studies on solid fuel ramjet in a broad sense. For this purpose, the researcher established the following search parameters: TITLE: (“solid fuel” or “solid-fuel” or “ramjet”) AND TOPIC: (“regression rate” or “additive*” or “swirl” or “combustion chamber”) NOT TOPIC: (“scramjet” or “turbojet”) AND YEAR PUBLISHED: (2011-2020) Time-span: 2011-2020.

As a result, one hundred-one documents were found. From this preliminary list, the author selected papers of interest based on the number of citations and field of study frequently mentioned as detailed following:

1. Paraffin-based fuel
2. Regression rate
3. Metallic Additives
4. Swirling Flows
5. Gel fuel
6. Hybrid rockets

In sequence, the software tool VOSviewer made it possible to visualize bibliometric networks. These networks based on bibliographic data identified co-authorship and country relations.

Text mining applying a minimum of two documents and one citation of an author as a threshold showed that the greater amount of documents came from China followed by the USA.

Figure 10 revealed the meaningful research contribution of authors such as Chen Xiong and Omer Musa.

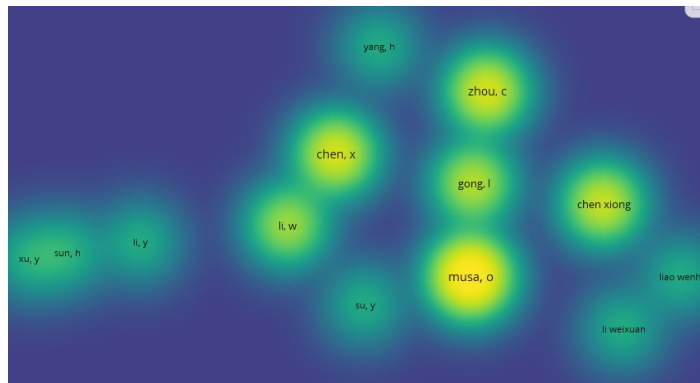


Fig. 10: Co-authorship density visualization.

In the second step of the search, the scope is refined to identify in the same period of time just the paraffin-based ramjet fuel surveys, which is the main field of research in Brazil for supersonic tactical missile development.

At this time the following parameters were used: TITLE: ("paraffin" or "ramjet") AND TOPIC: ("solid-fuel") NOT TOPIC: ("scramjet" or "turbojet") Refined by: Countries/Regions: (PEOPLES R CHINA OR USA OR INDIA OR RUSSIA) Timespan: 2011-2020.

Finally, a few papers from the nineties were added for comparison reason and tendencies identification.

Appendix B: Technical Requirements

Initially, for test and evaluation purposes, we suggest the United States Department of Defense Standard practice and the Standardization Agreement (STANAG) used by North Atlantic Treaty Organization members, both applicable to defense material, as technical guides accepted worldwide.

Next, we describe the technical requirements according to the specific systems' types. Nevertheless, complementary specifications may be necessary to fully incorporate the client's objectives.

Warhead (Damage mechanism):

- The warhead should mainly generate a blast fragmentation wave effect after the explosion.

Safe arming unit - SAU:

- The necessary acceleration to arm the explosive train should be compatible with the acceleration delivered by the booster.

Explosive train:

- The explosive train should have enough energy and power to initiate the warhead replenisher.

- The missile's electric signal for warhead detonation should be capable of initiating the safe arm unit electric detonator.

- The safe arming unit must meet the following test requirements detailed in the Standard Mil-STD-331D:

- a. 12 meters (40 ft) free-fall drop;
- b. 1,5 meters (5 ft) free-fall;
- c. extreme temperature;
- d. thermal shock;
- e. primary explosive safety; and
- f. electrostatic discharge.

Rocket booster:

- The rocket booster should meet the Standard MIL-R-25532A and STANAG 6016 specifications.

- The rocket booster electroexplosive initiator should meet the electromagnetic requirements of MIL-HDBK-1512.

- The rocket booster should meet the environmental test requirements of Standard MIL-STD-810E.

- The propellant should emit a reduced smoke signature following STANAG 6016.

- The rocket booster should follow the evaluations of standard MIL-STD-2105B as described?

- a. 12 meters (40 ft) free-fall drop;

- b. slow cook-off;

- c. fast cook-off;

- d. bullet impact; and

- e. sympathetic detonation (the rocket booster should receive the warhead's shrapnel impact).

Interface:

- The missile and its integrated subsystems should stand the typical static and dynamic load during the flight free of structural damage or deformation according to standard MIL-M-8856B.

Reliability

- The reliability analysis should observe the standard MIL-STD-721 and MIL-STD781C or later versions and the failure rates calculated according to standard MIL-HDBK-217FN2.

Marking and Painting:

- The external parts of the warhead and rocket booster should follow the criteria defined in Standard MIL-P-21960.

Environmental Requirements:

- The system, subsystems, and components should withstand the requirements of standard MIL-STD-810E regarding:

- a. Low pressure,

- b. High temperature,

- c. Low temperature,

- d. Thermal shock,

- e. Mechanical shock (during transportation),

- f. Humidity,
- g. Saline mist exposition,
- h. Vibration,
- i. Acceleration,
- j. Rain,
- k. Tightness/leakage,
- l. Fungus,
- m. Sand and dust,
- n. Solar radiation, and
- o. Ice.

Electromagnetic Interference:

- The electromagnetic interference requirements should follow the criteria defined in standards MIL-STD-461D, MIL-STD-462D and MIL-STD-464C.
- The electrical activation lines of the rocket booster should have HERO-safe device to protect from external electromagnetic fields, following standard MIL-STD-464D.

Vibration:

- The missile and its parts must operate steadily and reach the specified performance when subjected to the typical vibration parameters for high-performance missiles and platforms following the standard MIL-STD-810E.

Acceleration:

- The missile and its parts must operate steadily and reach the specified performance when subjected to the typical acceleration parameters for high-performance missiles following the standard MIL-STD-810E.

Combined Test (vibration, temperature, pressure, and humidity):

- The missile should be subjected to a combined tests of: temperature and vibration; temperature and humidity; pressure and temperature, for all subsystems following the standard MIL-STD-810.

Work Breakdown Structure (WBS)

- The WBS conception should follow the Standard MIL-STD-881 (Work Breakdown Structure for Defense Material Items).

Statement of Work (SOW)

- The SOW conception should follow as much as possible the standard Mil-HDBK-245C (Preparation of Statement of Work).

Configuration Management Plan

- The company should put into force and keep running during the contract term a Configuration Management System based on the standard Mil-STD-973.

Logistics and Reliability

- Calculations based on failure mode, effects, and criticality analysis (FMECA) or equivalent procedure should demonstrate the required reliability.

- The handbook MIL-HDBK-217-F is the basis to certify electronic systems' reliability.

- All components with a limited life cycle should present this condition through marks.

Specific requirements

Warhead:

- The warhead weight should remain within 150 kg to 250kg.

- Within a guidance error of 8 meters, the missile should penetrate the ship employing kinetic energy and then explode through delay fuze resulting in 80% probability of target total disability.

Proximity fuze:

- The proximity fuze should detonate as soon as the continuous shrinkage of distance changes to an increasing distance, meaning that the target was over-passed.

Safe arming unit - SAU:

- The safe arming unit should prevent the warhead detonation in the initial missile flight and provide the explosive train alignment at a distance not smaller than 500 meters from the launcher platform.

- Once armed in free flight, the explosive train must not return to misaligned condition.

- The missile should be capable of exceeding 4 G in flight to hamper the target defense system's.

- For maintenance and test's sake, it is desirable that the explosive train return to misaligned condition once armed.

- The explosive train condition (armed or disarmed) should be recognized visually.

- A single fail must not prompt the alignment of the safe arming unit.

- The SAU should not present paintings.

Rocket booster:

A rocket booster is usually a solid-propellant rocket required to assist take-off and accelerate a ramjet missile to its operational speed.

- The rocket booster and its components should meet the requirements applied for the

missile performance as a whole.

- The electric signal for rocket booster initiation should come from the launcher.
- The rocket booster should be isolated from humidity to preserve good conditions of its propellant and pyrotechnic devices.
- The rocket booster ignition system should incorporate hardware protection preventing activation in captive flight.
- The rocket booster should work employing solid composite propellant.
- The rocket booster should work in the temperature range between -76 °F and 170 °F.

Roll active control (RAC):

- The active roll control should provide missile stability and guidance throughout the flight and be consistent with global missile performance.

Life cycle:

- The missile life cycle is ten years. After that, an extension of 5 years should be guaranteed through an inspection and re-validation plan.
- An inspection and re-validation plan should foresee component replacement along the missile life cycle.

Reliability:

- The missile readiness should be higher than 95%.
- The missile should present a mean time between failure of 150 hours in typical mission conditions.

Interchangeability:

- All subsystems and modules of an exact part number (PN) associated with the missile and ground support equipment should be interchangeable without any additional adjustment.
- All missile's mechanical components subject of mounting and dismounting procedure should be interchangeable between operational and training versions.
- The missile autodirector should be interchangeable between operational and training versions.

Transportability:

- The missile project should guarantee safe conditions for air, maritime, and ground transportation.
- The tools, ground support equipment, and test equipment should have dimensions and weigh compatible for aerial transportation.
- For transportation's sake, the warhead and the SAU category are class 1.1, and the rocket booster is class 1.3.

- When transporting the missile assembled, the weapon classification is class 1.1.

Storage:

- It is mandatory the definition of storage conditions and handling procedures of each component.

- The industry must define if the missile is stored as a whole or in pieces.
- In case of storage in pieces, all subsystems should have adequate cases.

Marking and Painting:

- It is mandatory for the identification of missile components that part number and serial number stand easily readable.

Calibration:

- The missile should not require external calibration for launch.

Built-in test:

- The missile should incorporate a pre-flight self-test at Organizational Level (O-Level) and reports the result through the umbilical connector.

Safety:

- The missile should contain the necessary safety devices for handling.
- Sharp edges and pointed parts should receive adequate coverage for handling.
- The following safety devices should be consider in the missile's project?
 - a. A mechanism for manual clearance of the explosive buster train, providing alignment before launch and not aligned condition when stored.
 - b. The SAU should allow the warhead deployment only in flight after a characteristic acceleration and after crossing a safety distance from the launch platform. The mechanic misalignment of the explosive train must grant the safe condition in the not armed status.
 - c. It is mandatory the definition of a specific procedure for the hypothesis of a launch failure.
 - d. The missile should have electromagnetic compatibility with the launch platform.

Electromagnetic Interference:

- The missile should not prompt electromagnetic interference to the launch platform.
- It is mandatory to undertake an environmental test for electro-explosive devices.

Temperature:

- The temperature range for storage should varies between -40°C to 71°C.
- The temperature range for deployment should vary between -70°C to 71°C.

Project and Construction:

- The processes applied throughout the phases, manufacture, and tests must follow the company standard procedures.
- The attachment of assembled missile to the launcher platform should not require any additional adjustment.
- All subsystems and modules with the same part number should be interchangeable without and further adjustment.

Product Manufacturing:

- The industrial development process defined for manufacturing the missile components should follow all technical requirements set by the client.
- The missile project should prevent the operator from incorrect assembling, plugging connectors and cables wrongly, or inverting connectors.
- The weaponry system items should not produce hazardous or restraining interference within this system or over other systems such as the launcher platform system.
- The following processes should observe related airspace manufacturing techniques:
 - a. Machining of mechanical parts,
 - b. Integration of electrical, mechanical, and optical components,
 - c. Weld of electric terminals,
 - d. Weld of mechanic components
 - e. Manufacturing of wiring, connectors, and printed circuit board.
 - f. Only qualified personnel should carry out Weapon systems manufacturing, observing specific training in each respective area.

Project Techniques:

- When developing the weapon system, it is mandatory to use related technical standards to avoid system degradation in a high-density electromagnetic field.
- The weapon system components should not cause harmful interference from one to another or over other systems such as the launch platform.
- The following project techniques should be considered, among others:
 - a. Signal filtering to satisfy emission requirements.
 - b. Electromagnetic isolation for subsystems, boards, and components resulting in protection like a Faraday's cage.
 - c. The usage of the metal boards between printed circuit boards.
 - d. Optical coupling mainly for the emission of high power control signals.

- e. Techniques for wiring interference reduction.
- f. Wiring assembling in accordance to type and level of the transported signal.
- g. Avoidance of long cables for low voltage signals. Instead, consider the positioning of pre-amplifiers as close as possible from the signal source.
- h. Adoption of the shortest cable length possible for high-power electric subsystems and components and high electric current.
- i. Wiring oriented to minimize the distance between signal emission and reception.
- j. The proximity between wires conducting weak and robust signals should be avoided. If necessary, these types of wires should cross in orthogonal intersections.
- k. The use of the grounded shield in high emissivity lines.
- l. Impedance balancing mainly for differential signals.
- m. Unless strictly necessary, ward off the high-frequency signal passing through micro-processor buses, cables, or connectors, assuring otherwise these components are adequate and tested for this condition.
- n. It would be better to use the single grounded point per module, as that its feed line and return remain in the same source.
- o. It would be better to isolate grounded devices for low and high power signals.

The wiring project for pyrotechnical devices should follow special care:

- a. Adequate barriers to protect components against radiation and electromagnetic Induction.
- b. Wiring should remain to short-circuit until the pyrotechnic devices become armed.
- c. The circuit wiring that commands pyrotechnics should be twisted for noise reduction and electrical properties preservation.
- d. Isolation from other circuits to avoid coupling.
- e. Prevent the container of pyrotechnic devices from working like a radiation resonant cavity that trespasses the missile hull.
- f. Use of a high-level signal to start burning the pyrotechnical device.
- g. The project should provide ways to forestall misassembling, misconnections, or cable inversions.

Logistic:

See logistic requirements.

Industrialization:

Development phase

- The development prototypes should provide the necessary information for project validation or adjustments.

- The prototypes flight tests should demonstrate the fulfillment of the general requirements.

- The development prototypes are not adequate for final acceptance regarding the performance or functionality established in the requirements.

Qualification phase

- The qualification prototypes should prove the accomplishment of technical requirements and missile' specifications.

- The manufacturing of the qualification prototypes should follow the specific technical dossier for the missile project defined in the timely notice by the customer.

Pre-serie

The pre-series prototypes' manufacturing should follow the specific technical dossier for missile configuration defined in the timely notice by the customer.

Serie

- The series prototypes' manufacturing should follow the specific technical dossier for missile configuration defined the timely notice by the customer.

- The series' missile should reach all operational capabilities defined in the requirements.

Training

- The captive training missile should use the same guidance system as the series missiles (for air to air version only).

- The captive training missile should have the same interface (mechanical, electric, and logical) to the launcher as the series missile.

- The captive training missile should present the same functionalities in simulations as the series missile.

- The warhead, SAU, booster, surfaces actuator, and RAC subsystems for the captive training missile should be non-functional modules and inert for simulations on board.

- The captive training missile should not execute a launch command received from the launcher interface.

- The captive training missile should have the same characteristics as the series missile:

- a. External dimensions; b. Center of gravity; c. Mass moment of inertia; d. Rigidity; e. Mass.

Missile for Educational Purpose

- It should provide the internal details of the series missile through a cut of sections.

- It should be assembled with inert materials that are similar to the active materials of the series missile.

- The electronic parts should be non-functional copies of the exact dimensions of those from the series missile.

- Structural cuts should provide a view of the internal parts of interest.

- It is desirable the availability of this missile also in Computer-Based Training - CBT.

Tests and evaluation for development

- Should provide information for the project's validation and adjustment, including missile subsystems.

- All evidence of requirement fulfillment verified should feed the certification process to decrease the effort at this phase.

- All launched prototypes should carry on-board telemetry.

Tests and evaluation for certification

- All missile's requirements, including its subsystems, should be verified in flight, except:
 - a. Those defined to reach the requirements on the ground test.
 - b. Those demonstrated in the test and evaluation for development.

- All launched prototypes should carry on-board telemetry.

Work Breakdown Structure (WBS)

- The company in charge of developing this project should prepare and submit a Work Breakdown Structure for approval.

- This structure should ultimately define the project's activities, going over the development, production, and logistic support phases. It should mirror the services and others tasks expected for the project's life cycle.

- The company should implement this Structure at the beginning of the development phase.

- This Structure should contain the product development activities, logistic support development, and responsibilities.

Statement of Work (SOW)

- The company in charge of developing this project should elaborate a detailed Statement of Work.

- The Statement of Work conception should keep consistency with the Work Breakdown Structure.

Technical Publications

Descriptive Functioning Report (DFR):

- The DFR should contain, at least, all calculation memorials, specifications, test reports, and analysis.

Engineering Descriptive Report (EDR):

- This report should contain the product description, drawings, source code, schemes, and all necessary documents to specify each item precisely and its parts.

- The EDR should contain the software for simulations, algorithms, and necessary instructions to set up the launch platform with algorithms for trajectory simulations.

Certification File

- The Certification File should contain the Certification Plan and all supporting documentation regarding the certification requirements.

Development Plan

- This Plan should define tasks, schedules, activities, and responsibilities.

- Should also define the development activities, the product engineering, and the certification process, reaching all project phases, integration, and systems tests.

- The Development Plan should define revision meetings and formal auditing.

Configuration Management Plan

- The company should submit the final version of the Configuration Management Plan to the certification body indicated by the customer within 30 days after the contract signing.

- The Configuration Management Plan should contain the development, production, and missile operation.

- The Configuration Management Plan should list the critical processes of manufacturing.

Certification, Qualification and Tests Plan

- The Certification Plan should describe the procedures and methodologies for verification and proof before the Certification Body, for compliance with the requirements that form the Certification basis, and this requirement, as well as the activities schedule.

- The Certification Plan should include information regarding specifications and projects of the production chain.

Functional Tests:

- The Functional Tests should aim to aid the development of weapon system items to reach functionality within the project activities.

Environmental Tests:

- The missile's modules should pass through a sequence of environmental tests that grant adequate performance under operational conditions.

Certification Tests?

- The Certification Test should demonstrate the systems and subsystems and weapon systems critical items achievement.

Acceptance Tests:

- The Acceptance Test should confirm the achievement of specifications described in this requirements of weapon systems. The tests include weapon systems working jointly with their interfaces in operational conditions.

Quality Assurance (Development Phase)

- The company should demonstrate the existence of a quality system that complies with ISO 9000 standards applicable to this project, covering all areas associated with development and missile's final production.

- Throughout the contract term, this quality system should be ready, working, and approved by the governmental quality assurance body of the country where the company has its factory.

- The company should contract suppliers that follow quality systems aligned with the prime contractor's standards and are able to furnish material and services that comply with the requirements defined in the contract.

Logistics requirements - Sizing parameters:

- The logistic support development should make part of project activities.

- The logistic support should keep the missile operational performance, and specified availability with regard to the use phase in the life-cycle.

- It is recommended that logistic support provides cost-optimized system availability.

- The sizing parameters should only provide guidelines for the dimensioning and conception of the missile's logistic support. These parameters do not entail any commitment for production acquisition.

- The logistic support planning should cover the factory third-level maintenance.

- The missile's availability should be over 95%.

- The missile's life expectancy in the use phase should be greater than ten years.

- The company should consider the support tools and means available at the customer's logistic system to avoid unnecessary redundancy.

- The customer should receive all calculations regarding missile deployment logistics support, considering aspects such as war effort, deployment, and the necessity of spare parts, specifying:

- a. Maintenance;

- b. Supply;

- c. Ground Support Equipment;
- d. Facilities;
- e. Personnel.

Integrated Logistics Support Plan (ILSP)

- Regarding the necessity of the logistics, the missile furnishing should cover an ILSP considering the entire life cycle.

- A Contractor Logistics Support (CLS) renewable entirely or in part is necessary to define the ILSP's parameters.

-To support the missile's deployment, maintenance, and ground support equipment, the ILSP should comply with the following activities:

- a. On the site service;
- b. On-call support;
- c. Tests to confirm defective or malfunctioning equipment;
- d. Technical visit to vendors;
- e. Fault investigation;
- f. Support for technical doubts;
- g. Configuration management;
- h. Publication update;
- i. Repair scheme;
- j. Weapon system's reliability analysis;
- l. Emergency support system for spare parts replacement.

- The ILSP should describe the planning, management, execution, control, interfaces, and the entire integrated logistics support, considering the adequate detail level to meet all requirements related to:

- a. Training program;
- b. Initial supply list (ISL);
- c. Ground Support Equipment (including test equipment and tools);
- d. Packing for handling, store, and transport;
- e. Data collection;
- f. Technical publication;
- g. Warranty;
- h. Technical support;

- i. Planned obsolescence;
- j. Infrastructure;
- l. Reliability;
- m. Maintainability;
- n. Availability;
- o. Supply;
- p. Cataloguing;
- q. Contractor Logistics Support.

Initial Supply List (ISL)

The company will provide an ISL including, but not limited to the following subjects:

- a. Demand for bulk material, repairable spares, accessories, ground support equipment, including test equipment, tools, calibration equipment for deployment and maintenance in first and second maintenance levels.
- b. Frequent displacement to remote sites;
- c. All ISL items should meet the availability required for missile deployment,
- d. The company should provide the logistics modeling guideline applied to define the ISL.
- e. The company should offer a buy-back program or equivalent option regarding the ISL items that present an underestimated consumption rate in the first five years of operation after missile acceptance into service.

Life-Cycle Cost Analysis

The company should elaborate a life-cycle cost analysis on the missile weapon system.

This analysis should include:

- Cost Breakdown Structure (CBS);
- Deemed cost components based on adequate logistics engineering and management reference.

Test Equipment

- The test equipment should be able to analyze all electrical and logic interfaces.
- The test equipment should be available with the necessary publication and frequent actualization to orient the calibration activities.
- The test equipment should meet the requirements for airlift;
- Should be able to verify the output voltage and current levels fed by the electrical source at the launcher platform.

- Should be able to perform analysis on the auto director and the electronic control section;

- Should be able to induce command to the actuators evaluating the sensors signals correspondent to the control surfaces positioning.

- The auto director test should verify the detectable view angle compared with the accurate angle.

- The test equipment should verify the booster electrical components' condition.

- The test equipment should allow the proximity fuse range measurement.

- Should allow the subsystems auto-test;

- All go/no-go test should be concluded within 10 minutes;

- Just one person should perform all go/no-go tests.

Ground Support Equipment (GSE)

- The GSE should be painted and receive anti-corrosion treatment.

- The GSE should be airlift compatible.

- The GSE should be delivered with adequate publication for operations and maintenance purposes.

Logistics and Reliability

- The weapon system, including the series and training missiles, and the GSE should have reliability higher than 95% performing the typical mission.

- The missile should withstand 300 on/off cycles without losing its reliability. This condition should not require preventive or corrective maintenance.

Maintenance

- The on-condition maintenance concept should be applied to restrain the preventive maintenance activities that threaten the platform and operator safety.

- An interval of at least 500 hours between significant inspections is necessary when the on-condition concept is not applicable.

Appendix C: Risk Management

Regarding the resources with impact on risks, we presented the general definition of each resource and identified specific risks applicable to this project up to the time been.

- Technical risk - Refers to the Technology maturity; definition status of requirements, internal and external interfaces, payloads, operations; availability of margins, support team, project team; etc.

The project could face delays due to the challenges presented by the development of new technology on solid propulsion.

- Economic risk - It is the probability that changes in the greater economy will result in a loss to the project or the organization.

The political environment could impact the economy and consequently harm the project. In this scenario, the budget and sources for funding the project's development will be scarce.

- External risk – This risk category is beyond the project manager's control. Natural disasters and anthropogenic hazards are possible risks to be considered.

The project depends on laboratories. Limited access due to floods or even accidents are possibilities to be considered.

- Human error – Stands for mistakes in the planning or executing of a task that fails to meet a goal.

The possibility of human error in the project's conceptual phase is minimal but not negligible.

- Investing risk – It refers to the potential impacts due to investment, assets or portfolio losses in value [78].

Limited available funding and inflation could restrain the completeness of the project.

- Liquidity risk - The liquidity risk refers to the potential Lack of trading capacity of an entity due to cash constraints and consequent difficulties to meet obligations. In many cases, capital is locked up in assets that are difficult to convert to cash [79].

- Passive risk - Refers to a potential for losses due to inaction.

A weak effort to disseminate this study could entail acquiring a similar missile in the international market to the detriment of a national solution.

- Political risk - Refers to the possibility that political facts or events impact project development resulting in losses [78].

For instance, presidential elections could invert a tendency to contract new systems to the armed forces.

- Pure risk - Refers to an unpredictable risk that can only result in losses. This term is used to differentiate between speculative risk taken for a chance of a gain and risks inherent in a situation but never positive [80].

An event of a fire in laboratories or unemployment condition would impact the schedule leading to a significant delay in the development process.

- Reputational risk - Refers to the chance of a loss due to damage or a decline in institutional or personal reputation [81].

- Revenue risk - Refers to an uncontrolled potential event or condition that negatively impacts future revenue [82].

- Speculative risk - Refers to action or inaction that has the potential for both gain and loss.

- Strategy risk - Refers to the chance that a strategy will result in loss.

The concentration of development effort seeking to satisfy the necessity of just one client (the Brazilian Navy) could reduce the chances of success.

Another crucial aspect is the selection of the project chief design. It could make the difference between success and failure.

- Systemic risk - Refers to the probability of losses due to the collapse of a financial system such as the global economy or the economy of a single nation. This risk is negligible for the project.

- Upside risk - Refers to the possibility that an asset or investment will increase in value beyond the expectation.

An international conflict involving Naval Warfare against Brazil would expedite the development and sales of the weapon.

- Compliance risk - Refers to the potential impact for a organization or project due to non-compliance with legislation [78].

This risk does not apply to the project at this phase.

- Country risk - Refers to the potential for losses due to investments or business activities in a particular country.

The elections process could result in economic fluctuations and impacts on the budget. This scenario could hamper sales for the Brazilian armed forces.

- Dread risk - This is a specific risk that people have a strong aversion to. In this case,

people are often willing to spend far more to reduce a dread risk than a regular risk.

Fratricide or friendly fire is an example of dread risk possible to happen during operational deployment of the project.

- Good risk - Refers to an attractive condition for organization, and managed by methodical process [78].

Despite the project’s objective in developing an anti-ship missile, there is a calculated risk regarding the interest of others buyers than the Brazilian Navy, such as the Brazilian Air Force and Brazilian Army, not to mention foreign armed forces.

- Legal risk - Refers to the possibility of damage as a consequence of regulatory or legal action [83].

This risk should be investigated and ranked later by the buyers.

- Project risk - It is the potential of a project to fail.

In the conceptual phase of this project, the following risks are likely to happen:

- a. The architectural design fails to satisfy the requirements;
- b. The unauthorized use of information could harm the project.;
- c. The project will not deliver as much feature as required;
- d. A partner will fail to deliver on their obligations; and
- e. Technology applied in the project becomes outdated.

- Supply risk - Refers to the probability that an inbound supply will disrupt an activity. This risk includes issues with suppliers, shipments, and markets [84].

It is possible to occur delays due to a shortage of components for laboratory experiments.

It is also possible that import license denials increase the overall project’s cost.

Risk index	Risk magnitude	Proposed actions
E4, E5, D5	Very high risk	Unacceptable risk: implement new team process or change baseline – seek project management attention at appropriate high management level as defined in the risk management plan.
E3, D4, C5	High risk	Unacceptable risk: see above.
E2, D3, C4, B5	Medium risk	Unacceptable risk: aggressively manage, consider alternative team process or baseline – seek attention at appropriate management level as defined in the risk management plan.
E1, D1, D2, C2, C3, B3, B4, A5	Low risk	Acceptable risk: control, monitor – seek responsible work package management attention.
C1, B1, A1, B2, A2, A3, A4	Very low risk	Acceptable risk: see above.

Fig. 11: Risk index: combination of severity and likelihood

Task 2 comprises the definition of risk management plan. This plan provides all elements necessary to ensure that the implementation of risk management commensurate with the project, organization, and management, while meeting clients requirements.

In this topic, we will present the necessary information to elaborate the risk management plan in later phases of the project.

The risk management plan should observe the orientation provided by the European Cooperation for Space Standardization, mainly the ECSS-M-ST-80C, released on July 31st, 2008, and the ECSS-M-ST-10C-Rev.1, released on March, 6th 2009.

The definition of each participant's duties and responsibilities in implementing the risk management plan depends on the phase of the project. It will require frequent updates to include new participants. At this conceptual and academic phase, the researcher is responsible for pushing forth the risk management plan concepts vis-a-vis the risk management policy previously described in this study.

The plan should provide a risk management process detailing continuous risk identification and assessment, evaluation, handling, and controlling procedures. In addition, the process defines the results documentation and follow-up activities.

One way to meet the risk management process requirements is implementing a framework containing at least the following documents:

- List of possible risk sources and categories,
- Impact and probability matrix,
- Risk reduction and action plan,
- Contingency plan, and
- Risk threshold and metrics.

Finally, a risk monitoring and communication cycle should provide the operational approach to track, monitor, update, iterate, and spread information on the status of each risk identified. For efficiency sake, the cycle must define documents format, responsibilities, and frequency of reports.

Step 2: Identify and assess the risks

Identifying risk scenarios based on step 1 outputs allows the magnitude's assessment of individual risks and their rank. Thus, by categories, a list of risks plotted at this project phase is adequate to develop task 3 (Identify risk scenarios).

Therefore, five categories provide a structured risk division under specific areas likely to deal with threats.

Technical

T1. The project could face delays due to the challenges presented by the development of new technology on solid propulsion.

T2. The possibility of human error in the project's conceptual phase.

T3. Fratricide or friendly fire is a dread risk possible to happen during operational deployment of the project.

T4. The conceptual design could fail to satisfy the requirements.

T5. The project could not deliver as many features as required.

T6. Technology applied in the project could become outdated.

External

E1. A political turnaround could impact the budget for the development of the project.

E2. The project depends on the University of Brasilia's laboratories. Access limitations to these facilities could impact project development.

E3. Cuts to the budget and inflation could lengthen the term of the project delivery.

E4. An international conflict involving Naval Warfare against Brazil would expedite the development and sales of the weapon.

E5. A partner could fail to deliver on their obligations.

Organizational

O1. An event of a fire in laboratories would impact the schedule leading to a significant delay in the development process.

O2. A lack of supplies for laboratory tests could delay the development phase.

Project management

P1. Little disclosure of this study could entail acquiring a similar missile in the international market to the detriment of a national solution.

P2. The project's objective of developing an anti-ship missile fired from a maritime platform could prompt the exclusion of other buyers, such as the Brazilian Air Force and Brazilian Army, not to mention foreign armed forces.

P3. Classified information Leakage could harm the project.

Cost

C1. Import license denials will increase the overall project cost.

All this information is now processed in task 3, which includes identification of risk scenarios, identification of the means of early warning (detection) for the occurrence of an undesirable event, and Identification of the project objectives at risk.

Task 3: Identify risk scenarios

This step brings up risk identification by category, suggesting a way to detect and point the project's objective at risk.

Table 7 details the necessary measures for Technical and External risks.

An essential characteristic of risk is its evolution. Some of them may disappear, and new ones may arise, which demands a frequent re-examination of the planning.

Table 7: Risk identification (Technical and External)

Risk	Identification of risk scenarios	Means of early warning	Objectives at risk
T1	Cause: studies in progress. Consequence: unforeseen activities.	Keeping up with related re-search studies.	schedule
T2	Cause: uniqueness and procedures yet to be established. Consequence: delay	Supervision	Project reliability.
T3	Cause: Operational mistake. Consequence: Casualties	Supervision	Project reliability
T4	Cause: System engineering. Consequence: Fall short of expectations	Supervision	Technical characteristics project reliability, and scope
T5	Cause: Technical challenges. Consequence: low performances	test and simulations	Scope and cost
T6	Cause: Discoveries. Consequence: project outdated	Tendency analysis	Cost and technical characteristics
E1	Cause: Political. Consequence: project discontinuity	Tendency analysis	Qualification and production
E2	Cause: Force majeure. Consequence: delay	Safety assessment	Schedule
E3	Cause: Economic. Consequence: delay	Tendency analysis	schedule
E4	Cause: International crisis. Consequence: Demand to anticipate deliveries	Tendency analysis	schedule
E5	Cause: lack of supply. Consequence: delay	Supervision	Schedule

For risk possibilities regarding areas such as organizational, project management, and cost, table 8 presents a list of foreseen impacts and recommended measures to reduce or eliminate the risk associated.

It is worth mentioning that action before a crisis strikes can be decisive for the project's success. Thus, risk management should seek to anticipate actions through adequate planning. Such a plan requires examining multiple scenarios, giving more attention to those with a higher probability of occurrence. The plan should also provide adaptation and flexibility margin. No crisis repeat the same patterns of previous one. Finally, continuous review of potential risks is strenuous, but a crisis could lurk just around the corner, which can make the difference between project success or failure.

Task 4: Assess the risks

Considering the criteria shown in Tables 1 and 2 and table 9, it is possible to allocate the severity, likelihood, and magnitude dimensions for each risk scenario, signaling the proper

Table 8: Risk identification (Organisational, Project Management. and Cost)

Risk	Identification of risk scenarios	Means of early warning	Objectives at risk
O1	Cause: lightening, spontaneous short circuit, and gas leakage. Consequence: delay.	Supervision	schedule
O2	Cause: export denials. Consequence: delay	Previous analysis of related cases	schedule
P1	Cause: little publication in defense and technology magazines. Consequence: Lack of new clients	Supervision	Production
P2	Cause: Choice on specific client Consequence: Difficulties to reach new clients	Marketing management	Production
P3	Classified information leakage Consequence: Prejudice to copyright and related rights.	Supervision and restriction on access to documents.	Copyright
C1	Cause: Changes on foreign trade legislation. Consequence: delay.	Scan legislation update continuously	Schedule

Table 9: Risk assessment [1]

Risk	likelihood	Severity	Magnitude	Proposed action
T1	C	2	Yellow	Keep up with new studies
T2	B	1	Green	Chose an expert for chief design
T3	B	1	Green	Attention to safety weaknesses
T4	B	4	Yellow	Employ qualified and tested systems
T5	D	4	Yellow	Effort in training
T6	A	3	Green	Present alternatives to the client.
E1	D	3	Yellow	Elaborate on a contingency plan
E2	B	2	Green	Same action
E3	C	4	Yellow	Same action
E4	A	3	Green	Same action
O1	B	1	Green	Consider using alternative infrastructure
O2	E	3	Red	Consider developing critical components or altering suppliers
P1	B	3	Green	Publicize the project
P2	d	3	Yellow	Publicize
P3	d	4	Red	Define an information access plan
C1	d	3	Yellow	Substitute components or change suppliers

actions.

Table 9 details the risk assessment.

The occurrence of the risk T3 (fratricide or friendly fire) is not relevant to this phase. Therefore, this risk will be subject to further analysis.

Appendix D: EES Code for Missile Profile Design

The project's source code is available in the following online repository: <https://github.com/Brigverissimo/EES-Code-fro-ramjet-missile>.

The missile sizing based on Nowell's correlations is available in the following online repository: <https://github.com/Brigverissimo/Missile-sizing>

The internal ballistic code estimations are presented through an EES diagram window that shows the program input and output. The mentioned code is available in the following online repository: <https://github.com/Brigverissimo/INTERNAL-BALLISTIC-CODE>

Appendix G: Accepted Publication

Paraffin-based ramjet missile preliminary design

Rogério L.V. Cruz¹, Carlos A.G. Veras^{*1} and Olexiy Shynkarenko²

¹*Mechanical Engineering Department, University of Brasília,
Campus Darcy Ribeiro, 910-900 Brasília-DF, Brazil*

²*Department of Aerospace Engineering, University of Brasília, Gama Leste, 72444-240 Brasília-DF, Brazil*

(Received February 15, 2023, Revised July 5, 2023, Accepted July 12, 2023)

Abstract. This paper presents a basic methodology and a set of numerical tools for the preliminary design of solid-fueled ramjet missiles. An elementary code determines the baseline system configuration comprised of warhead, guidance-control, and propulsion masses and geometries from specific correlations found in the literature. Then, the system is refined with the help of external and internal ballistics codes. Equations of motion are solved for the flight's ascending, cruising, and descending stages and the internal ballistic set of equations designs the ramjet engine based on liquefying fuels. The combined tools sized the booster and the ramjet sustainer engines for a long-range missile, intended to transport 200 kg of payload for more than 300 km range flying near 14,000 m altitude at Mach 3.0. The refined system configuration had 600 mm in diameter and 8,500 mm in length with overall mass of 2,128 kg and 890 kg/m³ density. Ramjet engine propellant mass fraction was estimated as 74%. Increased missile range can be attained with paraffin-polyethylene blend burning at near constant regression rate through primary air mass flow rate control and lateral 2-D air intakes.

Keywords: aerodynamics; liquefying fuels; ramjet preliminary design; solid-fueled ramjet propulsion

1. Introduction

The Brazilian Exclusive Economic Zone, an offshore area spanning 3.6 million square kilometers, poses complex surveillance and defense challenges for the Brazilian Navy. To ensure its protection, the deployment of state-of-the-art anti-ship weaponry is necessary. As part of this effort, the Brazilian industry (AVIBRAS) is currently qualifying a long-range subsonic missile (300 km) propelled by a gas turbine jet engine (ASTROS, 2014). In addition, ongoing research is being conducted by the Institute of Aeronautics and Space (IAE) and the Institute for Advanced Studies (IEAv) to develop hypersonic technology, as discussed by Martos *et al.* (2017). While Brazil has successfully developed and operated a broad range of sounding rockets based on solid propellant technology (Garcia *et al.* 2011), the country has limited experience in developing supersonic missile technology. Furthermore, only a few academic institutions are currently working on ramjet propulsion, which cannot be commercialized or transferred between countries in compliance with the directives of the Missile Technology Control Regime (Sidhu 2007).

The University of Brasília has been investigating ramjet and hybrid rocket propellant technology for over 20 years, as reported in Bertoldi *et al.* (2022). Recently, Shynkarenko *et al.*

*Corresponding author, Professor, E-mail: gurgel@unb.br

(2019) presented a novel test bench and associated methodology designed to investigate advanced propulsion technology for rockets and ramjets. The apparatus is capable of handling various propellants, including solid paraffin, high-density polyethylene, methane, and kerosene, with high-temperature air streams (ramjets), GOx, and N₂O (rockets). The research team has also focused on the development of numerical tools for the design and optimization of long-range tactical missiles (Neiva, 2016), launch vehicles (da Cás *et al.* 2019), and other propulsion systems (da Cás *et al.* 2012). Apart from that, no published work on the open international literature has addressed the design of long-range surface-to-surface missiles based on liquefying fuels. Here, we present a set of numerical tools for the preliminary design of supersonic anti-ship missiles. A preliminary code predicts baseline missiles' main subsections extracted from published correlations. An external ballistics code integrates the trajectory equations covering the flight's ascending, cruising, and descending stages and an additional code helps design the solid-fueled ramjet sustainer. Then, through a series of refinements, these combined codes are used to identify a preliminary missile configuration that meets the system's mission requirements. The primary focus of our efforts lies in the design of the booster and the ramjet sustainer engines, with the latter being based on solid paraffin-polyethylene blends.

2. Tactical missiles and ramjet propulsion

2.1 Tactical missiles

Missiles are self-propelled guided weapons classified as strategic or tactical, depending on their purpose, type of warhead, flight range, cost, inventory, and frequency of use for combat or deterrence scenarios (Fleeman 2012). The Brazilian coastal line stretches approximately 8.5 thousand kilometers and accommodates 80% of the country's population. This narrow strip of land runs alongside the entire shoreline, encompassing sixteen out of the twenty-seven state capitals, crucial ports and airports, two rocket launch bases, as well as oil and gas complexes comprising pipelines and offshore drilling refineries. Additionally, it serves as the primary infrastructure hub for maritime routes used in international commerce. To underscore the significance of this region, the Brazilian National Defense Policy emphasizes the strategic importance of the South Atlantic region, with the Brazilian Navy designated as the leading authority responsible for safeguarding all coastal assets, as outlined in the National Strategy of Defense (Decreto 2008). Currently, Brazil is developing the MANSUP, an anti-ship subsonic missile that may have limited effectiveness against a well-defended naval task force in certain scenarios. Therefore, it is crucial to consider the development of missiles with improved range and speed to address this limitation.

As discussed in Dutta (2014), the attacking missile detection range is a function of the radar cross-section, radar height, and the ASCM flight altitude. Therefore, low altitude flight, small diameter missiles traveling at very high speed implies less time to interception, increasing the probability of hitting the targeted ship. High-speed flight ($M \geq 2.5$) at low altitude causes excessive drag forces and occurs at enormous air stagnation temperature and pressure. For such high speed, cruising stage should take place at high altitudes.

For the preliminary design, the study should focus on concepts, theory, and initial assessment that precede the industrial stage. In this work, we presume that the Brazilian Navy is the primary customer. The European Cooperation for Space Standardization (ECSS 2022) recommends splitting new projects into seven phases (0, A-F), which are planned by the main stakeholders,

ranging from top-level customers to lower-level suppliers. As the top-level customer, the Navy should define system needs and performance criteria and actively participate in the execution of preliminary studies to guide Phase-zero of the missile development life-cycle in accordance with the ECSS recommendations.

2.2 Ramjet propulsion

In a solid-fueled ramjet, the system geometry is governed by the fuel-burning regime. The fuel regression rate depends on the heat transfer from the combustion zone to the solid grain and mass transfer from the grain surface to the burning region. These processes are complex and cannot be solved analytically as reviewed in Karabeyoglu *et al.* (2004). The literature describes mechanisms and ballistic models for liquefying (paraffin) and non-liquefying polymeric fuels applied to hybrid rocket and ramjet propulsion systems. The most known of these models gives the relationship between the regression rate and oxidizer mass flux in the form of

$$\dot{r} = \frac{dr}{dt} = a G^n \quad (1)$$

In Eq. (1), the empirical constants (ballistic coefficients) “*a*” and “*n*” are positive and *G* is the average oxidizer mass flux through the grain port. Since the grain’s port area grows during the flight, the regression rate decreases for constant oxidizer mass flow rate. The integration of the \dot{r} function along engine operation determines the instantaneous average grain thickness and its final diameter. Therefore

$$D_{iam}(t) = D_{ini} + 2 \int_{t_{i,r}}^{t_{f,r}} \dot{r} dt \quad (2)$$

The ballistic coefficients depend on the fuel and oxidizer compositions, flow structure, and the temperature of the hot air compressed through the ramjet’s supersonic diffuser. For the ramjet’s typical air mass flux range of 10-350 kg/m²s, the regression rate of polyethylene did not exceed 0.3 mm/s (Schulte *et al.* 1987). Motor low regression rate would claim long solid grains, penalizing the propellant mass fraction of the ramjet engine and missiles overall weight. The fuel, however, is a competitive candidate for long-range missiles since it can sustain extended operation times, as implied in Eq. (2).

Azevedo *et al.* (2019) observed regression rates in excess of 1.4 mm/s for paraffin-air combustion in an experimental ramjet motor. The high regression rate of paraffin suggests short grain lengths and reduced engine operating time, thus suitable for short-range missiles. The low melting temperature and grain mechanical strength of pure paraffin may need further assessment when applied to missile systems.

Fig. 1 shows pictures taken from the experimental test campaign conducted by Azevedo *et al.* (2019). As it can be seen the initial burn of paraffin in air takes place in lean combustion regime (Fig. 1A) as the blue clean flame (plume) suggests. Few seconds later, the combustion improves forming a bright yellow flame on account of soot radiation at high temperature. The picture also shows possible paraffin droplets emerging from the lower part of nozzle (Fig. 1B) along with unburnt gas phase by-products (smoke), despite engine overall *FA* ratio set for lean combustion. The liquid layer brought to the nozzle entrance was sprayed in a way similar to conical two-phase flow atomizers. Such fuel losses reduce overall combustion efficiency and facilitates missile

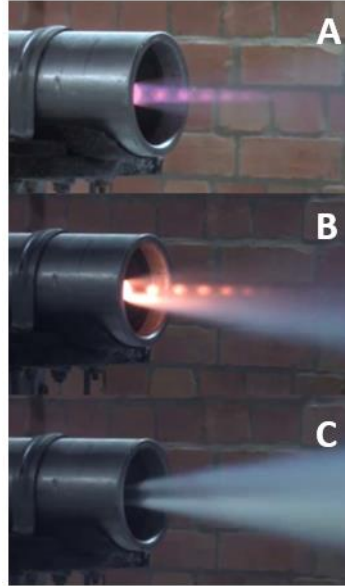


Fig. 1 Paraffin-based experimental ramjet engine at different burning stages.

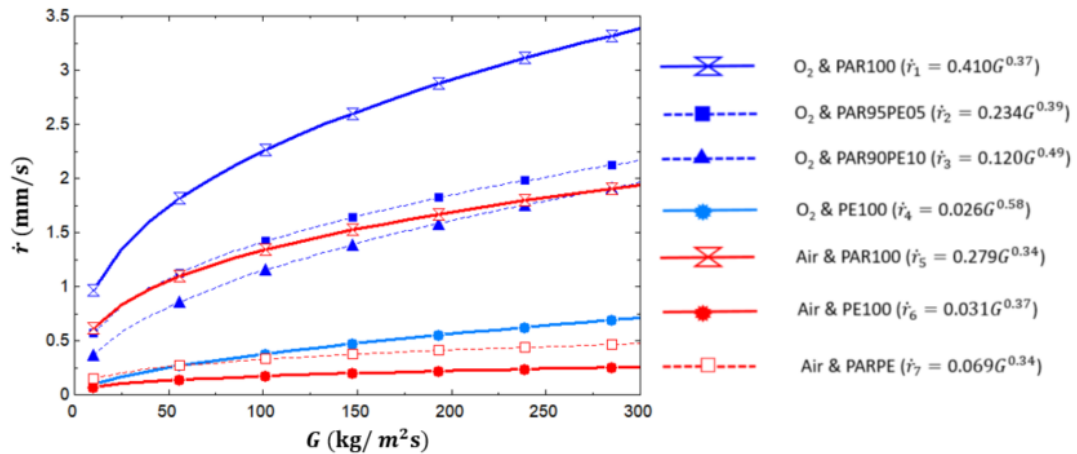


Fig. 2 Regression rate curves for different hybrid (blue) and ramjet (red) engine propellants: \dot{r}_1 to \dot{r}_4 (Kim *et al.* 2015), \dot{r}_4 (Azevedo *et al.*, 2019), \dot{r}_6 (Schulte *et al.* 1987), and \dot{r}_7 (this work)

tracking. The phenomenon was even more pronounced just after combustion extinguishment, as the accumulated liquid layer at the bottom of the grain emerged from the nozzle (Fig. 1C) in the form of long paraffin jet spray. Given the unpredictable mean diameter of droplet entrainment, which contributes to the high regression rate of paraffin, it is crucial to accurately estimate the minimum length required for the motor's post-combustion chamber. This estimation is vital to ensure complete combustion and achieve optimal system performance. Applying the D^2 law (Turns 2011) for liquid droplet evaporation under air flow conditions of 1600 K and 3.0 bar pressure, the recommended post-combustion chamber length is approximately 12 mm, 50 mm, 310 mm, and 1,240 mm for initial droplet diameters of 10 μm , 20 μm , 50 μm , and 100 μm ,

respectively, when issuing near the solid fuel grain exit. These predictions are conservative since the lifetime of the paraffin droplets decreases under oxidizing conditions, implying a shorter post-combustion chamber length. However, these concerns can be eliminated by choosing integrated rocket-ramjet engine technology, which offers increased residence times for droplet combustion within the system.

Fig. 2 shows regression rate curves for different pairs of propellants applied to hybrid rockets and ramjet engines. The ballistic coefficients for pure paraffin (\dot{r}_1), paraffin-polyethylene blends (\dot{r}_2 and \dot{r}_3), and pure polyethylene (PE100) burning with oxygen were taken from Kim *et al.* (2015). Paraffin-air and polyethylene-air ballistic data were taken from Azevedo *et al.* (2019) and Schulte *et al.* (1987), respectively. The difference in regression rates between paraffin and polyethylene is clear, whether applied to hybrid rocket or ramjet engine as shown in Fig. 2. Liquefying fuels have the additional effect of droplet entrainment caused by the melted layer instability. The entrainment rate depends on the liquid fuel properties which changes as the fuel composition is altered. Kim *et al.* (2015) reported decreased regression rate with the addition of only 5% of polyethylene in paraffin, as the curves \dot{r}_1 and \dot{r}_2 show. Further increase in the mass fraction of polyethylene (\dot{r}_3) had less effect in reducing the fuel regression rate. Such trends also hold when the oxidizer is air, as observed by Li *et al.* (2020) who measured regressions rates of 0.198, and 0.218, and 0.927 mm/s for PAR30PE70, PAR50PE50, and PAR100 respectively. In hybrid rocket engine burning with oxygen, Tang *et al.* (2017) reported decrease in regression rate between 10% and 50% as the polyethylene mass fraction in paraffin increased from 1% to 10%. It seems possible, therefore, to find a mix of liquefying and polymeric fuels whose regression rate approaches that of pure polyethylene in a broad range of air mass flux. In the absence of such correlation, we suggest the coefficients $a=0.069$ and $n=0.34$, curve R7 in Fig. 1 for the numerical predictions. As it can be seen, the regression rate (\dot{r}_1) is a weak function of air mass flux in the range of 100 to 300 kg/m²s. The blend would burn slightly faster than pure polyethylene and much lower than pure paraffin, but with improved fuel properties than the latter.

Paraffin-polyethylene blends have improved mechanical strength, higher density and melting temperature, and lower regression rate compared to pure paraffin. Depending on the mission and system requirements, paraffin-PE blend might be the primary choice for the solid fuel matrix for the propulsion of tactical missiles.

3. External and internal ballistics

3.1 Flight equations

Fig. 3 shows the main forces acting on a flight missile whose orthogonal frame is moving. The operational concepts and system architecture follow the aerodynamic, propulsion, and trajectory equations proposed by Fleeman (2012). The flight path estimation is based on a force balance, including thrust (T), drag (D), weight (W), and lift (L) applied to a material point, reducing the system to a two-degree of freedom. In Fig. 1, γ and α are, respectively, the flight path angle and missile angle of attack concerning the rocket axis. We assume that the flight trajectory changes with the help of control surfaces attached to the missile body, and the angle of attack (α) can attain values as high as 40 degrees (Lesieutre *et al.* 1987).

The flight path angle, therefore, changes accordingly. The system of equations of motion proposed by Campos *et al.* (2012) was adapted for missile systems. Missile velocity (V) and pitch

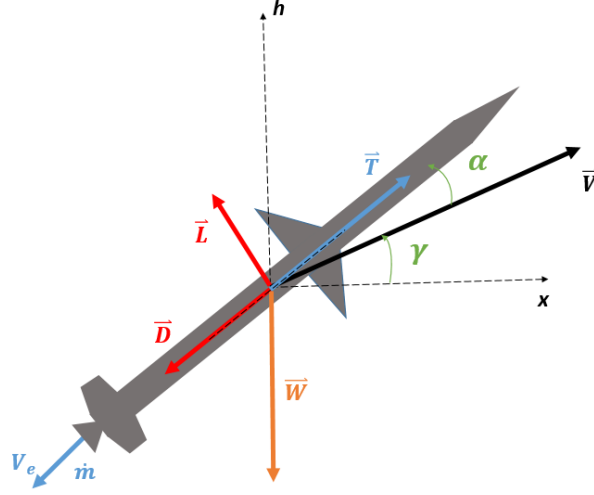


Fig. 3 Forces acting on a flying missile

angle (γ) are obtained after integrating the following equations

$$m(t) \frac{dV}{dt} = -W \sin(\gamma) - D \cos(\alpha) - L \sin(\alpha) + T \cos(\alpha) \quad (3)$$

$$m(t) V \frac{d\gamma}{dt} = -W \cos(\gamma) - D \sin(\alpha) + L \cos(\alpha) + T \sin(\alpha) \pm m(t) V K \quad (4)$$

Since the code is based on two degrees of freedom, rapid changes in pitch angle are accomplished by setting proper values to the constant K in Eq. (4).

The missile total propellant mass changes with time following

$$\frac{dm_p}{dt} = \frac{dm_{pb}}{dt} + \frac{dm_{pr}}{dt} \quad (5)$$

The rate of burning of the booster propellant is assumed to be constant; therefore, the booster propellant mass at time ' t ' is given by

$$m_{pb}(t) = m_{pb}(t_{i,b}) - \dot{c}_b(t - t_{i,b}) \quad (6)$$

for $t_{i,b} \leq t \leq t_{f,b}$. Outside this time range, the burning rate \dot{c}_b is zero. The burning rate of the solid-fueled ramjet, however, may vary with time, then

$$m_{pr}(t) = m_{pr}(t_{i,r}) - 2\pi L_{fuel} \rho_{fuel} \frac{dr}{dt} \quad (7)$$

for $t_{i,r} \leq t \leq t_{f,r}$. Outside this time range, the ramjet burning rate is zero. In Eq. (7), $t_{i,r}$ is larger than $t_{f,b}$, meaning that ramjet ignition takes place only after booster thrust termination. Total mass of the missile is given by

$$m(t) = m_{db} + m_{dr} + m_p(t) \quad (8)$$

In Eq. (8), m_{db} and m_{dr} are the booster and ramjet dry masses. The former separates from the missile just after $t_{f,b}$.

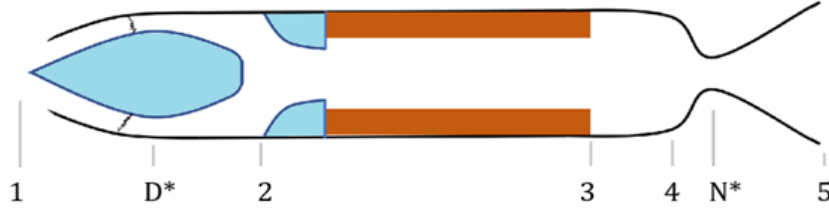


Fig. 4 Ramjet engine main stations

The missile altitude (h) and range (x) are inferred, respectively, by

$$\frac{dh}{dt} = V \sin(\gamma) \quad (9)$$

$$\frac{dx}{dt} = V \cos(\gamma) \quad (10)$$

In the equations of motion, weight, drag, lift and thrust are obtained, respectively, through

$$W = m(t)g \quad (11)$$

$$D = \frac{1}{2} C_d(\alpha) A_{ref} \gamma_{air} P_{air} M^2 \quad (12)$$

$$L = \frac{1}{2} C_n(\alpha) A_{ref} \gamma_{air} P_{air} M^2 \quad (13)$$

$$F = (\dot{m}_{air} + \dot{m}_{fuel}) V_e - \dot{m}_{air} V_{cf} \quad (14)$$

$C_d(\alpha)$ and $C_n(\alpha)$ are the drag and lift coefficients, respectively. A_{ref} is the missile reference area, γ_{air} and P_{air} are, respectively, the air's specific heat ratio and static pressure, and M is the missile Mach number. V_e and V_{cf} are the nozzle exhaust and missile cruise flight velocities, respectively. Drag and lift correlation for the body, fins, and tail were extracted from Fleeman (2012). Wave, ram, and skin drag effects are computed from low subsonic to high supersonic flight.

3.2 Ramjet engine

Fig. 4 presents the main stations of a ramjet engine. Engine main parameters at different stations are obtained after solving a system of equations for mass and energy conservation, assuming ideal gas behavior and isentropic processes, respectively, by

$$\dot{m} = \rho_i V_i A_i \quad (15)$$

$$\sum q + \sum w = (h_{i+1} - h_i) + \frac{1}{2} (V_{i+1}^2 - V_i^2) \quad (16)$$

$$P_i = \rho_i R_{gas} T_i \quad (17)$$

Conservation of momentum is given by Eq. (14) and Mach number is calculated from the flow velocity and the local speed of sound using

$$M_i = \frac{V_i}{\sqrt{\gamma_i R_i T_i}} \quad (18)$$

In Eqs. (15)-(18), i refers to engine stations (1-5) as depicted in Fig. 4. The ramjet internal ballistics code follows that proposed by Struchtrup (2014).

3.2.1 Intake diffuser

An isentropic diffuser is considered in the current design to maximize the ramjet performance. For station $i=1$, pressure and temperature are obtained from the atmospheric condition at the missile flight altitude and velocity. Actual intake pressure recovery is obtained from (NASA 2022)

$$\frac{P_2}{P_1} = \eta_{int} (1 - 0.075(M - 1)^{1.35}) \quad (19)$$

In Eq. (19), η_{int} is the intake efficiency.

3.2.2 Burner and nozzle

The combustion process is considered isobaric and material constraint limits the combustor exit gas temperature (T_3). The solid fuel combustion regime gives the combustor exit area (A_3), which should be dominated by convective heat transfer. At high mass flux, the flame may extinguish due to the small Damköhler number or strong lean combustion process resulting from an excess of oxidizer. Solid fuel burning must occur in the convective heat transfer regime. Energy conservation gives the total heat supplied by the combustor, and the exit burner temperature defines the combustor's overall equivalence ratio adjusting the (FA) ratio.

$$(FA)_{act} = \frac{\dot{m}_{fuel}}{\dot{m}_{air}} \quad (20)$$

The solid fuel mass flux, internal receding area, and density, combined with the average fuel regression rate help determine the fuel grain length

$$\dot{m}_{fuel} = \dot{r} A_{port} \rho_f \quad (21)$$

The thermodynamic states at the burner exit (station 3) define the inlet state of the nozzle (station 4). The stagnation temperature at station 4 is obtained from the balance of energy. The remaining thermodynamic conditions, at N^* and station 5, are obtained following the same steps used to define the diffuser's geometry (Struchtrup 2014).

3.2.3 Solid booster

Booster size and thrust are calculate by the external ballistics code. Booster thrust and propellant burning rate are inferred, respectively, by

$$F_b = W(8g_0) \quad (22)$$

$$Isp_b = F_b / (c_b g_0) \quad (23)$$

Missile minimum acceleration was set to eight g 's as in Eq. (22). Booster propellant mass is obtained from its burning time and rate. Operation time is that to bring the missile from rest to the cruise altitude and velocity. After inferring the mass of the propellant, dry booster mass is obtained from the following equation

$$PMF_b = m_{pb}/(m_{db} + m_{pb}) \quad (24)$$

The booster's specific impulse and propellant mass fraction depend on the system technology maturity. Brazil can produce solid fuel rockets whose propellant mass fraction is 83% with 270 s sea level specific impulse (da Cás *et al.* 2019).

3.3 Numerical solution and code validation

3.3.1 Internal and external ballistics codes

The system of equations was implemented in the Engineering Equation Solver (EES) platform. EES is an equation-solving program that handles thousands of coupled non-linear algebraic and differential equations (Klein and Nellis 2013). It also incorporates a high-accuracy thermodynamic and transport property database for hundreds of substances. The adjunct equations related to the thermodynamic state of the gases are obtained from the NASA polynomials for ideal gases stored in the internal function library of the EES platform. For numerical integration, EES uses a variant of the trapezoid rule along with a predictor-corrector algorithm (Klein and Nellis 2013). In EES, iteration halts when the relative residual of a variable is less than 10^{-6} or the change in variables during successive iterations falls below 10^{-9} . The solver saves the main parameters every second for post-processing mission profile analysis using the EES platform plot menu, including overlay plot capability for predicted performance comparison. The external and internal ballistics codes comprise 96 and 191 algebraic and differential equations, respectively. The solution to the initial value problems is provided through the following equation-based Integral function directive

$$F(t) = F(0) + \text{Integral}(dFdt; \text{LowerLimit}; \text{UpperLimit}; \text{StepSize}) \quad (25)$$

Drag and lift correlations at a given missile angle-of-attack are those listed in Fleeman (2012). All the coefficient equations were programmed as functions and procedures and stored in the EES external library. Drag and lift coefficients are obtained from call statements anywhere in the main code. Similar approach was taken for air density, static pressure, speed of sound, and temperature as a function of flying altitude. The atmospheric earth model (EAM 2022) infers thermodynamic properties with high accuracy up to 50,000 m altitude.

3.3.2 Ballistic codes validation

The internal ballistics code was validated by comparing ramjet engine predictions to those from a multi-platform tool designed for rocket engine analysis (Ponomarenko 2014). In the latter, the equilibrium composition of the combustion products is calculated minimizing the Gibbs free energy of the system for a broad range of rocket operating conditions. Table 1 gives the results from both methods for the combustion of hot air with paraffin wax ($C_{32}H_{66}$). As it can be seen, chamber thrust and effective velocity deviations from the proposed code to the equilibrium code are less than 2%. The chamber geometries are similar, with differences of less than 6.5%. Therefore, the internal ballistics code was deemed adequate for the preliminary design of solid fuel ramjet missiles.

The data of the Aerobee 150A sounding rocket and its mission profile were used to validate the external ballistics code. The vehicle is a four-fin sounding rocket, approximately 9.0 meters long and 38 cm in diameter, consisting of a solid rocket booster and a second stage (sustainer) based on a liquid propellant rocket engine. Comprehensive data on the Aerobee 150A is available in the NASA Technical Report R-226 (Busse and Leffler 1966). The platform was designed to carry

Table 1 Engine performance predictions comparisons

Input/output	Ramjet (Internal Ballistics Code)	RPA	Diff.
Chamber pressure (bar)	4.465	4.465	
Ambient pressure (bar)	0.2644	0.2644	
Inlet air temperature	500.4	500.4	
O/F ratio	26.1/1	26.1/1	
Gross Thrust (kN)	11.89	11.71	+1.52%
Nozzle throat diameter (mm)	156.2	164.76	-5.2%
Nozzle exit diameter (mm)	259.5	276.94	-6.3%
Effective exhaust velocity (m/s)	1,400	1,379	+1.54%

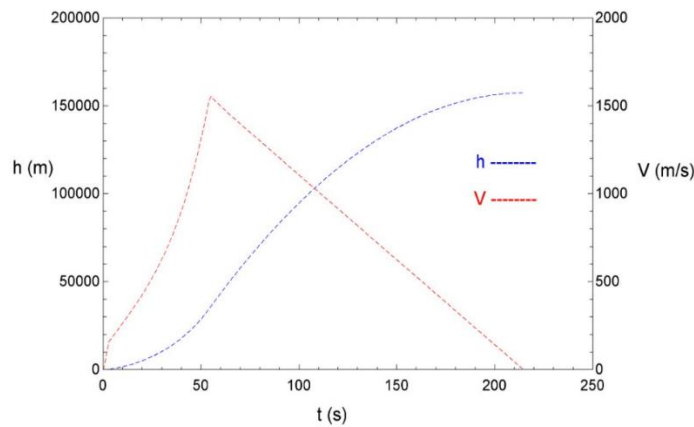


Fig. 5 External ballistics code predicted velocity and climbing profile of the Aerobee 150A sounding rocket

payloads of up to 136 kg to altitudes ranging from 120 to 300 km, depending on the transported mass. Sounding rockets like the Aerobee 150A were launched from the Wallops Island base in the USA. The long operating time of the Aerobee sustainer engine (51.5 s), compared to its booster (2.5 s), bears some resemblance to certain long-range missiles based on liquid ramjet technology, although with distinct mission profiles. The numerical solution predicted the maximum flight altitude reached by the Aerobee 150A as 156 km when transporting a 136 kg payload, as depicted in Fig. 5. This result closely aligned with the reported regular flights of the Aerobee, differing by less than 5% from the reported values (Busse and Leffler 1966). The external ballistics code was thus considered validated and deemed suitable for executing the preliminary missile design phase of long-range missiles.

4. System preliminary design

The top-level customer sets the missile requirements according to its specific needs and expected performance. Considering the Brazilian Navy is interested in new developments, and the country lacks similar systems in its inventory, the task must start with the definition of a basic missile configuration followed by an iterative designing process to improve the solution. Missile range, warhead mass, reference diameter, and flight program are predefined inputs from mission

Paraffin-based ramjet missile preliminary design

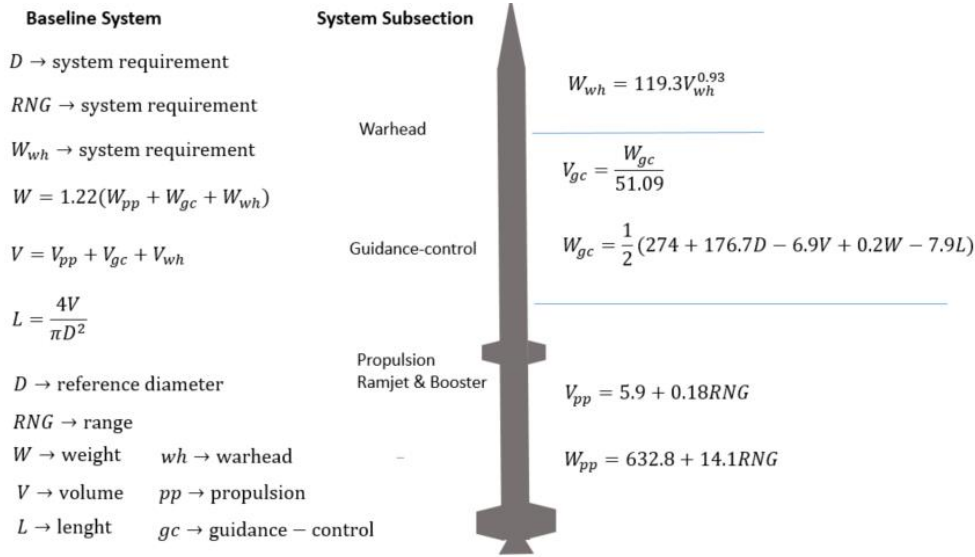


Fig. 6 Baseline missile subsection correlations (Nowell 1992)

requirements (Phase-0) as presented in Fig. 6. The baseline missile’s subsections, masses, and geometries are calculated from published correlations available in Nowell (1992). The correlations in Fig. 6 are in Imperial units (lbm, ft) and the range (RNG) in nautical miles. Guidance-control mass was adjusted using the average mass of a large number of surface-to-surface missiles (274 lbm) and a total spectrum correlation ($R^2=90\%$) where system diameter, volume, length, and mass are the independent variables (Nowell 1992). Auxiliary correlations were also employed for preliminary wing mass and area predictions for the booster and the sustainer, considering short and long-range missiles, respectively. Wing mass is negligible compared to the missile’s total mass. Wing area, however, is relevant for overall system drag estimations.

As depicted in Fig. 5, overall missile mass (W) and geometry (V , L) are obtained by summing the estimated data from its main subsections, i.e., warhead (WH), guidance-control (GC), and propulsion (PP). Warhead and guidance-control subsections must be accommodated in 80% of the missile reference diameter allowing compressed air to flow-by and reach the ramjet combustor. The provision increases the length of the WH and GC subsections accordingly.

Fig. 7 shows the preliminary design flow chart. Phase-0 gives the missile reference diameter (D), warhead mass (W), flight altitude (h) and speed (M), and the expected range (RNG). Applying Nowell’s correlations presented in Fig. 6, the baseline missile total mass, volume and length were calculated from its main subsections.

During system refinement, warhead and guidance-control masses and geometries are kept frozen. Therefore, the main objective of the code was to design the booster and ramjet sustainer engines able to carry out the prescribed system mission. The external ballistics code was then applied to size the booster thrust, dry, and propellant masses. Once the booster mass and geometry were calculated, the initial guess for the ramjet engine mass can be estimated. Preliminary ramjet mass was obtained subtracting the initial mass of the booster from the estimated total mass of the propulsion system from Nowell’s correlations

$$m_r = W_{pp} - m_b \quad (26)$$

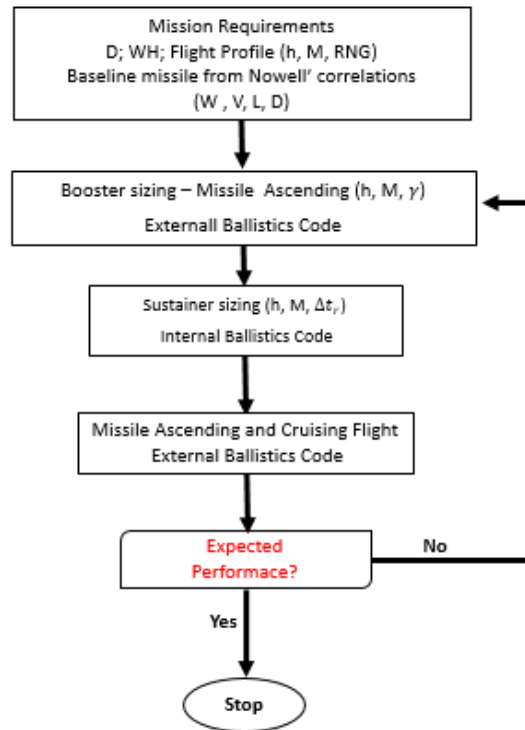


Fig. 7 Flow chart of the missile preliminary design

The sustainer thrust must overcome the total drag forces ($F=D$), which is a function of the system geometry, speed, and flight angle, while lift force must compensate the gravitational force ($L=G$) providing near-constant pitch flight angle ($d\gamma/dt \approx 0$) throughout the cruise phase. The internal ballistics code performs ramjet engine sizing comprised of the solid-fueled grain, post-combustion chamber and main nozzle dimensions. Nozzle contraction area ratio was set to two followed by a conical exit nozzle with a 22° half-angle. A post-combustion section was included to increase the flue gases' residence time for improved combustion efficiency with a diameter-to-length ratio of two. Post combustion chamber is not needed when considering integrated rocket-ramjet configuration, as discussed earlier. Engine dry mass was estimated using the vessel thickness calculation method proposed by Buthod (2001). Ramjet intake area, solid-fuel initial and final diameters, and length were predicted by the internal ballistics code. Ramjet total drag was updated and the external ballistics code executed the missile ascending and cruising phases. Minor adjustments to the combined propulsion system are carried out, and the process was repeated until a converged solution was obtained. The process stops when the missile's total mass alteration is less than 1.0% between two successive refinements. During ascending, the ramjet intake is protected by a conical ogive, which must be ejected before the ramjet motor ignition. Cold booster separation takes place after its propellant mass is exhausted. For some required payload and flight profiles, total missile size and weight strongly rely on the geometry and mass of the combined propulsion system. Therefore, most of the effort in the search process is to determine the optimized sustainer propulsion volume and mass. In most cases, the preliminary design, as claimed by Phase-0, converges after few iterations. Some operational missiles help define the range of parameters for

Table 2 Engine performance predictions comparisons

Data	Baseline	1 st	2 nd	3 rd
Total missile mass (kg)	2,092	2,092	2,116	2,128
Total missile length (m)	7.9	7.9	8.3	8.5
Inlet length (m)	-	0.5	0.5	0.5
Total ramjet length (m)	-	4.5	4.9	5.1
Ramjet engine length (m)	-	-	3.0	3.2
Warhead length (m)	0.64	0.64	0.64	0.64
GC length (m)	1.3	1.3	1.3	1.3
Booster length (m)	-	2.9	2.9	2.9
Warhead mass (kg)	200	200	200	200
GC (kg)	192	192	192	192
Propulsion mass (kg)	1,323	1,323	1,343	1,357
m_{pb} (kg)		908	908	908
m_{db} (kg)		186	186	186
m_{pr} (kg)		229	183	194
m_{dr} (kg)			66	69
Body structure mass (kg)	377	377	381	385
Missile density (kg/m ³)	934	934	942	890
$\Delta t_p/\Delta t_r$ (s)	-		14/293	14/296

preliminary technical and operational requirements of a tactical surface-to-surface missile, as follows:

- Range-from 100 km to 300 km;
- Flight regime-supersonic, up to Mach 3;
- Launch weight-up to 3,000 kg;
- Cruise altitude-10 to 20 km;
- Diameter-less than 700 mm;
- Warhead mass-from 100 to 300 kg of highly-explosive material (HE).

5. Results and discussion

We suppose the Brazilian Navy needs to develop a long-range surface-to-surface missile for 300 km range, carrying 200 kg of warhead, cruising at 14,000 m altitude at Mach 3, with 600 mm reference diameter. Nowell's correlations defined the subsections masses and geometries of the baseline missile, comprised of guidance-control (GC), warhead (WH), and propulsion (PP). Factor 1.22 in the mass equation accounts for additional weight from the missile structure, as recommended by Fleeman (2012). Table II presents the baseline system and the first three refinements following the preliminary design flow illustrated in Fig. 7. After running the external ballistics code, booster sizing and performance characteristics determine the first refined solution. The booster impulse places the missile at the designated altitude, Mach number, and pitch angle. Then, missile drag, including the share of the ramjet engine (ram-drag), can be estimated as a first guess to the ramjet sustainer thrust. A total drag force of 35.4 kN was obtained in the initial assessment. At the start of the cruising flight, the mass of the ramjet, comprised of propellant and

Table 3 Ramjet main parameters

Parameter	Station 1	Station 2	Station 4	Station 5
P (bar)	0.142	3.682	3.462	0.142
T (K)	216	601.6	1,679-1,384	547.4
\dot{m} (kg/s)		28.78	29.453	
D (mm)	426	600	600	564
Mach	3	0.2	0.17	2.8
F (kN)				17-13
F_{gross} (kN)				42-38
I_{sp} (s)				1,847-1,967

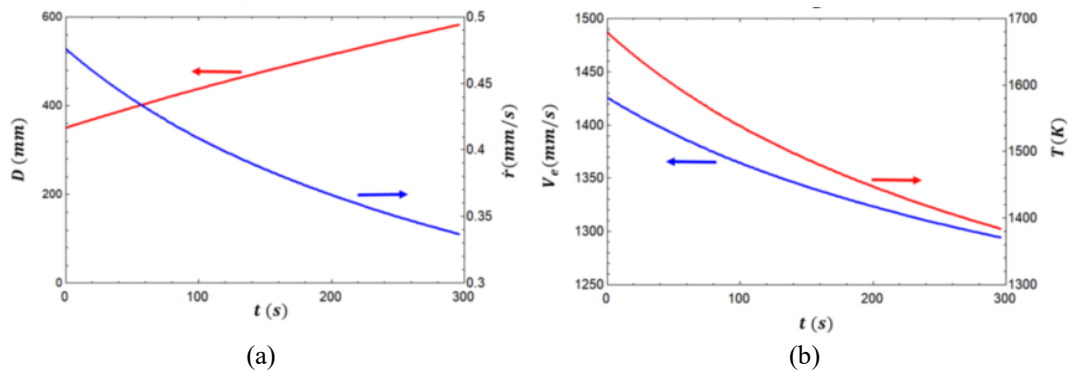


Fig. 8 Fuel regression rate, grain port diameter, exhaust velocity, and burner exit temperature during cruise flight

structure, was set to 229 kg, obtained by subtracting the booster mass (1,094 kg) from the baseline missile initial mass (1,323 kg).

Ramjet thrust depends on the air intake area and the combustion parameters. The dynamic evolution of the solid fuel port diameter sets the maximum engine operation time as the grain port approaches the missile reference diameter (600 mm). Increased burning times can be attained reducing the initial port diameter as long as the air mass flux does not exceed $350 \text{ kg/m}^2\text{s}$. Booster and the ramjet burning times were 14 and 296 seconds, respectively (Table 2). For the ramjet, the maximum combustion products temperature was set to 1,700 K to avoid expensive materials for the post-combustion chamber and nozzle. The internal ballistics code gives the solid fuel and total engine lengths and masses. For that, the calorific value and density of the solid-fuel were set to $42,150 \text{ kJ/kg}$ and 910 kg/m^3 , respectively.

After pre-sizing the ramjet engine, the external ballistics code is executed again to update the booster engine parameters and the initial cruising flight drag. As shown in Table II, the sizing of the booster converged after the first refinement since the mass of the ramjet engine went through minor changes due to the good propulsion mass estimate from Nowell’s correlation. To some degree, that was fortuitous. For example, applying the correlations (Fig. 6) to the MGM-52 Lance long-range missile (Lance 2023), the difference in total mass between the baseline predictions and the actual system was less than 7.5%. However, for the propulsion subsection, the difference in mass prediction was 31%. The actual propulsion mass of the Lance was 1,021 kg, and the model predicted 702 kg. In any case, a converged solution can always be obtained after a few

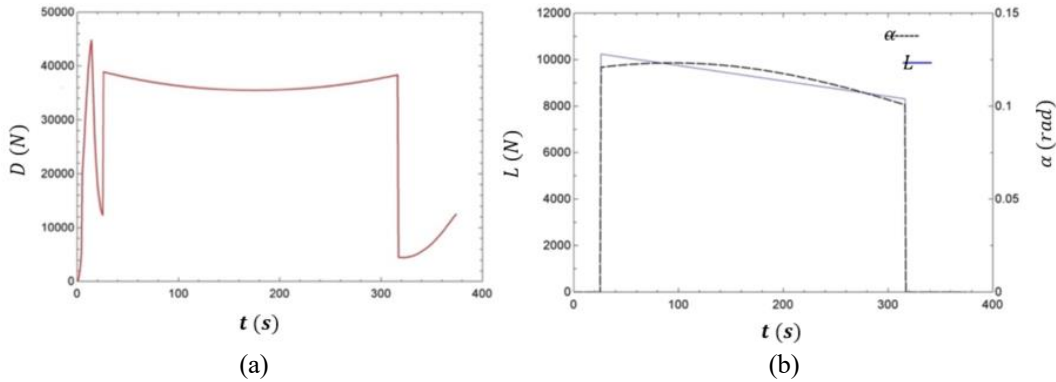


Fig. 9 Time variation of drag force (A); lift force and missile angle of attack (B)

adjustments.

Following booster separation, the ramjet missile was 5,100 mm long, weighing 1,038 kg, flying with 194 kg paraffin-polyethylene fuel. Table 3 presents relevant parameters for the solid-fueled ramjet engine. The efficiency of the isentropic intake was set to 90%, leading to 72.8% stagnation pressure recovery, or 368 kPa at station 2 (Fig. 3). The ramjet intake area of 0.1425 m² captured 28.8 kg/s of air for the combustor, which provided 15 kN of average net thrust.

Fig. 8 (a) shows the instantaneous fuel regression rate and solid fuel grain port diameter and Fig. 8 (b) shows the exhaust velocity and burner exit temperature throughout the cruise flight for a fixed grain length of 1,900 mm. The port diameter varied from 350 to 582 mm causing engine mass flux to vary from 299 to 108 kg/m²s. The change in mass flux altered the fuel regression rate, that ranged from 0.48 to 0.34 mm/s. For a fixed air mass flow rate, the reduction in the fuel-to-air ratio decreases the burner exit temperature (1679-1384 K), nozzle exhaust velocity (14126-1294 m/s), and engine gross thrust (42-38 kN). The averaged fuel burning rate and fuel-to-air ratio were 2,853 kg/h and 0.0312, respectively. In this preliminary assessment, the fuel regression rate decreases as the grain port increases, causing alterations on the overall fuel-to-air ratio.

The required ramjet sustainer thrust, shown on Fig. 9 (a), must compensate the total system drag forces whose main contributions are from the motor itself, along with those related to variations in the missile angle of attack. During cruise flight, drag forces varied from 38.8 to 38.3 kN. Along the cruise phase, gravitational forces are compensated through lift obtained by adjusting the missile angle of attack, as shown in Fig. 9 (b). Lift forces varied from about 10.3 to 8.3 kN for an average missile angle of attack of about 6.3 degrees (0.11 rad). Missile lift increases drag, which, in turn, claims higher thrust. The coupling of these counterbalanced forces sets the missile pitch and angle of attack for near-constant flight altitude. The missile flight profile comprised a rapid ascending (~20 s), cruising (~300 s) and descending. (~40 s) phases. Booster impulse brought the system to the required flight altitude, velocity, and near zero pitch angle in less than 40 s. Booster cold separation took place 15 s after take-off when the missile reached Mach 3.7, decaying to the desired cruise speed by the action of the drag forces. A rapid adjustment in pitch angle was provided by setting a proper value to the constant K in Eq. (4). The nose cone is ejected and the ramjet missile engine fired up, burning for about 296 s. The non-powered descending phase starts after 340 s from the time of launch. The missile can reach a target more than 300 km from its launch location at a steep angle and Mach 1.64.

The influence of the fuel composition on regression rate and mission performance was further

investigated taking the correlations listed in Fig. 1, for pure polyethylene and pure paraffin. For 100% PE fuel, the grain length should increase to 3,200 mm due to the lower regression rate range (0.26-0.20 mm/s) throughout motor operation (296 s). The initial and final grain diameters were estimated as 350 and 484 mm for the current mission. Ramjet engine fuel length increased by 38% to counterbalance the much lower regression rates, as compared to the PARPE blend (\dot{r}_7). The ramjet propellant mass fraction for this configuration was estimated as 67%, which is lower than that for the paraffin-polyethylene blend. Ramjet engine mass increased 27 kg, as a result of the additional 1,200 mm in the length of the motor.

A higher regression rate fuel would decrease motor length, fuel burning time, and missile range. For instance, applying the ballistics coefficients of Azevedo *et al.* (2019), the regression rate of pure paraffin varied from 2.0 to 1.4 mm/s for mass flux of 299-101 kg/m²s. The maximum allowed fuel grain diameter (~600 mm) was reached after 79 s of motor operation, greatly decreasing missile range, for an initial diameter of 350 mm. To give the target motor combustion temperature, the grain length was only 460 mm. Therefore, apart from structural concerns, pure paraffin seems not adequate for long-range missile applications.

Finally, we investigated the use of bypass provision to keep the motor *FA* ratio constant during cruise flight. Fixed regression rate can be narrowly attained with constant grain port oxidizer mass flux. The latter can be achieved bypassing the core air with a flow control device. Numerical predictions were then carried out by the internal ballistics code for the fixed regression rate strategy using the ballistics coefficients from \dot{r}_7 (PARPE blend). For constant regression rate of 0.3 mm/s, achieved with 77 kg/m²s of air mass flux, the fuel length would have 2,150 mm to maintain the required overall (*FA*) ratio and motor net thrust (38 kN). For that, the bypass ratio varied from 74 to 27% and grain diameter reached 590 mm, after 400 s of operation. This additional burning time would increase missile range in excess of 90 km. The system, however, would claim room for air to pass around the fuel grain, decreasing its final diameter and burning time. Adopting lateral squared air intakes, similar to the French ASMP-A missile (ASMP 2022), and integrated rocket-ramjet engine, the final grain diameter can approach that of the reference missile (600 mm). Such configuration increased ramjet propellant mass fraction to 78%.

6. Conclusions

In this paper, we have presented a comprehensive set of tools for the preliminary design phase of an anti-ship supersonic missile propelled by a ramjet engine based on liquefying fuels. The proposed method enabled the determination of the system's fundamental configuration, incorporating the main missile subsystems, namely guidance-control, warhead, and combined propulsion. Starting from a baseline missile that was pre-sized using published correlations, the iterative process facilitated the refinement of the booster and ramjet sustainer engines to meet a range of missile requirements. The combination of these tools yielded a preliminary long-range surface-to-surface missile, 600 mm in diameter, capable of carrying a 200 kg warhead to distances exceeding 300 km. The refined final weight was calculated to be 2,128 kg, which reduced to 1,034 kg after booster separation. The ramjet sustainer was designed to fly at Mach 3, 14,000 m altitude. Overall ramjet density and propellant mass fraction were estimated as 890 kg/m³ and 74%, respectively. To further increase the range, we propose incorporating lateral intake and variable air mass flow rate, while maintaining a constant fuel regression rate using a paraffin-polyethylene blend.

Acknowledgments

The authors are grateful for the technical support of collaborators of the Chemical Propulsion Laboratory of the University of Brasilia. Also, this study was financed in part by the Coordenação de Aperfeiçoamento de Pessoal de Nível Superior-Brasil (CAPES)-Finance Code 001.

References

- Air-Sol Moyenne Portée-Wikipedia (2023), Air-Sol Moyenne Portée, Wikipedia Foundation, St. Petersburg, USA.
- ASTROS (2014), ASTROS 2020 MLRS: Brazil's Industrial Investment in Precision Strike, Defense Industry Daily, Vermont, USA.
- Azevedo, V.A., Alves, I. and Shynkarenko, O. (2019), "Experimental investigation of high regression rate paraffin for solid fuel ramjet propulsion", *Proceedings of the AIAA Propulsion and Energy 2019 Forum*, Indianapolis, USA, August.
- Bertoldi, A.E.M., Veras, C.A.G., Shynkarenko, O., Andrianov A., Lee, J. and Domenico, S. (2022), "Overview of the past and current research on hybrid rocket propulsion at the University of Brasília", *Proceedings of the 9th European Conference for Aeronautics and Space Sciences (EUCASS)*, Lille, France, June.
- Busse, J.R. and Leffler, M.T.A (1996), "Compendium of aerobee sounding rocket launchings from 1959 through 1963", NASA Technical Report TR R-226, Goddard Space Flight Center, Greenbelt, USA.
- Buthod, P. (2001), *Pressure Vessel Handbook*, Pressure Vessel Publishing INC., Tulsa, OK, USA.
- Campos, L.M.B.C. and Gil, P.J.S. (2018), "On four new methods of analytical calculation of rocket trajectories", *Aerosp.*, **5**(3), 88. <https://doi.org/10.3390/aerospace5030088>.
- da Cás, P.L., Veras, C.A., Shynkarenko, O. and Leonardi, R. (2019), "A Brazilian space launch system for the small satellite market", *Aerosp.*, **6**(11), 123. <https://doi.org/10.3390/aerospace6110123>.
- da Cás, P.L.K. and Veras, C.A.G. (2012), "An optimized hybrid rocket motor for the SARA platform reentry system", *J. Aerosp. Technol. Manage.*, **4**(3), 317-330. <https://doi.org/10.5028/jatm.2012.04032312>.
- Decreto n. 6.703 (2008), Aprova a Estratégia Nacional de Defesa, Presidência da República, Brasília, Brazil. https://www.planalto.gov.br/ccivil_03/_ato2007-2010/2008/decreto/d6703.htm.
- Dutta, D. (2014), "Probabilistic analysis of anti-ship missile defence effectiveness", *Def. Sci. J.*, **64**(2), 123-129. <https://doi.org/10.14429/dsj.64.3532>.
- EAM (2021), Earth Atmosphere Model, NASA, Cleveland, USA.
- ECSS (2017), System Engineering General Requirements; European Cooperation for Space Standardization, Noordwijk, The Netherlands. <https://ecss.nl/standard/ecss-e-st-10c-rev-1-system-engineering-general-requirements-15-february-2017/>
- Fleeman, E. (2012), *Missile Design and System Engineering*, American Institute of Aeronautics and Astronautics, Inc, Reston, VA, USA.
- Garcia, A., Yamanaka, S.S.C., Barbosa, A.N., Bizarria, F.C.P., Jung, W. and Scheuerpflug, F. (2011), "VSB-30 sounding rocket: History of flight performance", *J. Aerosp. Technol. Manage.*, **3**, 325-330.
- Karabeyoglu, A., Zilliac, G., Cantwell, B.J., DeZilwa, S. and Castellucci, P. (2004), "Scale-up tests of high regression rate paraffin-based hybrid rocket fuels", *J. Propuls. Power*, **20**(6), 1037-1045. <https://doi.org/10.2514/1.3340>.
- Karabeyoglu, M.A., Altman, D. and Cantwell, B.J. (2002), "Combustion of liquefying hybrid propellants: Part 1, General theory", *J. Propuls. Power*, **18**(3), 610-620. <https://doi.org/10.2514/2.5975>.
- Kim, S., Moon, H., Kim, J. and Cho, J. (2015). "Evaluation of paraffin-polyethylene blends as novel solid fuel for hybrid rockets", *J. Propuls. Power*, **31**(6), 1750-1760. <https://doi.org/10.2514/1.B35565>.
- Klein, S.A. and Nellis, G. (2013), *Mastering EES, f-Chart Software*, Madison, MI, USA.
- Lesieutre, D., Mendenhall, M., Nazario, S. and Hensch, M. (1987), "Aerodynamic characteristics of

- cruciform missiles at high angles of attack”, *Proceedings of the 25th AIAA Aerospace Sciences Meeting*, Reno, United States, March.
- Li, W., Chen, X., Zhao, D., Wang, B., Ma, K. and Cai, T. (2020), “Swirling effect on thermodynamic performance in a solid fueled ramjet with paraffin-polyethylene”, *Aerosp. Sci. Technol.*, **107**, 106341. <https://doi.org/10.1016/j.ast.2020.106341>.
- Martos, J.F.A., Rêgo, I.S., Laiton, S.N.P., Lima, B.C., Costa, F.J. and Toro, P.G.P. (2017), “Experimental investigation of Brazilian 14-XB hypersonic scramjet aerospace vehicle”, *Int. J. Aerosp. Eng.*, **2017**, Article ID 5496527. <https://doi.org/10.1155/2017/5496527>.
- MGM-52 (2023), MGM-52 Lance, Wikipedia Foundation, Inc., San Francisco, USA. https://en.wikipedia.org/wiki/MGM-52_Lance
- NASA (2021), Inlet Performance, National Aeronautics and Space Administration, Cleveland, USA.
- Neiva, R.Q. (2016), “Técnica de otimização aplicada em projeto conceitual de mísseis táticos”, M.Sc. Thesis, University of Brasília, Brasília.
- Nowell Jr., J.B. (1992), “Missile total and subsection weight and size estimation equations”, M.Sc. Thesis, Naval Postgraduate School, Monterrey.
- Ponomarenko, A. (2014), “RPA-Tool for rocket propulsion analysis”, *Proceedings of the Space Propulsion Conference*, Cologne, Germany, May.
- Sidhu, W.P.S. (2007), *Looking Back: The Missile Technology Control Regime, Arms Control Today*, April.
- Struchtrup, H. (2014), *Thermodynamics and Energy Conversion*, Springer, Berlin, Germany.
- Tang, Y., Chen, S., Zhang, W., Shen, DeLuca, L.T. and Ye, Y. (2017), “Mechanical modifications of paraffin-based fuels and the effects on combustion performance”, *Propell. Explos. Pyrotech.*, **42**, 1268.1277. <https://doi.org/10.1002/prop.201700136>.
- Turns, S.R. (2011), *An Introduction to Combustion*, McGraw-Hill Education, Godfrey, IL, USA.